EXTRACELLULAR VESICLES IN OVARIAN ANTRAL FOLLICLES: CHARACTERIZATION AND FUNCTIONS

By
Wei-Ting Hung

Submitted to the graduate degree program in Molecular and Integrative Physiology and the Graduate Faculty of the University of Kansas in partial fulfillment of the requirements for the degree of Doctor of Philosophy.

Dissertation Committee:

Chair: Lane K. Christenson, Ph.D

William H. Kinsey, Ph.D

V. Gustavo Blanco, Ph.D

Warren B. Nothnick, Ph.D

Vargheese M. Chennathukuzhi, Ph.D

Francesca E. Duncan, Ph.D

Date Defended: July 28th, 2016

The dissertation committee for Wei-Ting Hung certifies that this is the approved version of the following dissertation:

EXTRACELLULAR VESICLES IN OVARIAN ANTRAL FOLLICLES: CHARACTERIZATION AND FUNCTIONS

_____

Chair: Lane K. Christenson, Ph.D

Date approved: Oct 12th, 2016

III. Abstract

Formation of the follicular fluid antrum within the ovarian follicle provides a unique environment for the developing oocyte. Follicular fluid contains factors including nucleic acids, proteins, lipids, hormones, and metabolic factors secreted by both ovarian somatic cells and the oocyte that are critical for follicle development. In addition, lipid bi-layer extracellular vesicles (EVs) comprised of exosomes and microvesicles are highly abundant in follicular fluid. Whether these EVs play a role in ovarian cell signaling, provide a mechanism for transport of metabolic products or are nonfunctional within the ovarian follicle is unknown. In this dissertation, I will test the hypothesis that ovarian follicular fluid EVs are unique and determine whether they can elicit functional effects on the cumulus-oocyte-complex and the mural granulosa cells. To accomplish these goals, follicular fluid from three different sizes of bovine antral follicles, [i.e. small (3-5 mm), medium (6-9 mm), and large (>9 mm)] were collected and EVs were isolated and characterized by electron microscopy, nanoparticle tracking analysis (NTA), protein marker analysis, and small RNAseq. Electron microscopy and NTA indicated the presence of a uniform (50-200 nm) population of EVs that had different microRNA within them based on follicle size. An EV marker, CD81, showed decreased abundance in EVs as follicle size increased. Fluorescent labeling of the follicular fluid EVs

followed by culture indicated that both cumulus and mural granulosa cells took up the fluorescent-labeled EVs. To test for functional activity, cumulus-oocyte-complexes and granulosa cells were exposed to EVs isolated from different size follicles. Extracellular vesicle treatment caused expansion of cumulus cells and increased expression of prostaglandin-endoperoxide synthase 2 (*Ptgs2*), pentraxin-related protein 3 (*Ptx3*), and tumor necrosis factor, alpha-induced protein 6 (*Tnfaip6*) genes, genes associated with normal cumulus expansion. Additionally, EVs from small follicles induced granulosa cell proliferation, and we determined that the Src and JNK pathways were involved in the cell proliferation induced by EVs. Moreover, we determined that the differential ability of EVs to affect granulosa cell proliferation was primarily a result of preferential uptake by EVs from small follicles versus those of medium and large follicles. In summary, these studies provide insight into the unique characteristics of EVs isolated from three different stages of antral follicles. This work also provides the first functional evidence that EVs from ovarian follicular fluid are able to elicit functional physiologic changes in both cumulus and granulosa cells and provides clues to the cell signaling pathways that are modulated in cells following exposure to these small lipid enclosed vesicles. Lastly, this study provides an approach to further purify EVs, and indicates the ovarian follicle as an excellent model for studying general extracellular vesicle biology.

IV. Acknowledgement

It has been a great five years to stay in Kansas City. I still can remember the moment after I decided to come to Kansas City for graduate study. I took the advantage of google map and tried to get some ideas of the place I am going to stay for years. I saw several fast food stores on Rainbow Blvd, which means I am going to have some food at least and that was all I could see around the campus. But after five years, Kansas City is another home. The reason is that I have so many people around me showing their kindness and support.

For sure, it would not be easy without all the help and support from a good mentor, Dr. Lane K. Christenson. I always have a good fortune to meet great mentors or bosses and Lane in certainly one of them. He gave me plenty of room for independent thinking and provided me suggestions and advise whenever I needed. Other than the mentor, a great environment for research is critical. Lane's Lab always sticks together and helps each other. The ideas generated from discussion in the lab were such an important part on pushing the projects forward. Help from the other groups inside and outside the campus also played a huge role. I am very fortune to have worked at the University of Kansas Medical Center because of its strong reproductive group. I can easily find the answers to my questions just by talking to different researchers working on different topics of

reproduction.

I am not the type of person who can always be alone. Other than doing research in school, I am very lucky to meet a lot of great people in Kansas City. The Taiwanese group has been very helpful since the first day I arrived here. We help each other and hang out together. It has been really great to have every one of you here. Other than my Taiwanese friends, I also got the chance to know people from all over the world. Although we started our relationship using English, which I may not be very good at in the beginning, I still made a lot of good friends. Compared with friends from Taiwan, it may be more difficult to meet each other after I leave, but the friendship will be always there.

In the end, I would like to thank my family. My parents Chen-Yin and Ming-Tsai are always on my side and provide all the help I ask for. I am really happy that they made the trip here to attend my defense. My sister, Jui-Hsin grew up with me and shared a lot of memories together. I would like to let them know I love them.

It may be the end of the story in Kansas City. But I am looking forward to see you guys soon. See you in San Diego!

Wei-Ting

V. Table of Contents

VI. List of Tables and Figures

Figures

Tables

VII. Chapter I: Introduction

Eukaryotic cells are highly specialized cells with different organelles including endoplasmic reticulum, trans-Golgi network, mitochondria, carrying out distinct functions. Within cells the crosstalk between organelles through exchange of bio-informative materials, such as nucleic acid and proteins, is critical for maintaining a healthy cellular function. One mechanism used by these organelles to communicate is via membrane derived bi-layer vesicles. These vesicles are known to be capable of transferring molecules from one organelle to the other in a well-controlled manner of secretion and uptake (Vassilieva and Nusrat 2008).

Vesicles outside the cells were first observed by Dr. H. Clark Anderson, a University of Kansas Medical Center faculty soon after the invention of electron microscopy in 1967 (Anderson 1967). In 1971, Dr. N. Crawford reported the observation of proteins on/in the vesicles and studies have been focused on the vesicle-associated proteins in different systems (Crawford 1971). Dendritic cells and B lymphocytes secreted vesicles, which contained the major histocompatibility complex (MHC) class II antigen, were able to induce antigen-specific MHC class II-restricted T cell responses (Raposo, Nijman et al. 1996, Thery, Duban et al. 2002). Oligodendrocytes, which are responsible for myelinating axons in the brain, released vesicles containing proteolipid protein (PLP), myelin proteins and proteins associated with protection against oxidative stress (Kramer-

Albers, Bretz et al. 2007, Fruhbeis, Frohlich et al. 2013, Frohlich, Kuo et al. 2014, Budnik, Ruiz-Canada et al. 2016). Sphingomyelin present on tumor secreted vesicles was capable of stimulating endothelial cell migration and angiogenesis (Kim, Lee et al. 2002). In 2007, RNA transcripts were shown to be present in extracellular vesicles and this single manuscript, which has now been cited over >2500 times, signaled the start of a major effort in understanding of the potential biological roles these extracellular vesicles might have on cell, tissue and organ systems (Valadi, Ekstrom et al. 2007). Additionally, it was discovered that cancer cells excrete large numbers of vesicles and this lead to the hypothesis that these vesicles might be important in mediating changes in those cells immediately adjacent to the tumor cells to provide a niche for tumor growth. This also led to a large number of studies looking at vesicles in bodily fluids as biomarkers for cancers, and a significant portion of these papers focus on the composition of microRNA (miRNA) present in the vesicles (Ciardiello, Cavallini et al. 2016). What has lagged behind is the potential of these vesicles to elicit important functions in normal physiology. I believe that the antral ovarian follicle, due to its unique structure and well-established cross talk across this fluid filled space provides an excellent opportunity to study extracellular vesicles in a normal physiologic environment.

Vesicles can be released into extracellular space by different cellular mechanisms

and are categorized by the type of biogenesis and secretory method. Two major mechanisms are thought to predominate during the formation and secretion of vesicles. These include the direct budding of the plasma membrane into the extracellular space (microvesicles) and the fusion of multivesicular bodies (MVB), which contain small intraluminal vesicles (commonly referred to as exosomes). In addition, the process of apoptosis can also contribute a population of vesicles into the extracellular space. Since there is a lack of knowledge/methodologies to distinguish the vesicles once released by the cells, they are more appropriately called extracellular vesicles (EVs), to indicate the unknown source of these biofluid vesicles. The two most recognized populations of EVs (i.e. exosomes and microvesicles) will be discussed below with regard to their biogenesis.

1. Extracellular vesicle biogenesis

Exosome biogenesis

Exosomes are a product of the endocytic pathway. In endocytosis, the late endosome, also called MVB, contains intraluminal vesicles (ILV), produced by inward budding of the MVB membrane (Kowal, Tkach et al. 2014). The well-established downstream pathway for MVB is to fuse with the lysosome to degrade the cellular

products contained within. Alternatively, the MVB can fuse with the plasma membrane and the contents including the ILVs are then released into the extracellular space. This was first described by two groups studying reticulocyte maturation and these endocytic small vesicles (ILV) were named exosomes for the first time by Johnstone *et al.* in 1987 (Johnstone, Adam et al. 1987).

Since exosomes originate from ILV the regulation of the biogenesis of ILV affects exosome production. As a structure with a lipid bi-layer shell, production of ILV requires lipids these are mostly provided by recycling of the plasma membrane. Endosomal Sorting Complex Required for Transport (ESCRT) machinery is known to regulate membrane remodeling and then affect ILV formation in MVB (Hurley 2015). There are four complexes of ESCRT (ESCRT-0, ESCRT-I, ESCRT-II, ESCRT-III) and accessory proteins, which are also necessary for remodeling of plasma membrane. The components of ESCRT are well described by Williams *et al.* (Figure 1) (Williams and Urbe 2007).

Figure 1 The ESCRTs

The four ESCRTs are recruited to endosomes by their interactions with membranes, clathrin, ubiquitin (Ub) and with each other. Features common to both yeast and mammalian pathways are included. Lipid recognition of either phosphatidylinositol-3-phosphate (PtdIns3P) by the FYVE domain of Vps27 (ESCRT-0) or the GLUE domain of Vps36 (ESCRT-II), or PtdIns(3,5)P_2 by Vps24 (ESCRT-III) might contribute to the early or late endosomal localization of the components. All of the ESCRTs except ESCRT-III recognize and bind the ubiquitylated cargo, either through an ubiquitin-interacting motif (UIM) (ESCRT-0), an ubiquitin E2 variant (UEV) domain (ESCRT-I) or the GLUE domain of Vps36 (ESCRT-II). ESCRT-III orchestrates the last steps in the pathway in which ubiquitin is removed by a de-ubiquitinase (degradation of alpha-4 (Doa4)), and the complexes are disassembled by the AAA+ ATPase Vps4. Budding away from the cytosol is depicted as being facilitated by a curvature-inducing factor that could flex the membrane by being localized to the neck of the budding vesicle. The ESCRT components might facilitate the recruitment of such curvature-inducing factors or the concentration of inverted cone-shaped components in the endosomal membrane, such as lysobisphosphatidic acid (LBPA), and non-cargo transmembrane proteins that have bulky glycosylations on the luminal side of the membrane, such as tetraspannins. Did2, Vps2

and Vps60 are shown interacting with the Vps4–Vta1 complex. The bottom panels list ESCRT subunits and accessory proteins from *Saccharomyces cerevisiae* and their mammalian homologues. AMSH, associated molecule with the SH3 domain of STAM; CHMP, charged MVB proteins; SH3, Src-homology-3; STAM, signal transducing adaptor molecule; UBPY, ubiquitin-specific protease Y. (Williams and Urbe 2007)

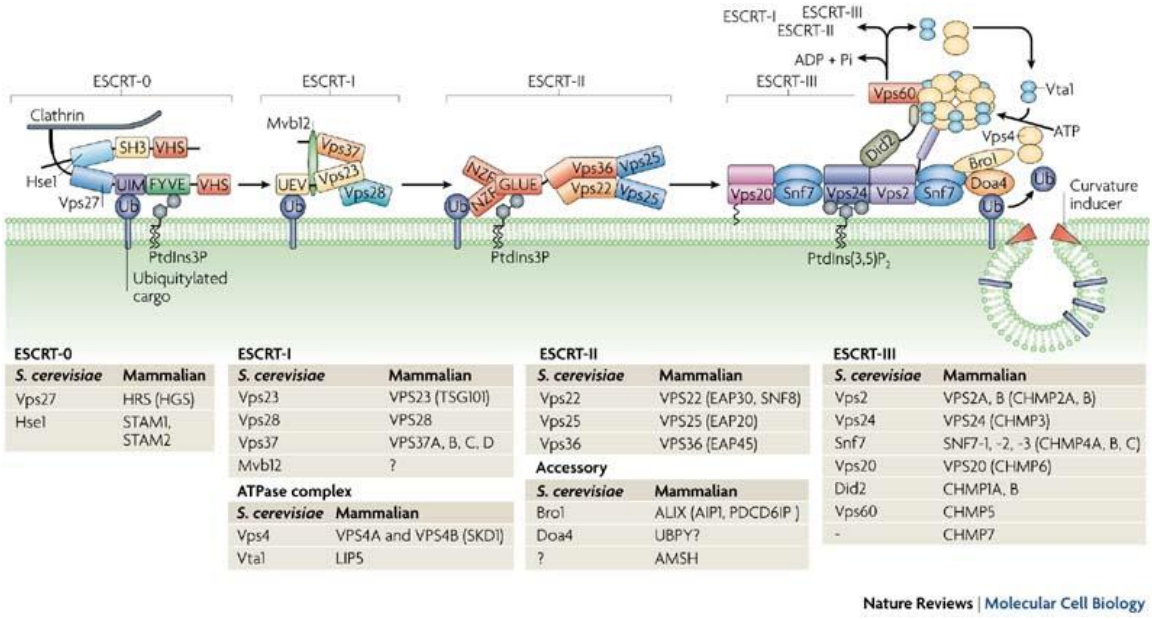

ESCRT-0

S. cerevisiae	Mammalian
Vps27	HRS (HGS)
Hse1	STAM1, STAM2

ESCRT-I

S. cerevisiae	Mammalian
Vps23	VPS23 (TSG101)
Vps28	VPS28
Vps37	VPS37A, B, C, D
Mvb12	?

ATPase complex

S. cerevisiae	Mammalian
Vps4	VPS4A and VPS4B (SKD1)
Vta1	LIP5

ESCRT-II

S. cerevisiae	Mammalian
Vps22	VPS22 (EAP30, SNF8)
Vps25	VPS25 (EAP20)
Vps36	VPS36 (EAP45)

Accessory

S. cerevisiae	Mammalian
Bro1	ALIX (AIP1, PDCD6IP)
Doa4	UBPY?
?	AMSH

ESCRT-III

S. cerevisiae	Mammalian
Vps2	VPS2A, B (CHMP2A, B)
Vps24	VPS24 (CHMP3)
Snf7	SNF7-1, -2, -3 (CHMP4A, B, C)
Vps20	VPS20 (CHMP6)
Did2	CHMP1A, B
Vps60	CHMP5
-	CHMP7

Nature Reviews | Molecular Cell Biology

Permission to use this figure was kindly provided by the author, Dr. Roger Williams.

ESCRT-0 is responsible for cargo loading in an ubiquitin-dependent manner. Two key components of ESCRT-0 have been reported to affect the production of exosomes, HGF-regulated tyrosine kinase substrate (HRS) and signal transducing adaptor molecule (STAM1), in which depletion of these two factors decreases the number of exosomes released (Colombo, Moita et al. 2013). ESCRT-I is also involved in exosome secretion since depletion of Tumor Susceptibility 101 (TSG101) caused a decrease in exosome production (Colombo, Moita et al. 2013). Within components of ESCRT-II and ESCRT-III, the effect of single protein depletion is divergent except for CHMP4C (Baietti, Zhang et al. 2012, Colombo, Moita et al. 2013). Knocking down the expression of CHMP4C decreased secretion of exosomes. Alix is an ESCRT accessory protein that has been widely used as an exosome marker because of its consistent presence in different exosome preparations (Mathivanan, Ji et al. 2010). Studies have tried to identify the influence of alix depletion on exosome secretion because of its ability to induce ILV budding (Baietti, Zhang et al. 2012). While there is evidence showing that alix can affect specific populations of exosomes including CD81, CD63, MHC class II positive exosomes, the effect is not clear for the total number of exosomes produced by cells (Colombo, Moita et al. 2013, Romancino, Paterniti et al. 2013, Kowal, Tkach et al. 2014). Another critical protein in the ESCRT pathway is VPS4, an ATPase involved in

membrane scission (Hanson and Cashikar 2012). The role of VPS4 in exosome biogenesis is not clear, as its effects on exosome secretion are dependent upon the cell line being studied (Baietti, Zhang et al. 2012, Abrami, Brandi et al. 2013, Colombo, Moita et al. 2013).

In addition to the ESCRT pathway, there are also ESCRT-independent mechanisms capable of producing exosomes. Ceramide, a major component of the lipid bi-layer, is able to induce inward budding and increase the production of exosomes by inducing the inward curvature of MVB membranes (Trajkovic, Hsu et al. 2008). Accumulation of cholesterol, another major component of the plasma membrane, can also increase the number of exosomes (Strauss, Goebel et al. 2010). Phospholipase D2 (PLD2) is also reported to have similar actions as ceramide, since the increase of PLD2 results in ILV inward budding and therefore increased exosome production (Laulagnier, Grand et al. 2004, Ghossoub, Lembo et al. 2014).

Other than vesicle formation, regulation of MVB trafficking and fusion with plasma membrane is another factor critical to exosome secretion. RABs, which are small GTPase proteins, play important roles in several steps of vesicle trafficking and are essential for membrane budding, vesicle movement, and membrane docking and fusion (Stenmark 2009). Within the RAB family, individual RABs including RAB2B,

RAB5A, RAB7, RAB9A, RAB11A, RAB27A, RAB27B, and RAB35 have been shown to be involved in various steps of vesicle trafficking and having different roles based on the cell type (Savina, Fader et al. 2005, Hsu, Morohashi et al. 2010, Ostrowski, Carmo et al. 2010, Baietti, Zhang et al. 2012, Bobrie, Krumeich et al. 2012, Peinado, Aleckovic et al. 2012, Abrami, Brandi et al. 2013, Fruhbeis, Frohlich et al. 2013).

Microvesicle biogenesis

In 1991, Stein and Luzio first defined microvesicles as vesicles shedding from plasma membrane (Stein and Luzio 1991). Since both exosomes and microvesicles originate from lipid bi-layer membranes, they share some of the biogenesis machinery. ESCRT complexes, which I described above as important for exosome biogenesis, were originally shown to be important in membrane budding, docking, and scission reactions involved in microvesicle formation. TSG101, an ESCRT-I subunit, interacts with alix and another accessory protein, arrestin-domain containing-1 (ARRDC1) in microvesicles (Nabhan, Hu et al. 2012). Another similarity of exosome and microvesicle production can be observed by the enrichment of cholesterol, sphingomyelin, and ceramide implying that they are both related to lipid raft formation which is a microdomain of the plasma membrane with the enrichment of glycosphingolipids and membrane receptors (Bianco,

Perrotta et al. 2009). A special mechanism to generate microvesicles is dependent on a membrane-binding motor, myosin-1a (Myo1a). The activity of this motor results in the accumulation of membrane at microvillar tips, which then leads to the formation of microvesicles (McConnell and Tyska 2007, McConnell, Higginbotham et al. 2009).

The regulation of exosomes and microvesicles production has been pursued in various cell types and focused on different cellular pathways. Since they are both membrane-enclosed vesicles and require sources of membrane for biogenesis, some fundamental genes of membrane remodeling contribute to both exosomes and microvesicles. Moreover, after being released into the extracellular space, it is difficult to distinguish and separate them from one to the other. Therefore, the field has started to use the term "extracellular vesicle, EV" to refer to the vesicles isolated from biofluids (Cocucci and Meldolesi 2015). I will use the inclusive EV term in my dissertation.

2. Extracellular vesicles uptake

In order for cells to use EV and the molecules (ie., nucleic acids, proteins, and lipids) contained within the recipient cells must have mechanisms to internalize or fuse with the EVs. The ability of the cells to take up EVs has been proven by different methods, indirect and direct. The transfer of mRNA, miRNA, or protein between cells from

different species by EVs has been shown by use of species specific primers or antibodies (Valadi, Ekstrom et al. 2007, Alvarez-Erviti, Seow et al. 2011). Another mechanism is through use of reporter-based experiments where EVs were loaded with substrate that upon deliver/fusion to recipient cells can activate expression of a reporter construct in the recipient cells (Montecalvo, Larregina et al. 2012). Other than the observation of cargo delivery, the uptake of EVs can also be visualized directly by labeling EVs with fluorescence markers (Montecalvo, Larregina et al. 2012). Lipophilic dyes are the most common methodology to label the lipid bi-layers of EVs, these include PKH26, PKH67, rhodamine B (R18), DiI, and DiD. Permeable dyes are the other alternative way to stain EVs, such as carboxyfluorescein succinimidyl ester (CFSE) and 5(6)-carboxyfluorescein diacetate (CFDA) (Mulcahy, Pink et al. 2014). These compounds become confined to the cytosolic lumen and fluoresce as a consequence of esterification (Mulcahy, Pink et al. 2014). To determine the uptake of EVs in recipient cells, flow cytometry and confocal microscopy are two general approaches used. Confocal microscopy can only show uptake of the EVs and the localization of EVs in the cells after internalization. Flow cytometry can quantify the relative level of uptake and is capable of making comparison across experimental subjects. When observing labeled EVs under confocal microscopy, it is also worthwhile noticing that it is not a single EV but a group of EVs that are

typically being detected due to the limited resolution of light based microscopes. There are several ways that recipient cells can take up EVs in the extracellular space including various types of endocytosis, membrane fusion, and specific protein-dependent internalization, which will be discussed below.

Clathrin-dependent endocytosis

This type of endocytosis requires clathrin for the formation of clathrin coated vesicles to internalize extracellular materials (Kirchhausen 2000). Since this pathway has been well studied, there are numerous approaches to manipulate the process and to test the role of clathrin-dependent endocytosis on EV uptake. Chlorpromazine prevents formation of clathrin-coated pits at the plasma membrane and treatment with chlorpromazine decreased the uptake of EVs in ovarian cancer cells (Wang, Rothberg et al. 1993, Feng, Zhao et al. 2010, Escrevente, Keller et al. 2011). Two proteins, dynamin2 and epidermal growth factor receptor pathway substrate clone 15 (EPS15) are essential components in clathrin-dependent endocytosis. Regulating these proteins negatively in the cells decreased EV uptake (Barres, Blanc et al. 2010, Feng, Zhao et al. 2010, Fitzner, Schnaars et al. 2011).

Caveolin-dependent endocytosis

Caveolin-dependent endocytosis shares some similarities with clathrin-dependent endocytosis but requires the formation of caveolae, a type of lipid raft present on the plasma membrane. Dynamin2 is also a component in this process, therefore the decrease of EV uptake by blocking dynamin2 illustrates that EVs are taken up at least partially through this pathway (Barres, Blanc et al. 2010, Menck, Klemm et al. 2013, Nanbo, Kawanishi et al. 2013). In order to look into the role of caveolin-dependent endocytosis on EV uptake more specifically, knock-down of caveolin-1 (CAV1), which is required and sufficient for the formation of caveolae, was performed, and impaired EV uptake was observed (Nanbo, Kawanishi et al. 2013). However, knock-down of CAV1 resulted in increased EV uptake in another study using a different cell type (Svensson, Christianson et al. 2013).

Macropinocytosis

Macropinocytosis is a type of endocytosis, which involves the formation of invaginated membrane ruffles and inward membrane budding at these sites. This mechanism is rac1-, actin- and cholesterol-dependent and requires Na+/H+ exchanger activity (Kerr and Teasdale 2009). Inhibition of Na+/H+ exchanger with amiloride was

able to decrease uptake of EVs by microglia cells (Fitzner, Schnaars et al. 2011). Treatment with a small molecule inhibitor of rac1, NSC23766, inhibited the uptake of EVs by microglia (Fitzner, Schnaars et al. 2011). However, studies with other cell types did not observe inhibition of EV uptake following blockade of macropinocytosis (Feng, Zhao et al. 2010, Christianson, Svensson et al. 2013, Nanbo, Kawanishi et al. 2013). Therefore, the role of macropinocytosis on EV uptake appears to be cell type dependent.

Phagocytosis

Phagocytosis is yet another type of endocytosis. Phagocytosis usually happens in a receptor mediated manner and is known to internalize larger extracellular materials. Phosphatidylinositol-4,5-bisphosphate 3-kinase (PI3K) is critical in phagocytic processes, particularly in enabling membrane insertion into the forming phagosomes (Stephens, Ellson et al. 2002, Mulcahy, Pink et al. 2014). Inhibition of PI3K activity using small molecule inhibitors, such as LY294002 and wortmannin, can abolish EV uptake in a dose-dependent manner (Feng, Zhao et al. 2010). Phosphatidylserine (PS), a phospholipid of the membrane, is another molecule that has been shown to play a role in phagocytosis-mediated EV uptake. Macrophages cultured in presence of an antibody against T-cell immunoglobulin mucin protein 4 (TIM4), which is a critical receptor

involved in PS-dependent phagocytosis, reduced the uptake of EVs (Miyanishi, Tada et al. 2007, Feng, Zhao et al. 2010). Additionally, treatment with a PS analogue reduced uptake of EVs by dendritic cells as did incubation of macrophages and natural killer cells with a PS-binding protein, annexin-V (Nolte-'t Hoen, Buschow et al. 2009, Yuyama, Sun et al. 2012).

Lipid rafts

Lipid rafts are specialized regions on the plasma membrane, which are rich in protein receptors, sphingolipids, and cholesterol (Nabi and Le 2003). Endocytosis depending on cholesterol are highly associated with lipid rafts, such as clathrin- and caveolin-dependent endocytosis. Flotillins represent another type of protein in the lipid rafts, which are also involved in endocytosis (Palecek, Schmidt et al. 1996). The endocytosis mediated by flotillins are independent from clathrin and caveolin and likely work through binding to GPI-anchored proteins (Glebov, Bright et al. 2006, Frick, Bright et al. 2007, Otto and Nichols 2011). Disruption of lipid rafts composition using drugs, such as fumonisin B1, N-butyldeoxynojirimycin hydrochloride, MβCD, filipin and simvastatin were all shown to influenced EV uptake, indicating the critical role of lipid rafts in EV uptake (Parolini, Federici et al. 2009, Feng, Zhao et al. 2010, Escrevente, Keller et al.

2011, Koumangoye, Sakwe et al. 2011, Montecalvo, Larregina et al. 2012, Svensson, Christianson et al. 2013).

Membrane fusion

The other way to deliver signaling molecule by EVs is through membrane fusion which is dependent on Soluble NSF Attachment Protein Receptors (SNAREs), Rab proteins, and Sec1/Munc-18 related proteins (SM-proteins) (Jahn and Sudhof 1999). Fusion of EVs to recipient cells can be observed by using fluorescence lipid dequenching, followed by detection of delivered materials using specific primers or antibodies (Parolini, Federici et al. 2009). While the tools for measuring membrane fusion are available, currently very little is known/published regarding whether this is a mechanism that is used by EVs to deliver material from one cell to another cell.

Specific protein interaction

Other than known cellular mechanisms, EV uptake through interaction with individual membrane surface proteins has been explored as well. Tetraspanins are a family of proteins with four transmembrane domains that are rich in EV preparations (Escola, Kleijmeer et al. 1998, Zoller 2009). CD9, CD63, and CD81 from this family

are broadly used as markers for EVs (Escola, Kleijmeer et al. 1998, Thery, Regnault et al. 1999). Treatment of cells with CD9 or CD81 antibodies decreased EV uptake, suggesting an active role of these two tetraspanins in EV uptake (Morelli, Larregina et al. 2004). Another tetraspanin, Tspan8, is known to form a complex with CD49d and then is able to be taken up by endothelial cells and pancreatic cells through interactions with its ligand, intercellular adhesion molecule 1 (ICAM1/CD54) (Nazarenko, Rana et al. 2010).

The importance of integrins and immunoglobulins on EV uptake has been studied mostly in immune cells. Blocking CD11a, ICAM1, CD51, and CD61 resulted in reduced EV uptake (Morelli, Larregina et al. 2004, Nolte-'t Hoen, Buschow et al. 2009). Naïve T-cells have been shown to internalize EVs through T-cell receptor (TCR), CD28, and function-associated antigen (LFA1; (Hwang, Shen et al. 2003). CD4+ cells also require TCR-major histocompatibility complex (MHC) and LFA1-ICAM1 interaction to take up EVs (Hao, Bai et al. 2007). These results emphasize the role of protein-protein interaction on EV uptake.

Proteoglycans are proteins with high levels of carbohydrate. The heparin sulphate proteoglycans (HSPGs) are proteins with sulphated glycosaminoglycan polysaccharides that participate in viral entry (Shukla, Liu et al. 1999). Cells that have lost the ability to

produce normal HSPGs also show impaired ability to uptake EVs (Christianson, Svensson et al. 2013). Extracellular vesicles pre-treated with heparinase to remove proteoglycans have reduced uptake by recipient cells indicating the importance of cell surface proteoglycans (Christianson, Svensson et al. 2013).

Lectins are another group of proteins, which have been shown to be critical for EV uptake. Treatment with antibodies against DC-SIGN or DE-205, both C-type lectin receptors, abolished EV uptake by dendritic cells (Hao, Bai et al. 2007, Naslund, Paquin-Proulx et al. 2014). Another leptin, galectin-5, has been found to associate with EVs, and co-incubation of EVs and excess galectin-5 reduced EV uptake (Barres, Blanc et al. 2010). Addition of asialofetuin, which binds to galetin-5, also reduced EV uptake (Barres, Blanc et al. 2010).

The evidence provided above has shown that EVs can be taken up by the cells through different mechanisms and that they rely on different cellular proteins in a cell type dependent manner. The EV uptake mechanisms in individual cell types and organ systems require to be further determined, and modulation of the identified EV uptake mechanisms can serve as an additional approach to study cell-cell communication.

3. Ovarian antral follicle

Ovarian antral follicle

The most critical functions of the ovary are generation of a fertilizable and healthy oocyte and its role as an endocrine organ. Ovarian follicles are functional units within the ovary, they are composed of three major cell types: the endocrine granulosa and theca cells, and the germ line, oocytes. Granulosa cells, located inside the basal lamina of the follicle, are a major cell population within the ovary, while the less predominant theca cells reside just outside the basal lamina. Orchestrated cross talk between these distinct cell types in addition to crucial gonadotropins from the pituitary, follicle-stimulating hormone (FSH) and luteinizing hormone (LH), ensures healthy folliculogenesis in which follicles grow from tiny primodial follicle (<0.1 mm) into a large periovulatory follicles (>15 mm) in women (Baerwald, Adams et al. 2012). The structure of a follicle changes with growing follicle size, and a significant difference is the presence and expansion of the fluid-filled space, the antrum, within the follicle. This space effectively separates the oocyte from the highly metabolic mural granulosa cells. This specific feature gives rise to the name antral follicle. The size of antral follicles is dependent upon the proliferation of granulosa cells and the accumulation of follicular fluid (Rodgers and Irving-Rodgers 2010).

Follicular fluid

The antral space within the growing follicle contains follicular fluid, this fluid like most bodily fluids is thought to originate from osmotic differences and movement of fluids out of the vascular system into the tissues (Rodgers and Irving-Rodgers 2010). Thecal layers outside the basal lamina contain a vast capillary network that serves the growing follicle's need for nutrients and removal of metabolic waste. However, providing a route and a force to make the fluid flow into the antrum is another issue. The basal lamina and granulosa cells that separate the vasculature in the theca cell layer, and the antrum are tightly connected with each other, therefore channels or pumps are likely to play roles in this fluid transportation. It has been found that aquaporins are responsible for pulling water into the follicular antrum and the isoforms of aquaporins required for this process are species dependent (McConnell, Yunus et al. 2002, Skowronski, Kwon et al. 2009). One of the forces directing fluid flow is osmolality. It has been shown that the tight basal lamina and granulosa cells prevent large molecules from moving in and out of follicles. Therefore, the concentration of molecules in the follicular fluid may be able to control the osmolality between capillaries and follicular fluid, and then further control the fluid flow into the follicular antrum. The volume of follicular fluid progressively increases in the growing follicle reaching it maximal

volume in the periovulatory follicle, immediately before ovulation (Rodgers and Irving-Rodgers 2010). It has been reported that increased concentrations of hyaluronan and versican are able to create osmolality differences, and the expression of both are controlled by LH (Clarke, Hope et al. 2006).

Other than supporting the structure of the follicle, the follicular fluid also provides an environment for exchanging information between different ovarian cell types. Therefore, the components in the follicular fluid are dynamic and physiologically relevant. Proteomic studies using mass spectrometry (MS) is a powerful tool to reveal the composition of follicular fluid (Angelucci, Ciavardelli et al. 2006, Schweigert, Gericke et al. 2006, Hanrieder, Nyakas et al. 2008). One of the study using three protein fractionation methods to deplete abundant serum-like proteins, 480 proteins were identified by MS analysis in human follicular fluid (Ambekar, Nirujogi et al. 2013). These proteins involve in metabolism, extracellular matrix (ECM) remodeling, and immune responses (Ambekar, Nirujogi et al. 2013). Studies focusing on individual proteins such as cytokines and growth factors in follicular fluid have also been described. Improved oocyte quality has been linked with increased levels of granulocyte-colony stimulating factor (Ledee, Munaut et al. 2010, Ledee, Petitbarat et al. 2011, Ledee, Gridelet et al. 2013); interleukin (IL)-12, IL-6, IL-8, and IL-18 (Bedaiwy, Shahin et al.

2007, Sarapik, Velthut et al. 2012); brain derived neurotropic factor (Wu, Hu et al. 2012); and bone morphogenic protein 2 (Sugiyama, Fuzitou et al. 2010), as well as decreased levels of IL-1 and IL-12 (Mendoza, Ruiz-Requena et al. 2002) and vascular endothelial growth factor isoform 165 (Savchev, Moragianni et al. 2010). Other than proteins, the balance between reactive oxygen species (ROS) and antioxidants in follicular fluid is critical to the production of a competent oocyte (Hennet and Combelles 2012). Blocking or suppressing ROS with antioxidants reversibly inhibited the resumption of meiosis in rat oocytes *in vitro* (Takami, Preston et al. 1999). Excessive levels of ROS have been shown to cause aberrations to the microtubule organization and chromosomal alignment of metaphase II meiotic spindles in mouse oocytes *in vitro* (Choi, Banerjee et al. 2007), and to inhibit oocyte maturation in the mouse (Tamura, Takasaki et al. 2008). There are also hormones found in follicular fluid include FSH, LH, growth hormone (GH), human chorionic gonadotropin (hCG), progesterone, and estradiol (Hennet and Combelles 2012). High follicular fluid concentrations of FSH, hCG, and LH seem to promote oocyte maturation and are correlated with a high probability of fertilization (Hennet and Combelles 2012). High estradiol levels, especially in relation to androgen levels are also associated with high-quality oocytes and healthy follicles (Revelli, Delle Piane et al. 2009). Metabolites including amino acids, lipids, nucleotides, and other

small molecules also present in follicular fluid (Hennet and Combelles 2012). Linoleic acid, oleic acid, stearic acid, and palmitic acid have been shown abundant in the bovine FF (Bender, Walsh et al. 2010). Evidence suggests that competent human oocytes generally contain relatively low levels of saturated fatty acids such as palmitic acid and stearic acid (Haggarty, Wood et al. 2006). Moreover, saturated fatty acid levels in the FF of a high-fertility bovine model (heifers) are lower than those of a low-fertility model (cows) (Bender, Walsh et al. 2010). Experimental exposure of cumulus-oocyte-complex to linoleic acid inhibited cumulus cell expansion and decreased the number of oocytes reaching metaphase-II (Marei, Wathes et al. 2010).

Granulosa cell proliferation

One of the factors inducing the growth of antral follicle size is the increasing number of granulosa cells. This process is the result of decreased apoptosis and increased cell proliferation which are regulated by various signaling molecules. Small antral follicles undergo high levels of cell proliferation until they reach the ovulatory stage. Due to the importance of granulosa cell proliferation, a lot of work has been dedicated to understanding the various factors that can impinge upon this cellular aspect. Below I describe several of the major pathways and factors that are implicated in granulosa cell

growth and proliferation.

Estradiol

In addition to being involved in the feedback loop of the hypothalamo-pituitary - ovarian axis, granulosa cell produced estradiol can serve as autocrine and paracrine factors within the ovary. Their receptors, ERα and ERβ are also expressed in granulosa cells in a species dependent manner (Rosenfeld, Wagner et al. 2001, Berisha, Pfaffl et al. 2002, LaVoie, DeSimone et al. 2002, Juengel, Heath et al. 2006). Deletion of either receptor results in complete or partial loss of fertility (Dupont, Krust et al. 2000). Estradiol signaling has been reported to inhibit the expression of *p53* and *Bcl2 homologous antagonist/killer (Bax)* in granulosa cells, which are both proapoptotic genes (Britt, Drummond et al. 2000, Toda, Takeda et al. 2001).

Insulin-like growth factor (IGF)

IGF and its receptor, type-I IGF receptor (IGF-IR) are both expressed in granulosa cells (Zhou, Chin et al. 1991, Yuan, Lucy et al. 1996, Adashi, Resnick et al. 1997, Wandji, Wood et al. 1998, Armstrong, Gutierrez et al. 2000, Liu, Koenigsfeld et al. 2000, Hastie and Haresign 2006). Mice of IGF-1 knockout are infertile, and no large antral

follicles are observed indicating the importance of IGF signaling to antral follicle growth (Baker, Hardy et al. 1996, Zhou, Kumar et al. 1997). One of the explanations is that IGF regulates the expression of FSH and LH receptors and the secretion of estradiol by granulosa cells (Adashi, Resnick et al. 1985, Hsu and Hammond 1987, Maruo, Hayashi et al. 1988, Monniaux and Pisselet 1992, Zhou, Kumar et al. 1997, Khalid, Haresign et al. 2000, Glister, Tannetta et al. 2001).

Phosphophatidylinositol 3-kinase (PI3K)-AKT signaling

PI3K-AKT signaling is at the center of the anti-apoptosis signaling in granulosa cells. The activation of this pathway results in phosphorylation of the forkhead box O (FOXO) subfamily of forkhead transcription factors (Brunet, Bonni et al. 1999, Dijkers, Birkenkamp et al. 2002, Stahl, Dijkers et al. 2002, Accili and Arden 2004). Phosphorylation of FOXO then prevents its translocation into the nucleus, and therefore the failure of translocation in turn then prevents expression of the cell death related genes, Fas ligand (FASLG) and BCL211 (Matsuda, Inoue et al. 2011).

Transforming growth factor β (TGFβ) superfamily

This is a large protein family including inhibin, activin, follistatin, TGF, bone

morphogenetic protein (BMP), growth differentiation factor (GDF), and anti-mullerian hormone (AMH). Activin has been shown to be expressed in the granulosa cells, and able to induce granulosa cell proliferation in the antral follicles of rat (Li, Phillips et al. 1995, Miro and Hillier 1996). Expression of AMH decreases with the increase of follicle size, and is also associated with the increase of aromatase expression indicating a role of AMH on follicle growth through the regulation of estradiol production (Andersen, Schmidt et al. 2010, Grondahl, Nielsen et al. 2011). BMPs and GDFs are widely expressed in the ovary in a cell type specific manner (Knight and Glister 2006). Oocyte-derived GDF9, BMP6, and BMP15 have been shown to be able to induce granulosa cell proliferation as paracrine agents at the antral stage. BMP2, BMP5, and BMP6 secreted from granulosa cells have described autocrine and paracrine roles of promoting granulosa cell proliferation in the antral follicle (Fatehi, van den Hurk et al. 2005).

Tumor necrosis factor alpha (TNFα)

Tumor necrosis factor alpha also plays a critical role in the antral follicle. Tumor necrosis factor alpha has been reported to be able to induce granulosa cell proliferation in the mouse through IGF signaling and the acute phase protein serum amyloid A3 (Son, Arai et al. 2004, Son, Roby et al. 2004). Tumor necrosis factor alpha is also known to

be able to activate nitric oxide synthase 2 (NOS2), in which its downstream product, NO can promote granulosa cell proliferation (Hattori, Sakamoto et al. 1996). Paradoxically, TNFα has also been linked to apoptosis while TNFα knockout mice showed increased granulosa cell proliferation (Cui, Yang et al. 2011). Tumor necrosis factor alpha was also shown as downstream of nerve growth factor (NGF) and mediated apoptosis of granulosa cell in mice (Son, Roby et al. 2004). The receptors for TNFα, TNF receptor 1 and 2 (TNFR1 and TNFR2) may play a critical role on this dual function of TNFα signaling since TNFR1 has been linked to cytotoxicity and TNFR2 to proliferation (Tartaglia, Weber et al. 1991).

4. Extracellular vesicles in ovarian antral follicles

Since EVs appear to be produced by all normal cells, it is not surprising that the ovarian cells also secrete EVs. These EVs would be predicted to be enriched in follicular fluid, particularly those from granulosa cells and cumulus cells due to immediate proximity to the fluid and the enclosed environment of ovarian follicle. In 2012, the first published observation of EVs in follicular fluid was made by da Silveira et al. (da Silveira, Veeramachaneni et al. 2012). These authors collected EVs from equine

follicular fluid of follicles (>35 mm) 32 h after hCG injection from mares of two different ages, young (3-13 years) and old (>20 years). EVs were collected by ultracentrifugation. Two-dimensional mass spectrometry was applied to the EVs taken from young mares and revealed proteins that had not previously been identified in/on EVs of different cellular origin. The EV-contained miRNA were compared between young and old mares using Human miRNome Profiler plates, and the differences were linked to WNT, MAPK, focal adhesion, and TGFβ pathways. *In vivo* uptake of EVs was also observed following injection of fluorescence labeled EVs back into antral follicles.

This study was followed by several other studies by other laboratories, which focused on the cargos of follicular EVs, particular miRNA. Sohel *et al*. collected bovine follicular fluid and classified them by the representative oocyte, as either mature or growing oocyte, using Brilliant Cresyl Blue (BCB) staining (Sohel, Hoelker et al. 2013). In this study, EVs were isolated from follicular fluid using Exoquick, an exosome precipitation kit. MicroRNA were profiled by ready-to-use PCR Human Panels (I+II), and the differential miRNA were linked to ubiquitin-mediated, neutrophin, MAPK, and insulin signaling.

Sang *et al.* collected follicular fluid from women undergoing *in vitro* fertilization

(IVF) who had polycystic ovary syndrome (PCOS) and were undergoing intracytoplasmic sperm injection treatment (ICSI) (Sang, Yao et al. 2013). Follicular fluid from follicles 18-20 mm in size were collected 34-36 h after hCG injection. In their study, it is worthwhile pointing out that microvesicles can be a significant part of their EV samples because of the ultracentrifugation protocol they used. The differential presented miRNA in follicular EVs between control and PCOS patients were determined by TaqMan Array Human MicroRNA A and B Cards Set version 3.0, and the miRNA were predicted to affect genes which have been shown important generally in ovary or particularly in PCOS including estrogen receptor (ESR1), pTEN, ILs, TGFβ1, HMGA, and RAB5B. MicroRNA-132 and -320 were present at a low level in the follicular fluid of PCOS patients, which might indicate a potential use as biomarkers clinically.

Santonocito *et al*. used the same protocol as Sang *et al*. to isolate follicular fluid from healthy women who were undergoing ISCI due to male factors, and their plasma samples were used as the control (Santonocito, Vento et al. 2014). EVs were isolated by ultracentrifugation, and the profile of miRNA was completed on TaqMan Human MicroRNA Array A cards. MicroRNA which were detected differentially between plasma and EVs linked to TGFβ, MAPK, ErbB, and WNT signaling.

Diez-Fraile *et al.* conducted a similar study comparing follicular EV-associated

microRNA between young (<31 years) and old (>38 years) women (Diez-Fraile, Lammens et al. 2014). The authors found four microRNA, which were specific to only one of the two groups including miR-21-5p in young women and miR-99b-3p, miR-134, miR-190b in old women. Targets of these microRNA were predicted to relate to heparan-sulfate biosynthesis, extracellular matrix–receptor interaction, carbohydrate digestion and absorption, p53 signaling, and cytokine–cytokine-receptor interaction.

The studies described above show that EVs are highly abundant in follicular fluid of different species (mare, cow, and women), and that the EVs contain microRNA that are physiological relevant. However, none of these studies demonstrated a functional effect of EVs within the ovary, the first study to do so was carried out by da Silveira *et al*. (da Silveira, Carnevale et al. 2014). In their study, they detected genes in the TGFβ/BMP pathway expressed in the mare granulosa cells of mid-estrus and pre-ovulatory follicles. They also found that the follicular EVs from the same staged follicles contained miRNAs (i.e., miR-27b, miR-372, and miR-382) that can target these TGFβ/ BMP pathway related genes. To demonstrate activity of follicular EVs, mare granulosa cells were treated with follicular EVs. They found that the EVs from both mid-estrus and pre-ovulatory follicles could decrease granulosa cell expression of inhibitor of DNA binding/differentiation 2 (ID2), which is a target of miR-27b, miR-372, and miR-382.

This result indicated for the first time that follicular EVs could elicit functional effect. But since the follicular EVs from both mid-estrus and pre-ovulatory follicles suppressed the expression of ID2 similarly, the physiological roles of follicular EVs are still not clear and needed to be further explored.

5. Significance

The increasing role of EVs as a cell-cell communication mediator has been proven in multiple organs and different types of cells. In cancer cells, EVs have been known to promote cancer cells metastasis (Tkach and Thery 2016). Tumor cells secreted EVs have the ability to facilitate remodeling of the extracellular matrix (ECM) (Clancy, Sedgwick et al. 2015, Hoshino, Costa-Silva et al. 2015, Sung, Ketova et al. 2015, Yue, Mu et al. 2015). Moreover, tumor cell secreted EVs can travel to pre-metastatic sites and set up the microenvironment favorable for tumor cells before metastasis (Peinado, Aleckovic et al. 2012, Zhou, Fong et al. 2014, Costa-Silva, Aiello et al. 2015, Hoshino, Costa-Silva et al. 2015). EVs also have been reported as critical players in the neurogenic niche (Batiz, Castro et al. 2015). In *Drosophila*, exosomes have been described as cell-cell communication mediators between pre- and post-synaptic cells (Korkut, Li et al. 2013). Cross-talk between different neuronal cell types by EVs also

has been shown (Fitzner, Schnaars et al. 2011, Fruhbeis, Frohlich et al. 2013, Fruhbeis, Frohlich et al. 2013, Bahrini, Song et al. 2015), and the function of EVs is specific to cellular environment such as nutrition deprivation (Fruhbeis, Frohlich et al. 2013). The existence of EVs in the ovarian follicles has been reported by several groups as discussed above, and the potential functions of these EVs have been predicted based on the EV-contained miRNA. However, demonstration of a physiological function for the follicular EVs has not been well explored. In this dissertation, follicular EVs from different sized follicles were first characterized, and their effects on ovarian granulosa cells and cumulus-enclosed oocytes were tested. These studies provide another layer of information on the cellular mechanisms responsible for appropriate follicle growth, and demonstrate for the first time specific functions of these membrane-enclosed vesicles, EVs, in the ovarian follicle.

VIII. Chapter II: Characterization and Small RNA Content of Extracellular Vesicles in Follicular Fluid of Developing Bovine Antral Follicles.

Introduction

Cell-to-cell communication between somatic cells (theca, granulosa, and cumulus) and germ cells (oocytes) are critical for the process of folliculogenesis (Eppig 2001, Matzuk, Burns et al. 2002). During folliculogenesis, the coordinated communication and signaling between the different follicular cell types is crucial for growth, maturation, and release of an oocyte that can be fertilized and undergo embryonic development. The endocrine hormones, follicle stimulating hormone (FSH) and luteinizing hormone (LH), play key regulatory roles in all aspects of this developmental progression from a preantral to a periovulatory follicle. Additionally, growth factors within the periovulatory follicle are essential for transmission of these endocrine signals to the deeper residing cumulus cells and oocyte within the follicle (Espey and Richards 2002, Park, Su et al. 2004, Conti, Hsieh et al. 2006, Carletti, Fiedler et al. 2010). Likewise the oocyte secretes factors (i.e., GDF-9, BMP15) that are able to influence the nearby mural granulosa cells (Galloway, Gregan et al. 2002, Mazerbourg and Hsueh 2003). The antrum that separates these distinct cells is filled with a complex fluid derived from both blood plasma that arises from increased permeability of the thecal capillaries and release of secretory factors from both types of granulosa cells and oocytes (Espey 1980, Cavender and Murdoch 1988). Hormones (e.g., FSH, LH, GH, inhibin, activin,

estrogens, and androgens), growth factors, proteins, lipoproteins, peptides, amino acids, and nucleotides have been found to be enriched in follicular fluid and provide an important microenvironment for follicle growth and oocyte maturation (Fortune 1994, Revelli, Delle Piane et al. 2009). However, with the exception of several growth factors and steroids, much of the material observed in follicular fluid has not been well characterized and very little is known about the functional role of these molecules.

Recent studies have demonstrated that membrane-enclosed vesicles called microvesicles which are heterogeneous in size (100–1000 nm) contain bioactive molecules such as proteins, messenger RNA (mRNA) and microRNA (miRNA) (Camussi, Deregibus et al. 2010, Muralidharan-Chari, Clancy et al. 2010) which are released from cells by outward budding and fission of the plasma membrane (Cocucci, Racchetti et al. 2009). Similar to microvesicles, exosomes also have a lipid bilayer but are more homogeneous and smaller in size (30–100 nm). Exosomes are derived from intraluminal invagination of the multivesicular bodies (MVBs), followed by fusion of the MVB with the plasma membrane and release of its exosomal cargo into the extracellular space (Valadi, Ekstrom et al. 2007, Lakkaraju and Rodriguez-Boulan 2008, Simpson, Lim et al. 2009, Vlassov, Magdaleno et al. 2012). It should be noted that following cellular release the distinction of exosomes from microvesicles cannot be determined; they will

be referred to extracellular vesicles (EVs) from here on. Recent evidence suggests that EVs can play important roles in cell-to-cell communication by transferring proteins, RNA, and miRNA molecules to target cells (Valadi, Ekstrom et al. 2007, Muralidharan-Chari, Clancy et al. 2010). Several studies have now confirmed the existence of EVs in follicular fluid of mares and women at different ages (da Silveira, Veeramachaneni et al. 2012, da Silveira, Carnevale et al. 2014, Diez-Fraile, Lammens et al. 2014, Santonocito, Vento et al. 2014), in women with polycystic ovarian syndrome (Sang, Yao et al. 2013, Roth, McCallie et al. 2014), and in cow follicles at a single stage of development (Sohel, Hoelker et al. 2013). Our recent work has documented that EVs from small and large cow follicles can differentially support cumulus expansion and changes in cumulus-oocyte-complex (COC) gene expression (Hung, Christenson et al. 2015). However, to date no studies have evaluated whether the numbers of vesicles and contents of these vesicles change during ovarian follicular development. The cow was chosen for these studies for several reasons: the cow is a monoovulatory species with a similar temporal follicular growth and regression dynamics to that of the human (endocrine profiles do however differ between these species), the cow follicle provides sufficient levels of readily available fluid from early (small, 3-5 mm) antral follicles, samples that cannot be feasibly collected in humans or rodents for comparison to later-staged (medium, 6-9 mm

and large >9mm) antral follicles and understanding ovarian physiology in the cow has intrinsic value to the livestock industry.

Materials and methods

Follicular fluid collection

Bovine ovaries were from a local abattoir: because the animals were not used specifically for research purposes our Institutional Animal Care and Use Committee ruled that the collection of ovaries from the abattoir does not constitute animal research and is exempt from further review. Ovaries (~150 ovaries / collection) were placed immediately into PBS and then transported 2.5 h to the University of Kansas Medical Center at 20-24 C temperature in preparation for ovarian follicular fluid aspiration. Follicular diameters were determined by individually measuring follicle diameters; follicles were designated into three different groups based on diameter (3-5 mm - small, 6-9 mm – medium and > 9 mm – large). Follicular fluid was aspirated using a tuberculin syringe (28 gauge needle) for small follicles and a 5 ml syringe with a 20-gauge needle for medium and large follicles. The volume aspirated was used to confirm classification status (small < 50 µl, medium ~100 µl to 350 µl and large > 400 µl). Three independent collections of follicular fluid were conducted over a two-month period for the RNAseq analysis. Each collection provided the approximate volumes of follicular fluid: 20 ml from small, 15 ml

from medium and 40 ml from large follicles. To determine relative follicle quality within the small, medium and large pools, 18-20 single follicles at each size were dissected free from the ovaries of a fourth collection of ovaries. The granulosa cells were then isolated by bisecting each follicle and scraping the cells into PBS. Cells were then fixed in 4% PFA, and stained with the DNA dye, Hoechst 33342 (Life Technologies, NY). The nuclei of a hundred granulosa cells from each follicle were then classified as healthy (i.e., intact nucleus) or as apoptotic/atretic (i.e., fragmentized nucleus). Additionally, RIA conducted at the University of Virginia Center for Research in Reproduction Ligand Assay and Analysis Core determined estradiol and progesterone levels for each of the pools. Each follicular fluid sample was diluted 1:15 fold in PBS for estradiol and 1:20 for progesterone prior to RIA. The sensitivity of estradiol assay is 10pg/ml with intra-assay CV of 6.3% and inter-assay CV of 8.1%. The sensitivity of progesterone assay is 0.15ng/ml with intra-assay CV of 5.7% and inter-assay CV of 7.1%.

Isolation of extracellular vesicles

Extracellular vesicles were isolated using a differential ultracentrifugation method developed for serum isolation of exosomes (Thery, Amigorena et al. 2006). Follicular fluid (15 ml) was diluted 1:1 with PBS and then spun at 800g and 2000g for 10 and 20

min each in an Optima^{TM} L-100XP to pellet all granulosa cells and the oocytes (the cell pellets were snap frozen at -80C or placed in Trizol). The follicular fluid was then centrifuged at 12000g for 45 min to remove cellular debris and other large particles (large microvesicles and apoptotic blebs). Samples were then filtered through a 0.22 μm pore filter to further remove vesicles bigger than 220 nm. Ultracentrifugation of the 1:1 mix follicular fluid:PBS was performed at 110000g for 3h in an Optima^{TM} L-100XP ultracentrifuge, using a swinging bucket SW32Ti rotor. The resulting EV pellets were then resuspended in 4 ml PBS and spun again for 1 h at 110000 g in a TLA 100.4 fixed angle rotor. A final wash with 1 ml of PBS was then performed and spun at 110000 g for 1 h using a TLA 55 fixed angle rotor. All centrifugations were performed at 4°C. The obtained pellets were re-suspended in PBS for further analysis.

Separation of extracellular vesicles on sucrose gradient

Extracellular vesicles isolated from follicular fluid using differential centrifugation were re-suspended in 100 μl of PBS and overlaid on the top of a continuous sucrose gradient (0.2 to 2.5 M sucrose in 20 mM HEPES, pH 7.4) which was made using a Hoefer SG30 gradient marker (GE Healthcare, Piscataway, NJ). The gradient tubes were centrifuged at 210,000g for 16 h at 4 °C in an SW41Ti swinging bucket rotor with an Optima-Max ultracentrifuge (Beckman Coulter). Eleven 1 ml fractions were collected from the top to

bottom of the gradient and the refractive index of each collected fraction was measured using a VEE GEE refractometer (VEE GEE Scientific, Washington, USA). The sucrose density was converted from refractive index to density (g/cm3). Each fraction was washed in 3 ml of PBS by ultracentrifugation at 110,000g for 1.5 h at 4 C using a TLA-100 rotor in an Optima-Max ultracentrifuge and the pellets were re-suspended in PBS and loaded onto 12% SDS-PAGE for Western blot analysis.

Western blot Analysis

EV samples (10 μg protein) were lysed in SDS sample buffer with 50 mM DTT, heated for 5 min at 95 °C and subjected to electrophoresis using 12% SDS-PAGE in running buffer at constant 120 V for 1.5 hrs. Proteins were then electrotransferred onto polyvinylidenedifluoride membranes, and the membranes were blocked with 5 % (w/v) skim milk powder in Tris-buffered saline with 0.05 % (v/v) Tween-20 (TTBS) for 1h at RT. Membranes were then probed with primary anti-CD81 (sc-166029), anti-Alix (sc49267), anti-GP96 (sc-11402) and anti-Actin (sc-1616) antibodies for 1 h in TTBS (50 mM Tris, 150 mM NaCl, 0.05 % Tween20) followed by incubation with the secondary anti-mouse IgG or anti-sheep goat antibodies for 1 h. All primary antibodies were purchased from Santa Cruz Biotechnology Inc. Membranes were washed three times in TTBS for 10 min after each incubation step and detected by enhanced

chemiluminescence (ECL) (GE Healthcare Bio-science, PA) per manufacturer's instructions.

Nanoparticle tracking analysis

To determine particle size and concentration, nanoparticle-tracking analysis (NTA) was performed with a Nanosight LM10 instrument (Nanosight, Salisbury, UK) outfitted with a LM14C laser. Each EV preparation was sampled three times to generate 3 independent dilutions. These dilutions range from ~1:1000 to 1:10,000 for each sample (the dilution is determined empirically for each sample) and then each of the three dilutions is analyzed 5 times (5 – 60 video tracks/dilution). The overall average of these three dilutions was used as the experimental result for each sample. If large discrepancies in counts were observed for a set of dilutions or if the range of particle concentrations were outside the optimum range, another dilution was then created from the stock and analyzed. From validation studies using dilution series, we determined that NTA is most accurate between particle concentrations in the range of 2×10^8 /ml to 2×10^9 /ml. Thus samples were diluted to this level and absolute concentrations were then back calculated according to the dilution factor.

Transmission electron microscopy

An aliquot of the EV sample was pelleted and the PBS was replaced with 2%

gluteraldehyde fixative in 0.1 M cacodylate buffer. Following overnight fixation, the fixative was carefully removed and replaced with 0.1M sodium cacodylate buffer 2 times for 5 min each. The pellet was then post-fixed in a solution of 1% osmium tetroxide plus with 1% potassium ferric cyanide buffered in 0.1 M cacodylate buffer for 1 h. Osmicated pellets were dehydrated through a series of graded ethanols, rinsed in propylene oxide 2 times for 10 minutes each and then embedded in fresh EMbed 812 resin and cured in a 60°C oven overnight. Sections were cut at 80 nm using a Leica UC-7 ultramicrotome, mounted on copper thin bar 300 mesh grids, and contrasted with 4 % uranyl acetate and Sato's lead stain. All samples are examined in a JEOL-JEM-1400 transmission electron microscope at an 80 kV with 25,000x magnification.

RNA preparation

Total RNA was isolated from EVs (20 µl) with Trizol (Invitrogen) according to the manufacturer's protocol. Briefly, EVs were disrupted and homogenized in 200 µl of Trizol reagent and incubated for 5 min at room temperature. Samples were then spun in a microcentrifuge at 12000 g for 15 min at 4 °C following addition of 40 µl of chloroform. Subsequently, the aqueous solution was mixed with 100 µl of isopropanol. In order to extract small RNA, 1 µl glycogen (20 µg/µl) was added together with RNA-isopropanol mixture solution and incubated at -80 °C for 30 min and spun at 12000 g for 15 min at 4

°C. The pellet was washed with 100 µl of 70 % ethanol followed by centrifugation at 7500 g for 5 min at 4 °C. The RNA pellet was dried at room temperature and dissolved in 10 µl of RNase free water. The RNA solution was then stored at -80 °C. RNA quality, yield, and sizes were assessed with the Agilent 2100 Bioanalyzer (Agilent Technologies, Foster City, CA) using the Agilent Small RNA chip. To confirm the absence of 18S and 28S ribosomal RNA we also ran the RNA of the Agilent RNA 6000 Nano chips. Briefly, 1 µl of RNA was analyzed on either the Agilent RNA 6000 Nano or Small RNA chips according to manufacturer's protocol. Electropherograms were analyzed using the Agilent 2100 Expert B.02.07 software that includes data collection, presentation and interpretation functions. The EV RNA purity was also evaluated using Nanodrop spectrophotometer ND-1000 (Thermo Scientific, Wilmington, DE) at the absorbance 230, 260 and 280 nm. The average A260/230 and A260/280 ratios were used to assess the presence of peptides, phenols, aromatic compounds, or carbohydrates and proteins.

Next generation sequencing

Small RNA sequencing was performed using the Illumina HiSeq2500 Sequencing System at the University of Kansas Medical Center – Genomics Core (Kansas City, KS). Extracellular vesicle RNA (ranging from 1.8 ng – 100 ng) was used to initiate the TruSeq Small RNA library preparation protocol (Illumina #RS200-0012 kit A). The EV RNA

was ligated with 3' and 5' RNA adapters followed by a modified reverse transcription reaction and modified PCR amplification. Due to low starting RNA quantities, the reverse transcription of the RNA adapter ligated samples was modified by performing two duplicate reactions containing 6 µl of the 3'/5' RNA ligated RNA. The 12.5 µl yield of each duplicate reverse transcription reaction was then pooled to obtain 25 µl of homogeneous cDNA. The subsequent PCR amplification, with index adapter incorporation, was modified by replacing 8.5 µl of ultra-pure water in the PCR master mix with 8.5 µl of the reverse transcribed and pooled cDNA (21 µl cDNA total). The modified PCR reaction was performed with 15 cycles of amplification. Size selection and purification of the cDNA library construct was conducted using 3 % marker H gel cassettes on the Pippin Prep size fractionation system (Sage Science). The Agilent 2100 Bioanalyzer was used with the High Sensitivity DNA kit (Agilent #5067-4626) or the DNA1000 kit (Agilent #5067-1504) to validate the purified libraries. Libraries were quantified on the Illumina ECO Real Time PCR System using KAPA SYBR Universal Library Quant kit – Illumina (KAPA Biosystems KK4824). Following quantification, libraries were adjusted to a 2 nM concentration and pooled for multiplexed sequencing. Libraries are denatured and diluted to the appropriate pM concentration (based on qPCR results) followed by clonal clustering onto the sequencing flow cell using the TruSeq

Rapid Single Read (SR) Cluster Kit-HS (Illumina GD402-4001). The clonal clustering procedure was performed using the automated Illumina cBOT Cluster Station. The clustered flow cell was sequenced on the Illumina HiSeq 2500 Sequencing System in Rapid Read mode with a 1x50 cycle read and index read using the TruSeq Rapid SBS kit-HS (Illumina FC402-4002). Following collection, sequence data was converted from .bcl file format to FASTQ files and de-multiplexed into individual sequences for further downstream analysis.

Bioinformatics

The three groups of EVs (small, medium and large) were analyzed in biological triplicates giving nine samples in total. After 3' adapter removal, the read sequences were mapped using the bwa software (v 0.7.5a, (Li and Durbin 2009)) to the bovine genome (assembly UMD3.1) and annotated for overlapped regions with the Ensemble gene annotation file for bovine (release 70) and miRBase (release 21).

Mapped reads from all 9 samples were merged and loci with an average read count per base (sum of the number of reads mapped at each base of the locus divided by its length) less than 45 were filtered out. These loci were then scanned for high-density regions defined as a contiguous region whose read count at each base is not less than 20% of the highest base read count for the locus. These high-density regions formed the effective

region of the locus and its length defined as its effective length. The number of reads mapped to the effective region of each sample formed the effective read counts that were used for down-stream analysis. To further limit the number of loci identified to a more conservative "biologically relevant" number; loci with an average read count (over the three replicate samples) of 100 or greater in at least one of the three conditions (small, medium or large) were included for further analysis.

Known and novel miRNA's were identified from these loci through a systematic filtering process beginning with a length filter that filtered loci to those with an effective length between 18 and 30 bases. Effective regions that mapped to mature miRNA were first identified, while the remaining effective regions were compared to known miRNA from both bovine and other species found in miRBase (release 21). A region was labeled as a miRNA by homology if it passed the following criteria; a gapless alignment of the effective region to the mature reference miRNA with at most 2 mismatches in the core and at most 1 gap/mismatch at the 5 and 3 prime ends and less than 10% mismatches in the alignment of the reference hair-pin sequence to the locus. Novel miRNAs were identified based on the criteria that the extended effective region should have a predicted pre-miRNA like hairpin structure (Jiang, Wu et al. 2007) with the effective region falling in the stem region with at least 80% pairing. The hybridization free energy cutoff was

set at -15 kcal/mol. The raw sequence data available as GEO (GSE74879) has been uploaded to miRBase for annonation, a sortable Excel file format depicting all of the identified loci is available upon request.

Exact statistical methods developed for multi-group experiments available from the edgeR software package (Robinson and Smyth 2008) were used to determine significantly differently expressed miRNAs between the different conditions. The edgeR package employs advance empirical Bayes methods to estimate miRNA-specific biological variation under minimal levels of biological replication. The associated p-values were corrected for multiple-hypothesis testing by the Benjamini and Hochberg method (Benjamini, Drai et al. 2001).

MiRNA function prediction

Differentially expressed miRNAs ($p < 0.05$ and false discovery rate, $FDR < 0.1$) between two different sizes of follicle groups (large versus small, medium versus small and large versus medium) were used. Selected miRNAs were used to predict potential function through the use of QIAGEN's Ingenuity® Pathway Analysis (IPA®, QIAGEN Redwood City, www.qiagen.com/ingenuity).

Statistical Analysis

All of the quantitative experiments (concentration of particles, steroid hormones

concentrations, ratio of miRNA in total small RNA) were repeated with at least independent three biological replicates. These results were analyzed by one-way ANOVA and Newman-Kuels multiple comparison tests were performed to determine differences amongst the means. The GraphPad Prism version 5.00 for Windows, GraphPad Software, San Diego California USA was used for these analyses. A $p<0.05$ was considered statistically significant. The Chi-square test of homogeneity was used to determine if differences in proportions of miRNA significantly up and down regulated differed across the three comparisons of follicular fluid pools. The statistical analysis details for the next generation sequencing results are explained in detail in that section.

Results

Quantitation and morphological characterization of follicular fluid EV from growing antral follicles.

Bovine follicles subdivided by size (small, 3-5 mm; medium, 6-9 mm; and large >9 mm) representing early to late stages of antral follicle growth were pooled by size to ensure enough material for initial EV collection and evaluation. To provide an indication of the relative numbers of healthy follicles versus atretic follicles in each of the 9 pools (i.e., three independent pools at each size), granulosa cells were isolated from a

subset (n=18-20) of individual follicles from each follicle stage. Individual follicles had between 28 and 100% normal intact nuclear staining with the majority (~70%) of the follicles in each group containing less than 25% fragmented nuclei. Compared across the follicular sizes, each pool thus contains between 71% to 81% intact nuclei (Fig II-1). Analysis of estrogen and progesterone levels in the 9 independent follicular fluid pools indicated that progesterone levels did not vary across the follicle sizes whereas estradiol concentrations increased with size as expected (Fig II-2).

Total EV concentrations (x 10^{12} particles/ml of follicular fluid) were highest in the smallest diameter (3-5 mm) follicles and the number decreased progressively as follicle diameter increased (Figure II-3A). EV size distributions ranged from ~30 to 300 nm as determined by nanoparticle tracking analysis (NTA) and there was no change in size distribution from the three different sized follicles (Figure II-3B). Additionally, the mode and mean size of EVs was not significantly different in the three different follicle diameter groups (Table II-1).

Figure II- 1 Percentage of non-apoptotic (normal) and apoptotic (fragmented DNA) granulosa cells from different size follicles.

A hundred cells were counted for each follicle. n=follicle numbers analyzed.

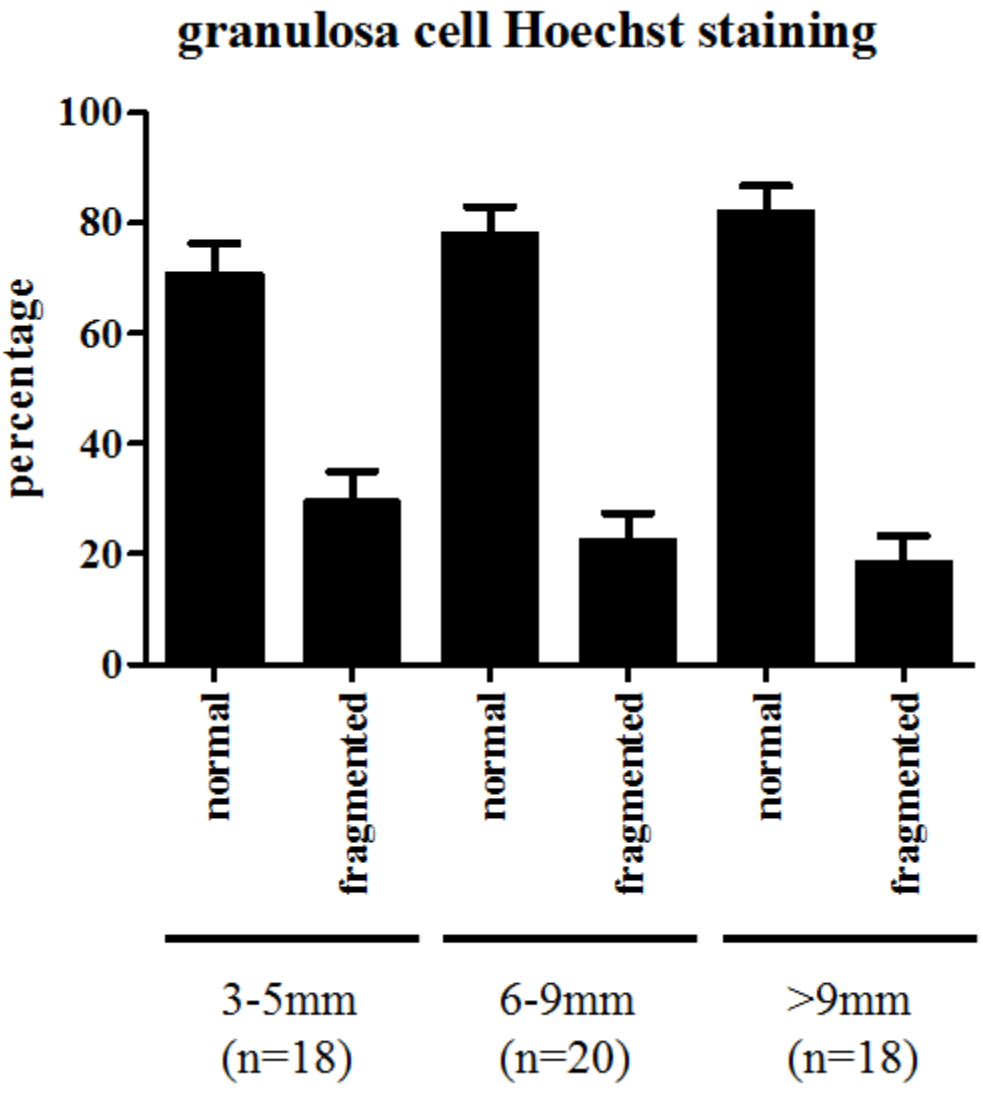
granulosa cell Hoechst staining
percentage
100
80
60
40
20
0
normal
fragmented
normal
fragmented
normal
fragmented
3-5mm
(n=18)
6-9mm
(n=20)
>9mm
(n=18)

Figure II- 2 Progesterone and estradiol concentrations in follicular fluid from different size follicles.

[a,b,c]Means ± SEM with different superscripts were statistically different ($P<0.05$).

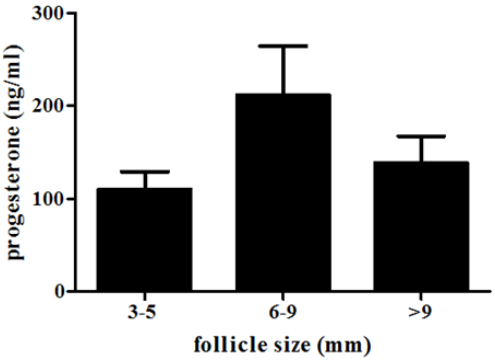
300
200
100
0
progesterone (ng/ml)
3-5
6-9
>9
follicle size (mm)

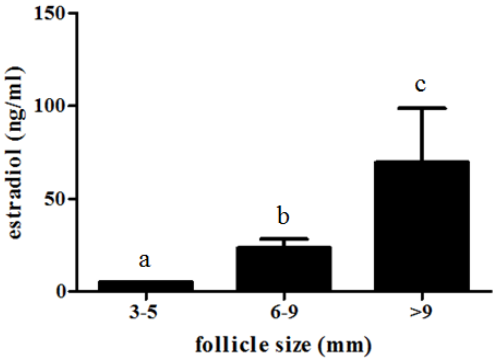
150
100
50
0
estradiol (ng/ml)
a
b
c
3-5
6-9
>9
follicle size (mm)

Figure II- 3 Particle concentrations and size distributions in EV preparations (n = 3) from small, medium and large follicles.

(A) Mean concentration of particles (x 1012 particles per ml of follicular fluid).

a,b,cMeans ± SEM with different superscripts were statistically different ($P < 0.0001$).

(B) Nanoparticle tracking analysis predicted concentration and size distribution of particles in three representative EV preparations from follicular fluid of small, medium and large follicles.

(A)

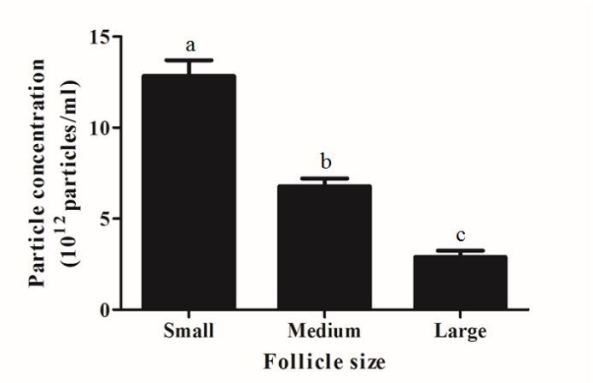
Particle concentration
(10^{12} particles/ml)
15
10
5
0
a
b
c
Small
Medium
Large
Follicle size

(B)

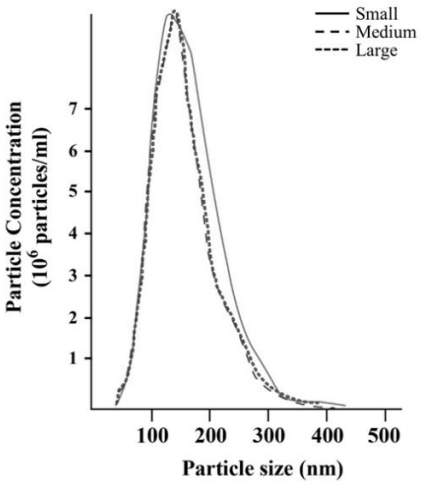
Small
Medium
Large
Particle Concentration
(10^6 particles/ml)
7
6
5
4
3
2
1
100
200
300
400
500
Particle size (nm)

Table II- 1The mode and mean size of EVs from different sized follicles were determined by NTA.

	follicle size (mm)		
	3-5	6-9	>9
Mode (nm)	109	113	106
Mean (nm)	124	134	127
Standard deviation (nm)	43	47	42

Several established exosome markers, tetraspanin CD81 and Alix were used to confirm the presence and enrichment of exosomes in the EV preparations (Figure II-4A). We found that the expression of CD81 was highly expressed in EVs as compared to granulosa cells that were isolated from the initial 800 g centrifugation run in the EV isolation protocol (FigureII-4A). Interestingly, the highest expression of CD81 was found in EVs (10 μg total loaded protein) derived from small follicles and decreased progressively in the EVs as follicle size increased (Figure II-4A). Alix another exosome marker was also abundant in the EV preparations compared to the cell lysates; however, it did not show the same decrease in levels as that detected for CD81 as follicle size increased. This later antibody/marker gene exhibited greater variation across samples and was considered less reliable. The endoplasmic reticulum marker GP96 was detected in cell lysates and was not detectable in the EV preparations indicating the absence of other cellular membrane contamination in the EV preparations. Actin was found in both EVs and cells (Figure II-4A). Western blot analysis of CD81 in sucrose gradient fractions of small, medium and large follicle EV preparations indicated that EVs were found in fractions 5-9 of small and medium follicles at densities (1.14 to 1.25 g/cm^3) that are consistent with extracellular vesicles (i.e, exosomes; Figure II-4B). The tetraspanin CD81 was not readily detectable in the large follicle EV preparations

following sucrose gradient analysis; this is likely due the decreased level of CD81 in the starting EV ultracentrifuge pellet "input" which is shown for each preparation (Figure II-4B). Transmission electron microscopy (TEM) revealed that the EV pellets contained a homogeneous population of circular bilayer enclosed vesicles with minimal evidence of protein contamination (very dark staining material that is not enclosed within a lipid bilayer: Figure II-4C). We observed no vesicles >130 nm in diameter by TEM; however because these are cross-sectional views exact sizes are not determinable using this approach.

Figure II- 4 Quantitative and qualitative analysis of the EVs from small, medium and large follicles.

(**A**) Western blot analysis of extracellular vesicle (CD81 and Alix), endoplasmic reticulum (GP96) and cellular (actin) markers in EV and cellular lysates. Equal amounts of total protein (10μg) were loaded into each lane. (**B**) Representative CD81 protein in sucrose gradient fractions of small, medium and large follicles. Each fraction density was determined by refractometry and an equal volume of the resulting resuspended pellets was loaded for western blot analysis (n = 3). Input represents an aliquot of the EV sample that was applied to the sucrose gradient. (**C**) Representative transmission electron microscopy image of a thin section through an EV pellet isolated from a small follicle– several vesicles diameters (nm) are labeled.

(A)

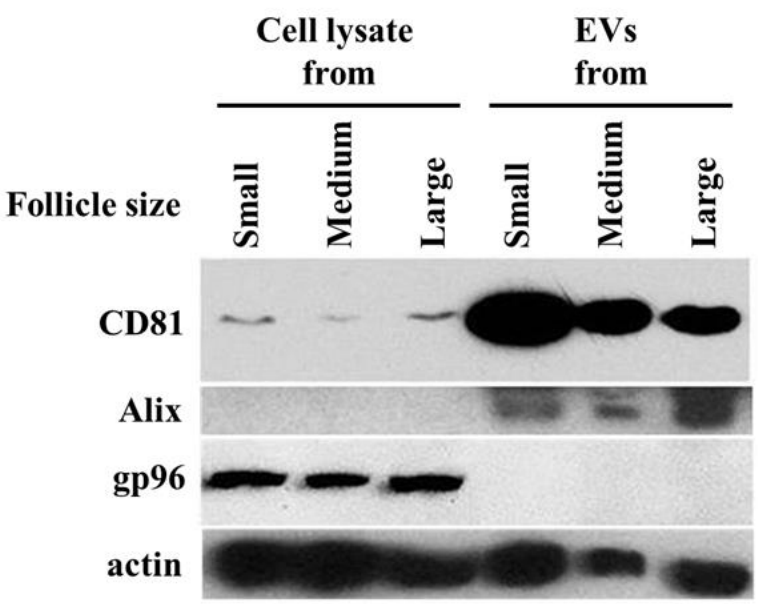
Cell lysate from
EVs from
Follicle size
Small
Medium
Large
Small
Medium
Large
CD81
Alix
gp96
actin

(B)

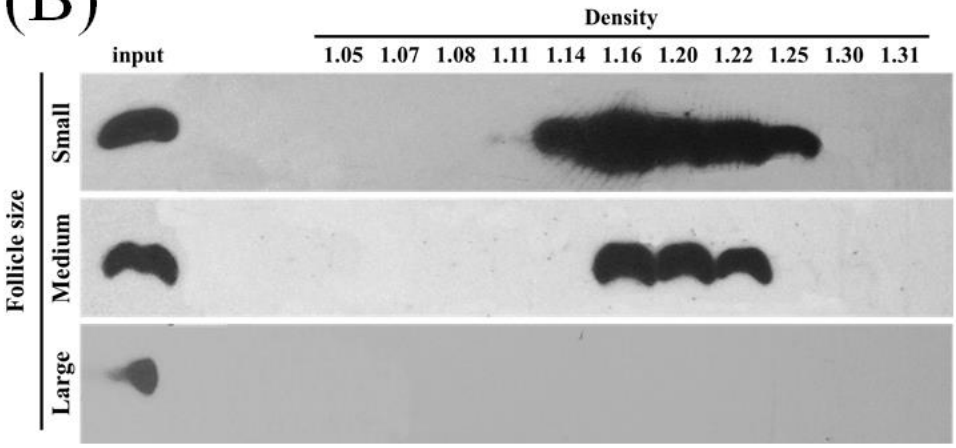
Density
input
1.05 1.07 1.08 1.11 1.14 1.16 1.20 1.22 1.25 1.30 1.31
Follicle size
Small
Medium
Large

(C)

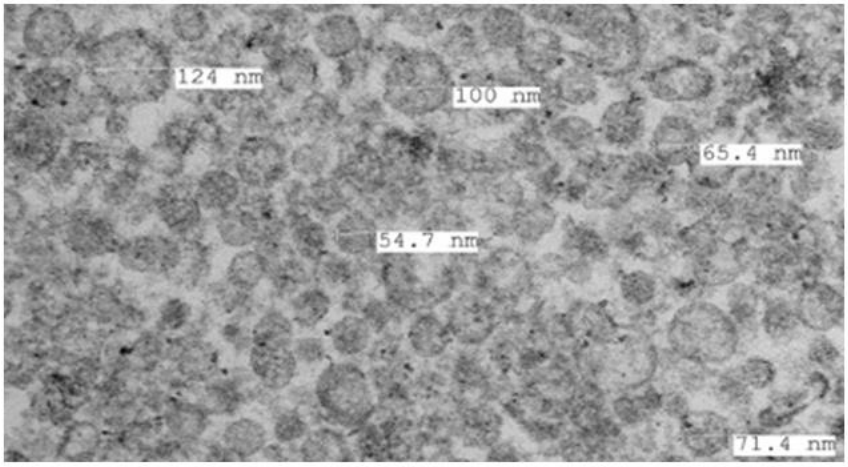
124 nm
100 nm
65.4 nm
54.7 nm
71.4 nm

Small RNAs within follicular fluid EVs

A representative electropherogram for small, medium and large follicles shows the size distribution of small RNAs derived from the EV RNA isolation in the interval of 6-150 nucleotides (Fig II-5A). Note that the majority of the small RNA ranged in size between 20 and 40 nucleotides in length consistent with microRNA (miRNA). Moreover, no detectable amounts of the highly abundant 18S and 28S ribosomal RNA (rRNA) were detected in the EV preparations indicating an absence of cellular contamination (data not shown). The percentage of EV RNA that was consistent with the size of miRNA (i.e., 18-24 nucleotides) differed across the follicle size groups with the greatest presence (84%) in the 3-5 mm, slightly lower (75%) amounts in 6-9 mm and the least 58 % in the > 9 mm diameter follicles ($p<0.0001$; Suppl Fig II-5B). The A260/280 and A260/230 values ranged from 1.56 -1.74 and 0.13 – 0.62, respectively.

Figure II- 5 RNA quality and miRNA percentage using the Agilent Small RNA analysis protocol.

A) Isolated RNA from different sized follicles were analyzed using the Agilent Small RNA chip. Distribution of different size of RNA was presented as intensity. The peak at 4 nucleotide represents the spiked in loading control. B) Small RNA with the length from 18-24 nt were considered as potential miRNA (Agilent protocol) and the percentage of miRNA in EVs from different sized follicles were plotted ($n=3$, $p<0.0001$).

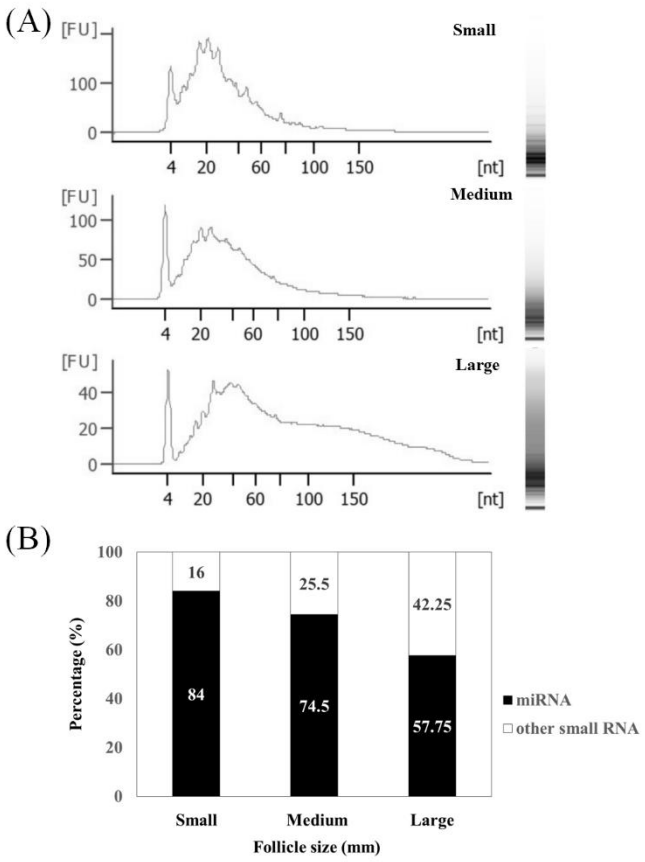
(A)
[FU]
Small
100
0
4 20 60 100 150
[nt]
[FU]
Medium
100
50
0
4 20 60 100 150
[nt]
[FU]
Large
40
20
0
4 20 60 100 150
[nt]
(B)
Percentage (%)
100
80
60
40
20
0
16
84
25.5
74.5
42.25
57.75
Small
Medium
Large
Follicle size (mm)
miRNA
other small RNA

Three independent small RNA libraries for each of the small, medium and large follicles were generated from the follicular fluid EVs. The total number of reads (Mean ± SEM) was 15,144,579 ± 900,792 reads/sample and this ranged from 12,480,394 to 21,361,359 reads/sample. Of the total reads for the nine independent pools (3 independent pools / size; n=9) 98.333% ± 0.001% mapped to the bovine genome. Mapping yielded a total of 11,770 different identified loci across all samples with the majority of these loci (8360) being located in unannotated regions (Figure II-6). Breakdown of loci falling within an annotated region (3410) indicated that 74.8% of these loci were detected within intronic regions of genes (2552) with the balance being in protein coding (238) and non-protein coding regions (620), which included miRNA (269), snoRNA (67), rRNA (128) and others (Figure II-6 shows complete breakdown of RNA subtypes). The number of read counts associated with each of these annotation types varied widely (Table II-2).. While only 269 bovine miRNA annotated loci were identified as present in EV RNA, the mean read count was 4384 counts/loci indicating that known miRNAs make up a large portion (12.2%) of the total number of reads (Table II-2).

Figure II- 6 Composite annotation and breakdown of small RNA generated from all small, medium and large EV preparations

(n = 9) following comparison to the annotated bovine genome (assembly UMD3.1, release 70).

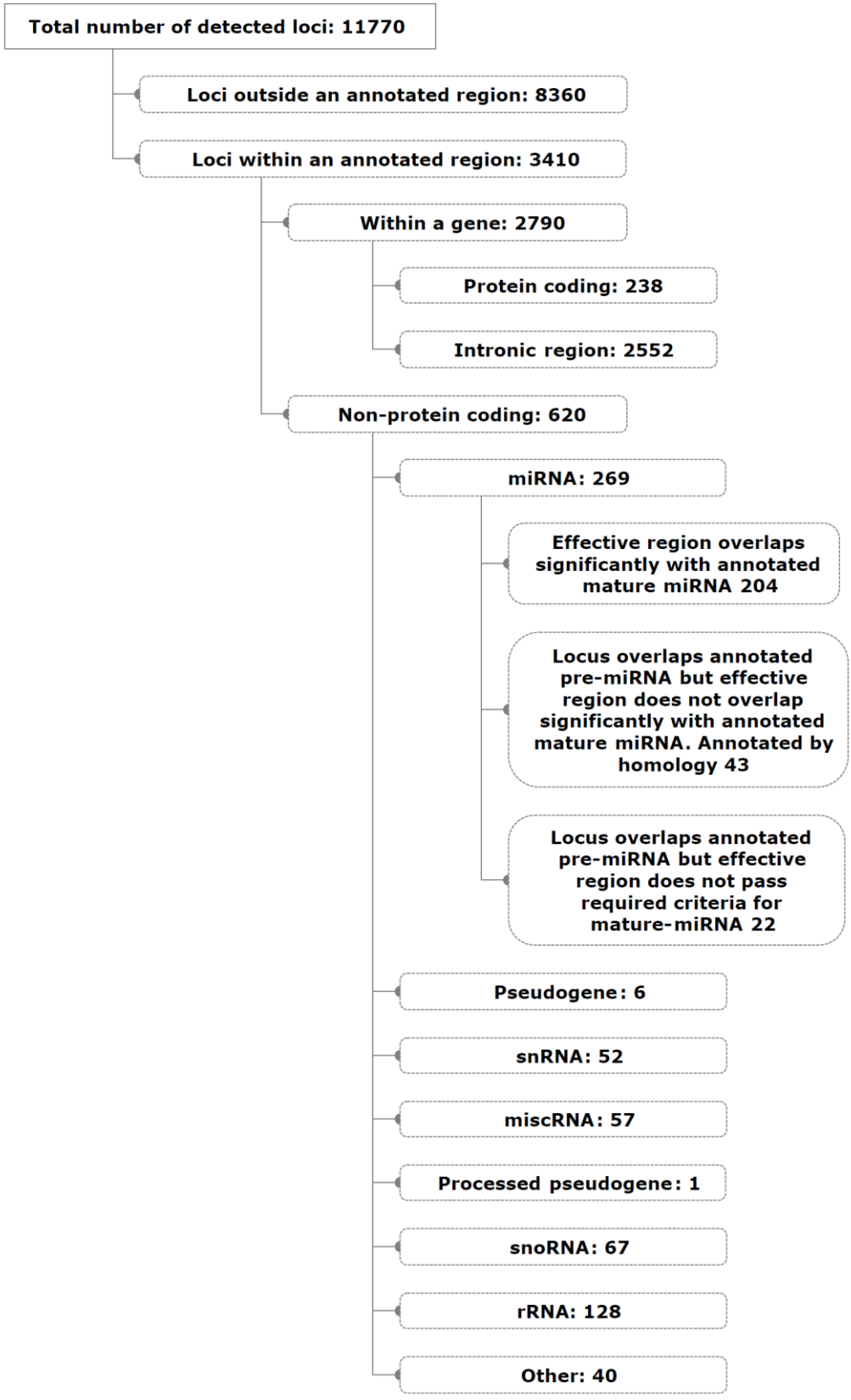
Total number of detected loci: 11770
Loci outside an annotated region: 8360
Loci within an annotated region: 3410
Within a gene: 2790
Protein coding: 238
Intronic region: 2552
Non-protein coding: 620
miRNA: 269
Effective region overlaps significantly with annotated mature miRNA 204
Locus overlaps annotated pre-miRNA but effective region does not overlap significantly with annotated mature miRNA. Annotated by homology 43
Locus overlaps annotated pre-miRNA but effective region does not pass required criteria for mature-miRNA 22
Pseudogene: 6
snRNA: 52
miscRNA: 57
Processed pseudogene: 1
snoRNA: 67
rRNA: 128
Other: 40

Table II- 2 The number of read counts associated with each of annotation types

Location	Count	Cumulative	Median	Mean	Std. Err.	Max	Min
Total number of detected loci	11770	9,629,592	143	818	63	597,958	37
Loci outside an annotated region	8360	5,207,955	144	623	73	597,958	37
Loci overlapping an annotated region	3410	4,421,637	140	1,297	125	126,917	38
Within a gene	2790	1,332,190	134	477	32	43,014	39
Protein coding	238	40,945	90	172	43	10,255	39
Intronic region	2552	1,291,245	136	506	34	43,014	41
Non-protein coding	620	3,089,447	279	4,983	654	126,917	38
miRNA	269	1,179,225	424	4,384	744	107,513	38
Pseudogene	6	851	53	142	84	561	42
snRNA	52	144,802	113	2,785	902	43,559	47
miscRNA	57	922,140	198	16,178	4,713	126,917	47
Processed pseudogene	1	86	86	86	0	86	86
snoRNA	67	15,568	163	232	34	2,255	59
rRNA	128	812,857	824	6,350	1,585	79,839	63
Mt-rRNA	30	10,579	193	353	142	4,420	72
Mt-tRNA	10	3,340	212	334	101	1,114	64

Following the general alignment to the bovine annotated sequence where we identified 269 miRNA as present within our samples, we then completed an unbiased approach to independently identify known and unknown miRNA within the bovine follicular fluid EVs. Using this unbiased approach we identified 704 loci that met our minimum read count requirements of ≥100 reads and the criteria for miRNA annotation within our EV samples (Figure II-7A). Of these 704 loci, 204 were exact matches for known bovine miRNAs (Ensemble gene annotation file for bovine; release 70). Of the remaining 500 miRNAs, 45 were mapped to a known miRNA of bovine or other species with very strong homology in both the mature and hairpin sequence. Of these 45 loci, 43 fell within a miRNA and 2 fell within a miscRNA annotated region in the bovine genome. Those 43 loci that fell within a miRNA annotated region, however, differed significantly from the previously annotated bovine miRNA. For example, the highly expressed region of the mature bta-miR-103 in the current study is 5 bases shorter than the reported bovine miRNA in miRBase v21 (Figure II-7B). Another example, miRNA-224, was also shown to differ with respect to its 3' end (the annotated bovine sequence has 23 bases) while the human and murine miR-224 are 21 bases in length (Figure II-7C). Upon closer inspection of the murine sequence (mmu-miR-224) within miRBase, one could easily propose that the mouse sequence is 22 bases in length based on the available data.

In our study we found that the EVs contained predominantly a 22 base miR-224 and to a lesser extent a 24 base version of miR-224 versus the bovine 23 base annotated sequence. Another example of a miRNA classification issue is found for a loci between bases 14462439 and 14462462 of chromosome 3 where a highly expressed mature miRNA like sequence aligns to bta-mir-9-5p which is currently annotated (miRBase v21) in two different locations within chromosomes 7 and 21, respectively. While the highly expressed mature sequence in the current study is a single base longer than the reported bta-mir-9-5p sequence, both its mature and stem-loop regions match exactly with the reported miR-9 regions in the four species *tupaia chinensis, canis familiaris, pan troglodytes* and *sus scrofa*. Lastly, the current study identified 455 novel miRNA sequences that met standard criteria as established in detail in the methods. Of these novel miRNA, 115 fell within and 340 fell outside an annotated feature (e.g., exons, etc.). Fig II-8A shows a novel miRNA located in the gene coding for *ADAMTS3* whereas the other novel miRNA in Fig II-8B is located outside any annotated feature. We have included the putative hairpin structures for all known bovine miRNA, miRNA previously identified in other species (i.e., homologous) and novel miRNA in Fig II-9.

Figure II- 7 Annotation breakdown and description of miRNA within the EVs using a comprehensive and unbiased approach.

(**A**) The flow chart shows the total number of loci and the classification of derivation (i.e., known, homologous to other species, and novel) that were associated with sequence loci with > 100 read average within a follicle size group that met the Sanger requirements to be considered a miRNA (see detailed description in Methods). (**B**,**C**) show two representative miRNA sequences derived from EVs and compares them to the established human and bovine annotated sequences. (**B**) The current miR-103 sequence is 5 bases shorter than the previous annotated bovine and human miR-103 transcripts. (**C**) The current miR-224 sequences were of two lengths 22 and 24 bases (denoted by two overlapping arrows) this differs from the previous annotated bovine sequence which was 23 bases.

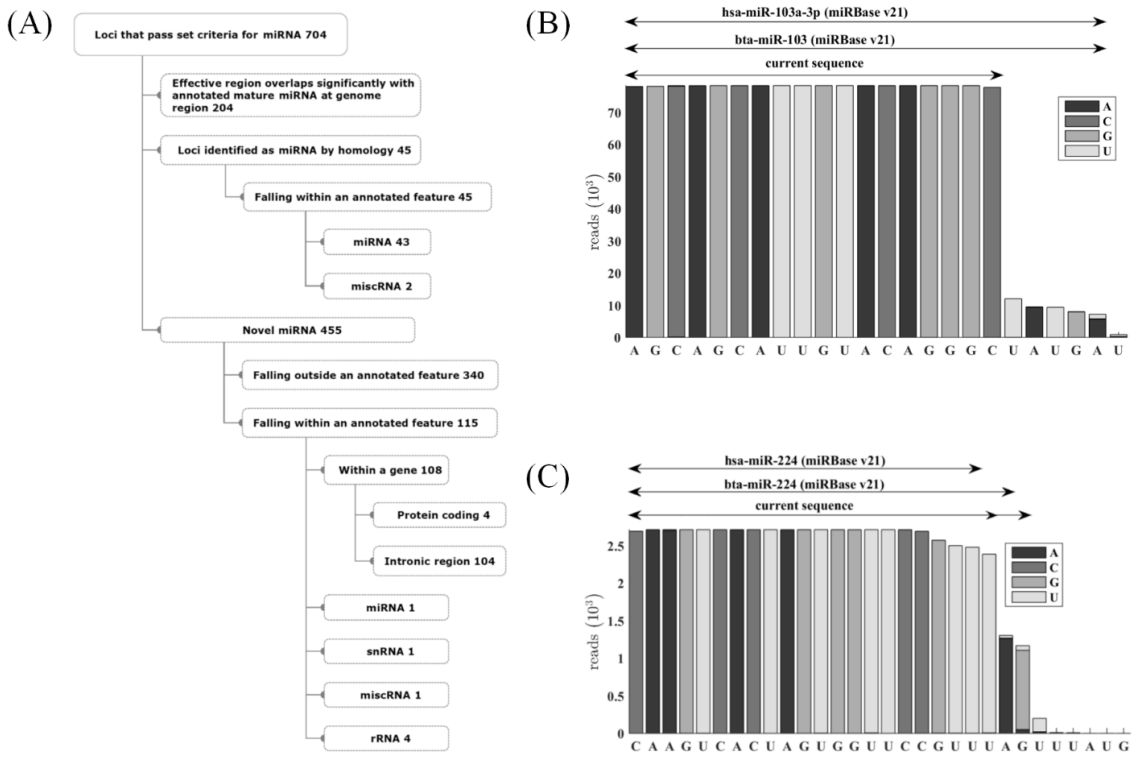
(A)
Loci that pass set criteria for miRNA 704
Effective region overlaps significantly with annotated mature miRNA at genome region 204
Loci identified as miRNA by homology 45
Falling within an annotated feature 45
miRNA 43
miscRNA 2
Novel miRNA 455
Falling outside an annotated feature 340
Falling within an annotated feature 115
Within a gene 108
Protein coding 4
Intronic region 104
miRNA 1
snRNA 1
miscRNA 1
rRNA 4
(B)
hsa-miR-103a-3p (miRBase v21)
bta-miR-103 (miRBase v21)
current sequence
A
C
G
U
reads (10^3)
0
10
20
30
40
50
60
70
A G C A G C A U U G U A C A G G G C U A U G A U
(C)
hsa-miR-224 (miRBase v21)
bta-miR-224 (miRBase v21)
current sequence
A
C
G
U
reads (10^3)
0
0.5
1
1.5
2
2.5
C A A G U C A C U A G U G G U U C C G U U U A G U U U A U G

Figure II- 8 Stem loop structure for two novel miRNA.

Location, read counts, predicted structure, and read intensity of two novel miRNA, A) one located in an annotated region A (ADAMTS3) and B) the other located outside an annotated feature.

(A)

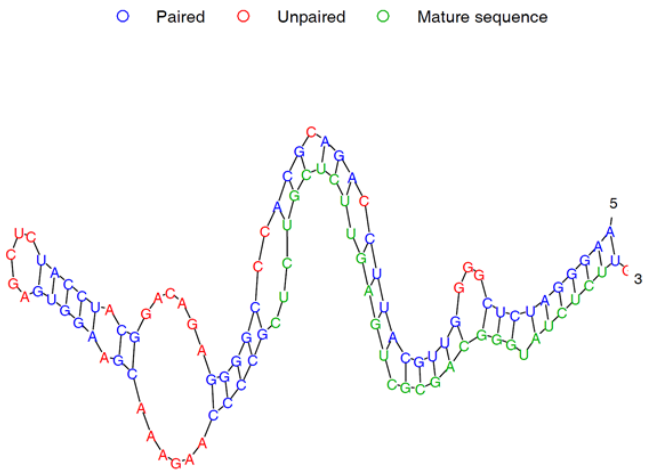

Stem loop (UMD3.1): chr6:89217310-89217416
Mature (UMD3.1): chr6:89217312-89217341
Average normalized counts: 6994.6
Total raw counts (9 samples): 53301
Average raw counts: 5922.3
Strand: Reverse
Orientation: 3p
Minimum free energy: -40.50

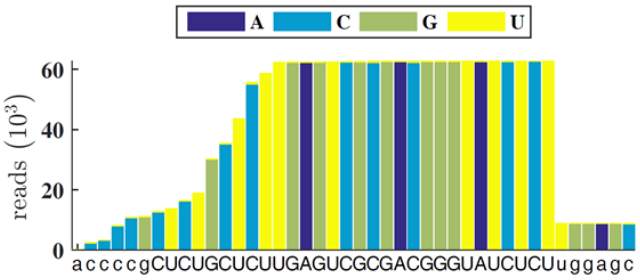

(B)

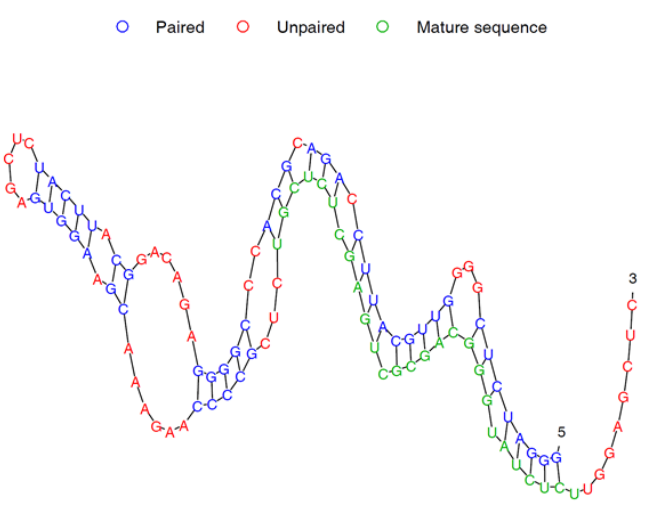

Stem loop (UMD3.1): chr19:38176-38286
Mature (UMD3.1): chr19:38252-38278
Average normalized counts: 1640.2
Total raw counts (9 samples): 12601
Average raw counts: 1400.1
Strand: Forward
Orientation: 3p
Minimum free energy: -34.90

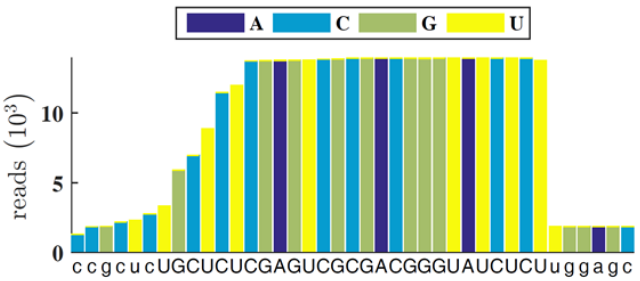

Figure II- 9 The 204 known bovine miRNA are followed by 45 (homologous miRNA) and then the list of 455 novel loci that are predicted to encode a miRNA.

See uploaded files (Navakanitworakul, Hung et al. 2016)

Differentially abundant miRNA within EVs of increasing sized follicles

Comparison of miRNA content within the EVs of small, medium and large follicles showed that the greatest differences were observed in the small versus large follicles (Table II-3). Small (3-5 mm) follicle EVs contained 83 miRNA that were more abundant in small versus large follicle EVs while 42 miRNA were more abundant in large versus small follicle EVs (Table II-3). Comparison of small to medium follicles indicated that 28 EV associated miRNA were more abundant in small and 8 more abundant in medium follicle EVs; comparison of medium and large follicles indicated that 42 were greater in medium and 17 more abundant in large follicles (Table II-3). The breakdown of known bovine miRNA, homologous miRNA and novel miRNA are shown in (Table II-3). The Chi-square test of homogeneity indicates that there is no significant difference in the proportion of up-regulated to down-regulated miRNA in the three comparisons (Yates' p-value =0.533). The relative fold changes in miRNA content across these different comparisons for individual miRNA ranged from 1.9 to 419.9.

Table II- 3 Distribution of miRNA that differed between small, medium, and large follicles*

Comparison		S vs L		S vs M		M vs L	
Increased in		small	large	small	medium	medium	large
miR annotation	Bovine	47	33	5	7	24	15
	Other species (homologous)	5	8	2	1	3	2
	Novel	31	1	21	0	15	0
	All	83	42	28	8	42	17

*The Chi-square test of homogeneity indicates there is no significant difference in the proportion of up-regulated to down-regulated miRNA in the three comparisons (Yates' p-value =0.533).

As the greatest number of miRNA and the biggest differences were observed for the small versus large follicle EV comparison, we have depicted all 80 known differentially detected miRNA for this comparison in Table II-4 and all 45 homologous and novel miRNA in Table II-5. For a complete breakdown of each of known and homologous miRNA and the novel miRNA that were observed in the different size follicles (see Tables II-6 and -7). Of the differentially present miRNA across follicle sizes, only 8 known miRNA exhibited changes across all three classification groups. Five miRNA (miR-204, miR-92b, miR-328a-3p, miR-424-3p and miR-450a) exhibited a significant progressive increase in read counts as follicle size increased (Table II-6). Two miRNA (miR-19a-3p and miR-335) exhibited a progressive decrease in read counts as follicle size increased (Table II-63). Additionally, 9 novel miRNA were shown to progressively decrease in abundance from small to large follicles and none were observed to progressively increase (Table II-7).

Table II- 4 Normalized read count and fold change of annotated bovine miRNA which differed between small and large follicles*

miR name	normalized read count (Average)		large vs small	miR name	normalized read count (Average)		Large vs small	miR name	normalized read count (Average)		Large vs small
	small	large	fold change		small	large	fold change		small	large	Fold change
bta-miR-150	8	416	51	bta-miR-542-5p	42	98	2.3	bta-miR-146b	946	302	-3.2
bta-miR-132	51	878	17.1	bta-miR-425-5p	699	1479	2.1	bta-miR-210	2438	714	-3.4
bta-miR-92b	1932	24175	12.5	bta-miR-30b-5p	735	1553	2.1	bta-miR-20a	416	121	-3.5
bta-miR-204	410	4117	10.1	bta-miR-151-5p	3218	6717	2.1	bta-miR-2284z	84	23	-3.6
bta-miR-486	949	9245	9.7	bta-miR-342	570	1124	2	bta-miR-215	534	143	-3.7
bta-miR-328	41	360	8.6	bta-miR-450b	2946	5497	1.9	bta-miR-21-3p	527	133	-3.9
bta-miR-424-3	120	838	7	bta-miR-10b	108030	56151	-1.9	bta-miR-101	2356	611	-3.9
bta-miR-1343	60	398	6.6	bta-miR-532	1867	885	-2.1	bta-miR-1839	3281	818	-4
bta-miR-30f	155	1015	6.6	bta-miR-27a-3p	1072	504	-2.1	bta-miR-29a	6079	1506	-4
bta-miR-450a-	68	444	6.5	bta-miR-15a	1534	686	-2.2	bta-miR-1388-5p	171	41	-4.1
bta-miR-450a-	71	425	6	bta-miR-103	8534	3785	-2.3	bta-miR-106b	752	180	-4.2
bta-miR-222	140	719	5.2	bta-miR-378	4819	2115	-2.3	bta-miR-17-3p	107	27	-4.3
bta-miR-1307	81	389	4.8	bta-miR-660	8723	3729	-2.3	bta-miR-2284w	62	12	-4.5
bta-miR-142-3	215	1018	4.8	bta-miR-143	15992	6642	-2.4	bta-miR-378c	100	20	-4.7
bta-miR-125b	335	1398	4.2	bta-miR-152	972	378	-2.6	bta-miR-192	6690	1393	-4.8
bta-miR-451	94	378	4.1	bta-miR-199a-3p	686	252	-2.7	bta-miR-130a	6823	1411	-4.8
bta-miR-339a	517	1873	3.6	bta-miR-17-5p	1317	484	-2.7	bta-miR-429	131	24	-5.1
bta-miR-125a	4165	14287	3.4	bta-miR-23a	2591	949	-2.7	bta-miR-1271	56	14	-5.4
bta-miR-2904	50	173	3.4	bta-miR-873	1319	482	-2.7	bta-miR-29c	319	54	-5.8
bta-miR-1468	416	1364	3.3	bta-miR-452	150	54	-2.8	bta-miR-19b	1271	212	-6.1
bta-miR-331-3	64	210	3.3	bta-miR-148a	48363	17154	-2.8	bta-miR-190b	136	18	-6.2
bta-miR-30d	12377	39580	3.2	bta-miR-2285k	68	21	-3.1	bta-miR-193a-3p	51	5	-7.9
bta-miR-744	268	796	3	bta-miR-18a	65	19	-3.1	bta-miR-449a	126	17	-8.7
bta-miR-484	285	828	2.9	bta-miR-592	233	72	-3.1	bta-miR-19a	764	52	-14.6
bta-miR-30c	2993	8015	2.7	bta-miR-107	8028	2543	-3.1	bta-miR-335	4689	231	-20.3
bta-149-5p	68	176	2.6	bta-miR-130b	246	75	-3.2	bta-miR-1388-3p	39	0	-419.9
bta-mIR-182	287	755	2.6	bta-miR-32	464	147	-3.2				

* All of the following genes were adjusted for multiple tests by the Benjamini and Hochberg method and had false discovery rates < 0.05. Additional details including raw counts, exact FDR values, as well as comparisons to medium sized follicles are present in Supplemental Table 3.

Table II- 5 Normalized read count and fold change of novel and homologous bovine miRNA which differed between small and large follicles*

Novel miRNA Locus	normalized read count (Average)		Large vs small
Locus ID (Chromosome:start-end; Strand)	**Small**	**large**	**fold change**
22:37936196-37936222 (-)	**600**	**892**	1.5
9:72616256-72616283 (+)	**821**	**453**	-1.8
14:4412105-4412134 (+)	**2352**	**1134**	-2.1
4:46639567-46639595 (-)	**1853**	**802**	-2.3
12:89782137-89782164 (+)	**1115**	**428**	-2.6
X:62079641-62079660 (-)	**4088**	**823**	-5.0
X:62078661-62078681 (-)	**4286**	**779**	-5.5
X:144087437-144087455 (+)	**1817**	**320**	-5.7
X:62080685-62080704 (-)	**2556**	**442**	-5.8
X:62081821-62081840 (-)	**2820**	**444**	-6.3
4:113198367-113198384 (-)	**1558**	**209**	-7.4
18:58243447-58243467 (+)	**1837**	**230**	-8.0
13:13589076-13589092 (-)	**5226**	**621**	-8.4
3:63639301-63639326 (-)	**8378**	**696**	-12.0
7:44900586-44900601 (-)	**2416**	**197**	-12.2
11:72567808-72567823 (+)	**2415**	**163**	-14.7
9:103492721-103492748 (-)	**2209**	**118**	-18.7
10:26814520-26814545 (+)	**16477**	**700**	-23.5
16:71150568-71150591 (+)	**3630**	**133**	-27.3
8:89663122-89663138 (-)	**8049**	**238**	-33.8
X:2676228-2676250 (+)	**3251**	**91**	-35.3
21:60864954-60864973 (+)	**152167**	**3229**	-47.1
28:25631928-25631956 (+)	**2787**	**57**	-48.0
20:55442871-55442887 (-)	**3718**	**69**	-53.2
7:20756731-20756752 (+)	**1908**	**32**	-58.3
X:29130246-29130269 (+)	**1394**	**22**	-62.1
9:94314513-94314529 (-)	**15284**	**232**	-65.9
27:27255989-27256011 (+)	**2563**	**37**	-69.2
8:111841867-111841889 (-)	**2674**	**36**	-71.4

7:64776449-64776465 (+)	**1825**	**23**	-77.7
18:22622903-22622918 (+)	**67609**	**671**	-100.6
X:30338371-30338390 (-)	**14428**	**116**	-123.8

Homologous miRNA	**normalized read count (Average)**		**Large vs small**
miRNA name (bovine chromosome:start-end: Strand)	**small**	**large**	**fold change**
efu-miR-181f 11:95709487-95709508	**181**	**826**	4.57
chi-let-7b-3p 5:117120245-117120266	**41**	**178**	4.24
chi-let-7d-3p 8:86887492-86887513	**545**	**2010**	3.69
chi-miR-28-3p 1:79250541-79250563	**2839**	**10157**	3.58
ssc-miR-1285 10:42863853-42863882	**72**	**231**	3.18
chi-miR-361-3p X:74328465-74328489	**167**	**509**	3.05
chi-miR-195-3p 19:27441353-27441377	**193**	**509**	2.64
chi-miR-1307-5p 26:24230159-24230179	**1281**	**522**	-2.44
eca-miR-199b-3p 11:98867681-98867702	**693**	**211**	-3.24
chi-miR-335-3p 4:95071042-95071063	**530**	**154**	-3.38
chi-miR-145-3p 7:62810788-62810808	**145**	**36**	-3.69
mml-miR-452-3p X:34665635-34665656	**113**	**25**	-4.13
chi-miR-708-3p 29:16686296-16686318	**52**	**7**	-5.91

* All of the following genes were adjusted for multiple tests by the Benjamini and Hochberg method and had false discovery rates < 0.05. Additional details including raw counts, exact FDR values, as well as comparisons to medium sized follicles are present in Supplemental Table 4.

Table II- 6, Table II- 7 See uploaded data set (Navakanitworakul, Hung et al. 2016)

Pathway analysis of miRNAs that differed between large and small follicle sizes

Because the greatest differences existed for the small versus large follicles, we then focused our Ingenuity Pathway Analysis (IPA) upon those miRNA. Because of the nature of IPA, only miRNA (211) which are annotated in human were used. MicroRNA that were more abundant in small and large follicle EVs were both highly linked to the associated Network functions IPA classification called Cancer, Organismal Injury and Abnormalies, Reproductive System Disease, which includes miRNA associated with reproductive tumors, endometriosis, preeclampsia, and azoospermia (Figure II-10). Molecular and cellular function predictions identified cellular development, cellular proliferation, cell death and survival and cell cycle as common among those miRNA that differed between these follicle sizes (Figure II-10). MicroRNA that are more abundant in large versus small follicles were predicted to be involved in inflammatory responses (Figure II-10).

Figure II- 10 Ingenuity Pathway Analysis predicted functional networks for miRNA enriched in EVs isolated from small or large follicles.

More in small follicles

Molecular and cellular function

Name	p-value	# Molecules
Cellular Development	3.52E-10 - 4.93E-02	24
Cellular Growth and Proliferation	3.52E-10 - 4.93E-02	24
Cellular Movement	3.39E-08 - 4.82E-02	18
Cell Death and Survival	7.36E-06 - 4.55E-02	20
Cell Cycle	2.49E-05 - 4.82E-02	10

Top networks

ID	Associated Network Functions	Score
1	Cancer, Organismal Injury and Abnormalities, Reproductive System Disease	73
2	Cancer, Organismal Injury and Abnormalities, Reproductive System Disease	32
3	Hereditary Disorder, Skeletal and Muscular Disorders, Developmental Disorder	23
4	Cancer, Gastrointestinal Disease, Inflammatory Response	16
5	Hereditary Disorder, Skeletal and Muscular Disorders, Cancer	8

More in large follicles

Molecular and cellular function

Name	p-value	# Molecules
Cellular Development	1.81E-07 - 4.21E-02	11
Cell-To-Cell Signaling and Interaction	2.69E-03 - 2.69E-03	2
Cell Cycle	4.03E-03 - 3.83E-02	3
Cellular Growth and Proliferation	4.03E-03 - 4.21E-02	8
Cell Death and Survival	5.36E-03 - 4.25E-02	7

Top networks

ID	Associated Network Functions	Score
1	Cancer, Inflammatory Disease, Inflammatory Response	32
2	Organismal Injury and Abnormalities, Reproductive System Disease, Cancer	26
3	Endocrine System Disorders, Organismal Injury and Abnormalities, Reproductive System Disease	3
4	Cancer, Hematological Disease, Immunological Disease	3

*Predicted molecular and cellular functions and top networks are depicted.

DISCUSSION

In this study we show for the first time that EVs within follicular fluid change in number and in their small RNA content when examined across different sizes of follicles. Previous work has indicated that small non-coding RNA (i.e., miRNA) exhibit dynamic changes during ovarian follicle development (Fitzgerald, George et al. 2016); we discuss several miRNA previously shown to be involved in ovarian function in the context of our new observation that they are now also known to be present in follicular fluid EVs. Our study points to the possibility that like hormones, cytokines and numerous other factors located within the follicular fluid, EVs also change dynamically over time and now must also be considered as a potential mechanism for cell-to-cell communication across the antral fluid barrier that spatially separates the cumulus oocyte complex from the mural granulosa cells. Indeed, we have recently shown that EVs from small and large follicles can elicit differential effects on cumulus-oocyte-complexes (Hung, Christenson et al. 2015).

In order to fully appreciate whether EVs undergo dynamic changes in the developing follicle, the current study took a robust approach to quantify and characterize EVs within the follicular fluid of growing bovine follicles. To confirm the proportion of viable healthy to atretic follicles within the pools, an analysis of 20 individually isolated

follicles from each size group indicated that a similar proportion of viable healthy to non-viable atretic follicles (~70 and 30%, respectively). Moreover, analysis of estrogen and progesterone levels in the pools of follicular fluid indicated an increase in estrogen levels as the follicle size increased which is typical of healthy growing follicles. Nanoparticle tracking analysis (NTA) indicated that the size of EVs is consistent with that attributed to the exosomes and small microvesicles. Interestingly, we observed no change in the distribution of particle sizes originating from the different sized follicles. Importantly, it must be pointed out though that our procedure effectively eliminates larger microvesicles (>220 um). Thus, we cannot be absolute in our statement that a population of larger microvesicles does not dynamically change during follicular growth. Analysis of the EV pellets by electron microscopy further indicated that a relatively homogenous population of small vesicles (< 130 nm in diameter) was isolated from the follicular fluid. Moreover, and consistent with the NTA, the size and morphology of vesicles by as evaluated by electron microscopy were also not different across the three follicle sizes. These observations might suggest that EVs are not dynamically changing during follicle development. However, the differential enrichment of CD81 within the EV preparations of the small, medium and large follicles suggests that changes within the EV pool are occurring. Conversely, the internal exosomal protein (Alix) was not found to vary in a

similar pattern as that of the transmembrane protein CD81 in the EV preps suggesting that either the levels of CD81 vary on individual EVs or that different populations of EVs exist in different size follicles. Furthermore, following differential ultracentrifugation, the EV pellets were subjected to sucrose gradient centrifugation/fractionation and western blot analysis for CD81. Consistent with an exosomal origin as evident by CD81 expression (Raposo, Nijman et al. 1996, Valadi, Ekstrom et al. 2007, Simpson, Lim et al. 2009), we found those fractions with a density of 1.14-1.22 g/ml to be enriched in CD81 and this was also differentially detected within the three different sizes of follicles. The absence of endoplasmic reticular protein GP96 within the EV prep was further evidence of the purity of these preparations (Thery, Regnault et al. 1999). Ultimately, this detailed characterization of the EVs in the current study is reassuring that the subsequent next generation sequencing results are originating from a population of EVs within the follicular fluid. The importance of this observation is highlighted by the recent observation that serum levels of miRNA are more highly enriched in the non-vesicle fractions of serum following ultracentrifugation (Chevillet, Kang et al. 2014). In previous analyses of human and bovine follicular fluid miRNA content, Sang et al. (Sang, Yao et al. 2013) and Sohel et al. (Sohel, Hoelker et al. 2013) both detected miRNA within the pelleted extracellular vesicle component and in the remaining supernatant. In both

cases the numbers of miRNA identified were greater in vesicular fraction and in the case of the bovine study, Sohel et al., (Sohel, Hoelker et al. 2013) suggested that the vesicle-mediated pathway may be the predominant mechanism of miRNA transport with the follicle. This clearly differs from observations in other bodily fluids (i.e., serum, urine, salvia) where it appears that non-vesicular miRNA maybe the predominant form (Chevillet, Kang et al. 2014). Our current study did not address this issue and additional studies will be required to determine the relative physiologic importance of these two different sources of miRNA within the follicular fluid.

Our study also shows for the first time that the tetraspanin CD81 exhibits differences in levels within the EV preparations of small, medium and large follicles. This protein belongs to a large family of tetraspanin proteins that are found in numerous cell types (Caplan, Kamsteeg et al. 2007) and are enriched in exosomes (Valadi, Ekstrom et al. 2007, Simpson, Lim et al. 2009). Previous studies demonstrated that CD81 was highly expressed by murine cumulus cells which surround oocytes (Tanigawa, Miyamoto et al. 2008) and by periovulatory bovine mural granulosa cells (Christenson, Gunewardena et al. 2013) before and after the LH surge. Immunohistochemistry indicated that the zona pellucida surrounding mouse oocytes was highly enriched in CD81 (Ohnami, Nakamura et al. 2012). A role for CD81 in murine ovarian function was demonstrated when

targeted deletion of the gene caused female mice to exhibit a 40% reduction in fertility (Rubinstein, Ziyyat et al. 2006). Further studies showed that this loss in fertility was due to the inability of oocyte to fuse with sperm (Rubinstein, Ziyyat et al. 2006). Interestingly, the source of the zona pellucida CD81 does not appear to be of oocyte origin as CD81 was not detected in the oocyte and furthermore oocytes microinjected with exogenous CD81 mRNA failed to produce CD81 or reverse the sperm fusion defect (Ohnami, Nakamura et al. 2012). In our study, the highest level of CD81 was found in EVs derived from 3-5 mm diameter follicles while the level of CD81 decreased in EVs from 6-9 mm and > 9 mm follicles. The biological meaning of this change in CD81 within the EVs isolated from the different size follicles as well as the source of the CD81, i.e., whether it is of serum or granulosa/cumulus derivation requires further investigation.

In our evaluation of RNA within the EVs, the preponderance of small RNA species ranged in size from 20 to 40 nucleotides in length, consistent with these small RNA species being of a size consistent with miRNA. Our sequencing results indicated that 12.2% of small RNAs were of miRNA origin which is consistent with that observed (15.4%) in the only other small RNAseq results for follicular fluid (Sang, Yao et al. 2013). In addition to the overall abundance of miRNA (43.3% of the total of non-protein coding loci), several other small RNA species were identified within EVs

including snRNA (8.3%), snoRNA (10.8%), rRNA (20.6%), miscRNA (9.2%). The presence of miRNA within EVs was previously documented in equine (da Silveira, Veeramachaneni et al. 2012), bovine (Sohel, Hoelker et al. 2013), and human (Sang, Yao et al. 2013, Diez-Fraile, Lammens et al. 2014, Santonocito, Vento et al. 2014) follicular fluid. In the bovine and equine studies, EVs were isolated using the ExoQuick precipitation method followed by qPCR arrays to identify miRNA. Recently it was shown that the Exoquick precipitation method generates a greater range of vesicle sizes and increased protein contamination when compared to the standard differential ultracentrifugation method used here (Santonocito, Vento et al. 2014). Additionally, these studies evaluated miRNA abundance using qPCR arrays designed for detection of human miRNA, which limits their observations to those miRNA with 100% homology to the human sequence. It should be noted though that many miRNA are 100% homologus with respect to the mature miRNA sequence across a large number of species (Griffiths-Jones, Saini et al. 2008). However, consistent with our observation of a large number of miRNA within the bovine follicular fluid, Sohel et al., (Sohel, Hoelker et al. 2013) observed 509 different miRNA in bovine follicular fluid isolated from 4-8 mm follicles. Using our unbiased small RNAseq approach, we detected the presence of 249 previously known miRNA (bovine or other species annotated) and the presence of 455 previously

unknown miRNA in bovine EVs. The large number (455) of novel miRNA found within bovine follicular fluid could indicate that this bodily fluid is exceptionally enriched in miRNA or could be a reflection of the incomplete annotation of miRNA species within the bovine. Currently, the bovine has 682 unique annotated miRNA and of these 36.5% were identified within our follicular fluid EVs. In addition to large numbers of novel miRNA, a number of miRNA (45) identified in the bovine EVs, not yet annotated in the bovine genome, were consistent with previously identified miRNA in other species. Recently, Maalouf et al., (Maalouf, Liu et al. 2014) in a small RNAseq analysis of bovine corpora lutea, identified 590 miRNA of which 46 were novel miRNA. This large difference in numbers of novel miRNA between our study and theirs is likely due to their restriction of identification of novel miRNAs to only regions within introns or antisense exon regions, a criteria we chose not to employ in our current study. Additionally, several novel miRNA structures identified in the current study were found replicated identically or nearly identically in both stem-loop and mature sequence in different locations across the genome; we considered each as a different putative novel miRNA. Recent analysis of miRNA sequences in 13 different human cell lines indicated the presence of a substantial number (3707) of previously unidentified microRNA (Londin, Loher et al. 2015). Follicular fluid EVs appear to be a rich source

of miRNA.

This study is the first to examine the differential abundance of miRNA within EVs across different stages of follicular growth. Previous studies have evaluated follicular fluid derived EVs isolated from follicles of young and old mares (da Silveira, Veeramachaneni et al. 2012), women with and without polycystic ovarian syndrome (Sang, Yao et al. 2013), IVF patients (Santonocito, Vento et al. 2014), and in young (age 31) versus old (age 38) IVF patients. In the previous bovine experiment, follicles within a single range of size 4-8 mm were classified based on oocyte brilliant cresyl blue staining which can define the oocyte as growing or fully grown (Sohel, Hoelker et al. 2013). Unfortunately, comparisons across these two studies are not possible based on the divergent experimental designs, methods of exosome isolation and miRNA identification methods. Not surprisingly, comparison of the miRNAs within the EVs of large (>9 mm) versus small (3-5 mm) follicles showed the greatest difference in number of differentially present miRNA, with 42 increased and 83 decreased. Changes in miRNA from small to medium and medium to large follicle EVs were intermediate as might also be expected. Five miRNAs exhibited significantly progressive increases in read counts as follicle size increased including miR-204, miR-92b, and miR-328a-3p, miR-424-3p and miR-450a. Mir-204 has been addressed as a cell proliferation inhibitor in several cell types (Shi,

Huang et al. 2015, Wu, Pan et al. 2015, Wu, Zeng et al. 2015, Wu, Wang et al. 2015, Xia, Liu et al. 2015, Yin, Liang et al. 2015), this could be possibly linked to the decrease in cell proliferation that occurs with increasing follicle size. MiR-92b was more abundant in large follicle than small follicle EVs. Significant changes in miR-92b expression levels have also been noted in the process of neointimal formation in a rat model of vascular injury (Ji, Cheng et al. 2007), in individuals with a cardiac rehabilitation following surgical coronary revascularization (Taurino, Miller et al. 2010) and in individuals with heart failure (Goren, Kushnir et al. 2012), indicating that miR-92 is also involved in neovascularization. However, the function of miR-92b in reproduction is still unknown. DNA methyltransferase 3a (Dnmt3a) is known as a target of miR-450a and ectopic miR-450a expression in HepG2 cells decreased Dnmt3a and blocked inhibition of cell proliferation (Weng, Wang et al. 2011). The roles of miR-328a-3p and miR-424-3p are currently poorly described. Conversely, levels of miR-19a-3p and miR-335 exhibited significant progressive decreases as follicle size increased. Mir-19a-3p has been reported to inhibit breast cancer progression (Yang, Zhang et al. 2014). Deletion of miR-335 is a common event in human breast cancer and also correlates with ovarian cancer recurrence (Png, Yoshida et al. 2011). Others showed that the level of miR-335 is highly elevated in astrocytoma cells and human malignant astrocytoma suggesting that

miR-335 might be a tumor promoter by promoting tumorigenic features such as growth and invasion of malignant astrocytoma (Shu, Zheng et al. 2011). Our bioinformatics analyses of pathways also pointed to the changes in vascularization, as evident by the significant association of the different miRNA observed in the small versus large follicle EVs and the inflammatory pathway. Interestingly, miR-150 which exhibited the most profound difference in small versus large follicles (Table II-2) was previously reported as an oncomiR because of its promotional effect on vascular endothelial growth factor (VEGF) (Liu, Zhou et al. 2004). During tumor development, tumor-associated macrophages (TAMs) secrete VEGF and other factors to promote angiogenesis. MiR-150 targets TAMs to up-regulate their secretion of VEGF *in vitro*. Angiogenesis is known to increase dramatically during development of follicle with a pronounced increase following selection of the dominant follicle (Beg and Ginther 2006). Human follicular fluid contains elevated VEGF production following induction by the surge of LH in in vitro fertilization patients (Anasti, Kalantaridou et al. 1998). Thus, miR-150, which was more abundant in the large follicle, might also be involved in the vascular development, follicle growth, and the ovulation of oocyte through its regulation of VEGF.

The importance of miRNA in the ovary has been illustrated in clinical studies and studies where key elements of the miRNA biogenetic pathway or where specific miRNA have

been genetically deleted. Loss of Dicer, the key enzyme of miRNA biogenesis, results in decreased fertility and ovulation rate were observed (Otsuka, Jing et al. 2007, Hong, Luense et al. 2008, Otsuka, Zheng et al. 2008). The change of follicular extracellular associated miRNA was also demonstrated in polycystic ovarian syndrome (Sang, Yao et al. 2013, Roth, McCallie et al. 2014). miR-224 which discussed above is known expressed higher in preantral follicle and is able to regulate estradiol production (Yao, Yin et al. 2010). miR-378 which decreased 2.4 fold from small to large antral follicle in our result was also reported to decrease during antral follicle growth and has the ability to regulate Cyp19A1, critical gene for estradiol production.

Taken together, the results of the present study demonstrate for the first time that EVs differ in number, presence of protein markers and miRNA contents as follicle size changes. Specifically, CD81, one of three major marker proteins used for exosome identification, exhibited decreased abundance as follicle size increased suggesting that changes in EV biogenesis or uptake is occurring during follicle maturation/development. Functional analyses of individual miRNA that are associated with changes in follicle development also await further study, yet the current study provides clear and robust data regarding which miRNA might be first to be evaluated. This in combination with the recent observations that follicular fluid EVs are biologically functional (induce cumulus

expansion and gene expression) and differ in their functional activity based on the size of follicle they were derived from is consistent with our current observations. Cumulatively, the observations point to the potential for a unique EV signaling mechanism existing within the ovarian antral follicle.

IX. Chapter III: Extracellular vesicles from bovine follicular fluid support cumulus expansion

INTRODUCTION

Antral follicles in the mammalian ovary enlarge with the secretion of follicular fluid that fills the growing cavity between the layers of granulosa cells (Rodgers and Irving-Rodgers 2010). This viscous fluid is a complex solution containing a mixture of water, electrolytes, proteins, RNA, and extracellular vesicles providing a route for autocrine and paracrine communication between theca, mural granulosa, and cumulus cells and the maturing oocyte (Gosden, Hunter et al. 1988). The content of follicular fluid correlates with the stage of the follicular growth and the developmental potential of the oocyte (Revelli, Delle Piane et al. 2009, Sohel, Hoelker et al. 2013).

Extracellular vesicles (EVs) such as exosomes and microvesicles (ectosomes) have been identified in follicular fluid in several mammalian species including human, bovine and equine (da Silveira, Veeramachaneni et al. 2012, Sang, Yao et al. 2013, Sohel, Hoelker et al. 2013, Diez-Fraile, Lammens et al. 2014). Studies of cancer cell lines, have demonstrated that cargos such as proteins and RNA within EVs can influence behavior and gene expression of cells both near and far (Vlassov, Magdaleno et al. 2012, Cocucci and Meldolesi 2015). Formation of EVs occurs either by budding from the cell surface (microvesicles) or release from multivesicular bodies (exosomes) following fusion with the plasma membrane (Cocucci and Meldolesi 2015). The size range of

these two distinct types of EVs overlaps with exosomes ranging from 30-200 nm in diameter and microvesicles typically considered to range from 50-1,000 nm (Gyorgy, Szabo et al. 2011). EVs are characterized by the presence of specific membrane associated proteins, which are enriched in the EVs as compared to intact cells. These markers include several tetraspanins, CD81, CD63 and CD9 as well as other proteins, such as Alix, a protein involved in endosomal transport and tumor suppressor gene 101 (Tsg101) and others (Bissig and Gruenberg 2014, Kumar, Gupta et al. 2014). Follicular fluid EVs have been associated with varying protein and RNA cargos depending on such factors as a woman's age (Diez-Fraile, Lammens et al. 2014) or the presence of ovarian pathologies such as polycystic ovarian syndrome (Sang, Yao et al. 2013). Follicular fluid EVs carry microRNA (miRNA) and can be taken-up by cultured granulosa cells (da Silveira, Veeramachaneni et al. 2012, Sohel, Hoelker et al. 2013) demonstrating that they could potentially act as a method for cell-to-cell communication within the antral follicle.

Communication between mural granulosa and the cumulus oocyte complex (COC) is known to occur bi-directionally across the antral follicular fluid (Su, Sugiura et al. 2010, Conti, Hsieh et al. 2012). As an example, the LH surge stimulates release of mural granulosa EGF-ligands that must then traverse the follicular fluid to affect the cumulus cells in order to induce the characteristic gene expression changes and expansion

of the COC(Su, Sugiura et al. 2010, Conti, Hsieh et al. 2012). The precise mechanism by which these and other signaling molecules move through the follicular fluid to rapidly affect cumulus cells remains unknown.

Transmission of signals through an EV-mediated system is a possible mechanism of signal transduction within the follicle. In cancer cell models, EVs released into the microenvironment can increase cell motility and cause rapid modifications to the extracellular matrix (Mu, Rana et al. 2013, Webber, Yeung et al. 2015). Similarly, cumulus expansion in response to the LH surge involves increased cumulus cell motility (Akison, Alvino et al. 2012, Kawashima, Liu et al. 2012), and rapid secretion of a hyaluronan-enriched extracellular matrix (Russell and Salustri 2006, Kimura, Hoshino et al. 2007). While the cargos carried by follicular EVs varies greatly under different physiologic states, no direct effects of EVs on ovarian physiology have been demonstrated to date. The objective of the present study was to determine whether follicular EVs could affect the morphology and gene expression of cumulus cells during COC maturation.

METHODS

COC collection

COC were collected from CF1 female mice (21-24 days old obtained from Harlan

Sprague-Dawley, Indianapolis IN USA or Charles River Labs, Wilmington MA USA). Mice were housed in a temperature and light-controlled room on a 14L:10D light cycle and experiments were conducted in accordance with NIH guidelines for the Care and Use of Laboratory Animals and approved by the University of Kansas Medical Center Internal Animal Care and Use Committee (IACUC). To stimulate synchronous follicular development, mice were administered 5 IU of equine chorionic gonadotropin IP (eCG; Calbiochem, San Diego CA USA). Mice were euthanized by isoflurane inhalation anesthesia followed by cervical dislocation. Ovaries were collected at 44-46 hr post-eCG and COC were released from large antral follicles by rupturing the follicles with a sterile needle into HEPES-buffered KSOM medium (Biggers and McGinnis 2001) supplemented with 4 mg/ml polyvinyl alcohol (PVA; and containing no bovine serum albumin (BSA) or fetal bovine serum (FBS)). Pools of COC were created from 5-10 females, and only COC that contained a GV stage oocyte (~>75 μm) surrounded by 2 or more intact layers of cumulus cells were selected for culture. COC containing dark, small or non-GV oocytes, or discontinuous cumulus layers were discarded. Unless otherwise stated, all chemicals and reagents were purchased from Sigma Chemical Corporation (St Louis MO,USA).

Murine COC culture

Sets of 3-5 COC were transferred to KSOM[aa] (Evolve; Zenith Biotech, Guilford CT USA) supplemented with 4 mg/ml polyvinyl alcohol (10,000 mw; no BSA) with or without FBS and/or follicular EVs (100 μg protein/ml) according to the individual experimental protocol (see results for details of each treatment). Follicular fluid EV levels approximated 80-120 μg protein/ml and preliminary dose response studies indicated that 100 μg/ml dose of follicular EVs yielded consistent responses in mouse COC assays. Mouse COC were cultured for 16 hr in 20 μl drops of media under oil in 35 mm petri dishes (NUNC from Thermo Scientific, Rochester NY USA) at 37.2℃ in an incubator with 6% CO_2 in humidified air. Each dish contained 3-5 culture drops of COC and each treatment was cultured in a separate dish to ensure no passage of treatment factors between drops of COC. The number of COC in each drop was determined on the day of culture according to the total number of COC collected on that day and all drops cultured on that day contained the same number of COC. COC collected each day were randomly distributed across all treatments.

Bovine follicular fluid and COC collection

Cow ovaries were obtained from a local abattoir in Omaha, Nebraska. Ovaries were

transported to the University of Kansas Medical Center in phosphate buffered saline (PBS) at room temperature in preparation for ovarian follicular fluid aspiration. Ovarian follicular fluid was collected by needle aspiration from follicles with diameters of 3-5 mm (small) and > 9 mm (large) antral follicles. Four independent collections of follicular fluid were conducted in a two-month period. Follicular fluids from small and large antral follicles were pooled on each collection day. All COC were collected by pulled glass pipet and transferred to 400 µl of warm HEPES-buffered TCM199. High quality COC from the small antral follicles were used for COC cultures in TCM199 media using the same supplements and culture set-up protocol as described for the mouse except that bovine COC were matured for 24 hr at 39°C and always in sets of 3 COC/drop with or without follicular EVs (200 µg protein/ml). Since very few COC (3-5/collection day) were found in follicular fluid from large follicles, none of the COC from large follicles were used in the culture experiments.

Follicular EV isolation by differential ultracentrifugation

Follicular EVs isolated from 15 ml of ovarian follicular fluid were obtained via a series of differential ultracentrifugation steps as described in (Thery, Amigorena et al. 2006). Follicular fluid was diluted with an equal volume of PBS prior to centrifugation. To eliminate residual granulosa cells and oocytes, samples were spun at 800 g for 10 min

followed by 2000 g for 20 min. Fluid was then centrifuged at 12000 g for 45 min to remove cell debris and large particles. The samples were then filtered through a 0.22 μm pore filter to remove particles larger than 200 nm. Ultracentrifugation was performed at 110,000 g for 3 hr in a Beckman X100 ultracentrifuge, using a swinging bucket SW32Ti rotor, to pellet the follicular EVs. The pellets were then washed twice in PBS by centrifuging at 110,000 g for 1.5 hr. All centrifugations were performed at 4°C. The obtained pellets were re-suspended in PBS for further analysis. For EVs staining, EVs were stained with PKH67 Green Fluorescent Cell Linker Kit (Sigma Chemical Corp, St Louis MO USA) per manual protocol and pelleted by ultracentrifugation following several washes in PBS before final resuspension in PBS.

Nanoparticle tracking analysis

To determine particle size and concentration within follicular fluid from follicles of varying sizes, nanoparticle tracking analysis (NTA) was performed with a NanoSight LM10 instrument (Malvern Instruments, Worcestershire UK). Follicular EV preparations were diluted first in PBS to meet the optimal concentration between 10^5-10^8 particles/ml. At least 300 μl of diluted sample was needed for each analysis and was mixed by vortexing before injection into the chamber. Three individual videos were collected and the resulting counts were averaged for each diluted sample. Triplicates of

the same dilution were performed and the overall average of these dilutions were used as the experimental result for each sample. Each video of moving particles was 60 s in duration, with a shutter speed of 30 ms and camera gain of 680. Software settings for analysis were: Detection threshold: 6, Blur: auto, Minimum expected particle size: 50 nm. A minimum of 200 completed particle tracks were completed for each video and the data was analyzed using the NTA 2.3 analytical software (Malvern Inc.). Data are presented as the average and standard deviation of the triplicate.

Western blot Analysis

EV samples (10 μg protein) were lysed in SDS sample buffer with 50 mM DTT, heated for 5 min at 95 °C and subjected to electrophoresis using 12% SDS-PAGE in running buffer at constant 120 V for 1.5 hrs. Proteins were then electrotransferred onto polyvinylidenedifluoride membranes, and the membranes were blocked with 5 % (w/v) skim milk powder in Tris-buffered saline with 0.05 % (v/v) Tween-20 (TTBS) for 1 h at RT. Membranes were then probed with primary anti-CD81 (sc-166029) and anti-Actin (sc-1616) antibodies for 1 h in TTBS (50 mM Tris, 150 mM NaCl, 0.05 % Tween20) followed by incubation with the secondary anti-mouse IgG or anti-sheep goat antibodies for 1 h. All primary antibodies were purchased from Santa Cruz Biotechnology Inc. Membranes were washed three times in TTBS for 10 min after each incubation step and

detected by enhanced chemiluminescence (ECL) (GE Healthcare Bio-science, PA) per manufacturer's instructions.

Nomarsky live microscopy

All COC were imaged by Nomarsky optics on a Nikon TE200 or DIC on an Olympus IX71 inverted microscope immediately after transfer to culture drops and again after 16 hr (murine) or 24 hr (bovine) of maturation. Images were captured with 110x UplanFl 0.30 Ph1 and 20x LCplanFl 0.40 Ph1 objectives and Olympus DP71 camera. The diameter of each murine COC was measured using ImageJ software (Schneider, Rasband et al. 2012). For each COC, two diameters were measured then averaged, resulting in an average diameter. The overall measure of expansion was the average change from 0 hr (start of culture) to 16 hr for all COC within each drop.

Transmission electron microscopy

EVs (10 mg/ml) were fixed overnight (2% glutaraldehyde and 0.1 M cacodylate buffer) and washed with 0.1 M sodium cacodylate buffer. The pellet was post-fixed in 1% osmium tetroxide with 1% potassium ferric cyanide buffered in 0.1 M cacodylate buffer for 1 hr. A glow discharge treated carbon film 300 mesh grid was inverted and floated upside down on the drop containing fixed EVs (20 min). Each grid was rinsed 7x with filtered distilled water then stained with 1% uranyl acetate. All samples are examined in

a JEOL-JEM-1400 transmission electron microscope at an 80-100 kV with 25,000x magnification.

RNA isolation and quantitative RT-PCR analysis

RNA was isolated using the Arcturus PicoPure RNA Isolation kit (Life Technologies, Carlsbad CA USA), with an on-column DNase I digestion. Concentration and purity of RNA were determined by using the Agilent RNA 6000 Pico kit (Agilent Technologies, Palo Alto CA USA) and Bioanalyzer (Agilent Technologies, Santa Clara CA USA). Total RNA was reverse-transcribed using SuperScriptTM II Reverse Transcriptase (Life Technologies) with random primer per manufacturer's instruction. Quantitative PCR was then performed with 1:5 dilution of cDNA on an Applied Biosystems HT7900 sequence detector. Primer sets for mouse *Ptgs2* (forward: TGA CCC CCA AGG CTC AAA TA, reverse: CCC AGG TCC TCG CTT ATG ATC), *Ptx3* (forward: CCC GCA GGT TGT GAA ACA G, reverse: TGC ACG CTT CCA AAA ATC TTC), *Tnfaip6* (forward: ATA CAA GCT CAC CTA CGC CGA, reverse: ATC CAT CCA GCA GCA CAG ACA T), bovine *Ptgs2* (forward: TGG GTG TGA AAG GGA GGA AA, reverse: GTG AAA GCT GGT CCT CGT TC), *Ptx3* (forward: CCG GCA GGT TGT GAA ACA G, reverse: CAG CGA CCA GTC TGT TTT CC), *Tnfaip6* (forward: AAC CCA CAT GCA AAG GAG TG, reverse: GCC GTG GAC ATC ATC GTA AC) and U6

(forward: CTC GCT TCG GCA GCA CA, reverse: AAC GCT TCA CGA ATT TGC GT) were designed using Primer Express 3.0 software (Applied Biosystems) and *GAPDH* primers and probe were purchased from Life Technologies. Samples were run in triplicate, and the ΔΔCt method was used to calculate the relative fold change between the samples after normalization with *GAPDH* or U6 for mouse or bovine COC, respectively. The presence of a single dissociation curve confirmed the amplification of a single transcript and lack of primer dimers.

Statistics

Results of multiple repeats were presented as means ± SEM. A one-way analysis of variance (ANOVA) followed by Newman-Keul multiple comparison test was used to determine statistical differences between groups. Bartlett's test was included to ensure equal variance in the group. If the data did not follow a normal distribution, the data sets were log transformed before performing the statistical analyses.

RESULTS

Characterization of follicular EVs

To confirm that follicular EVs were present in our isolates, we used a combination of techniques. Electron microscopy revealed a heterogeneously sized population of circular vesicles, 50-200 nm in diameter (Fig III-1A from small antral follicles; Fig III-1B

from large antral follicles), many with the characteristic concave centers that result from the collapsing of the EV upon drying on the film (Fig III-1*) . The purity of the follicular EV preparation was confirmed as few protein conglomerates were observed (dense/dark objects). We further characterized the follicular EVs from small and large follicles using nanoparticle tracking analysis (Fig III-1C). Follicular EVs ranged in size between ~30 to 325 nm with an average size of 142 and 128 nm for EV from small and large, respectively. CD81, an established exosome marker, was used to confirm the presence and enrichment of exosomes in the EV preparations. We found that CD81 was highly enriched in EVs with a higher level in EVs derived from small follicles (Figure III-1C).

Figure III- 1 Characterization of follicular EVs from bovine follicular fluid.

After centrifugation and washing isolated follicular EVs were examined by negative staining on an electron microscope to determine the presence and characteristics of the follicular EVs. Both small (A) and large (B) antral follicles contained EVs of varying sizes, mostly spherical and some with the concave centers that are characteristic of exosomes (*). (C) Nanoparticle tracking analysis (NTA) indicates that EVs collected from small and large follicles are similar in size. NTA was repeated on three isolates of follicular EVs collected on different days and are overlaid in this figure to graphically demonstrate the variation between these follicular EV isolates. The average diameters (nm) of particles are shown for each of the three independent preparations of small and large antral follicle EVs.

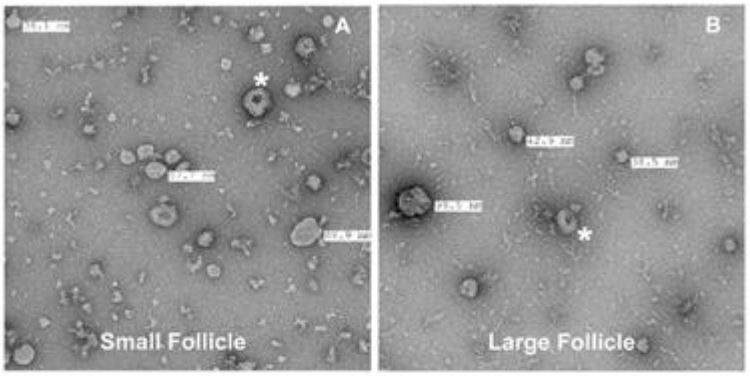
A
B
Small Follicle
Large Follicle

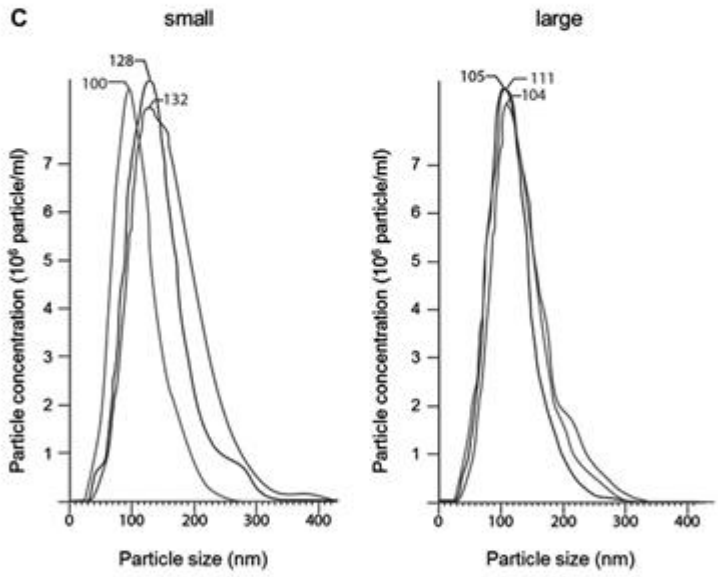
C
small
large
128
100
132
105
111
104
Particle concentration (10^6 particle/ml)
Particle size (nm)
0
100
200
300
400
1
2
3
4
5
6
7

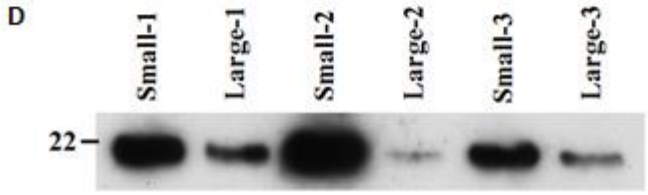
D
Small-1
Large-1
Small-2
Large-2
Small-3
Large-3
22

Uptake of follicular EVs by cumulus cells

To determine if bovine follicular EVs are taken up by mouse cumulus cells, PKH67-labeled follicular EVs were cultured with COC for 16 hr. Green fluorescent punctate spots (internalized EVs) were observed in the cytoplasm of cumulus cells and localized near the nucleus (Fig. III-2). Follicular EVs were detected in all layers of the expanded cumulus including those cells farthest from the oocyte (Fig. III-2A) as well as those cells next to the zona pellucida (i.e., corona radiata; Fig. III-2C). To ensure that nonspecific staining of cells from leftover dye was not occurring, we also cultured COC with the supernatant from the last wash, no staining was detected (Fig. III-2B). We also did not detect uptake of follicular EVs by the oocytes of intact COC although we did observe evidence of EVs associated with the transzonal processes, which span the zona pellucida to contact the oocyte (not shown).

Figure III- 2 Cumulus cells uptake follicular fluid EVs during COC culture.

Mouse COC were cultured 16 hr with PKH67 labeled bovine follicular EVs. Individual COC were imaged in serial z-sections on a Zeiss Pascal confocal microscope (40x) and examined for internalization of follicular EVs. In the expanded COC, internalized follicular EVs are evident as green spots within cumulus cells both in the outer layer of cumulus cells (A) and in cumulus cells located adjacent (C) to the oocyte (o=oocyte). To insure that the COC labeling was result of EV uptake, the final wash of the follicular EVs PKH67 labeling process was added to COCs and cumulus cells were all negative for PKH67 (B). Distance between serial z-stack A and C was 30 μm within the same COC. A' and C' are same as A and C but with DIC turned off. A'' and C'' are enlargements from the boxes identified in A' and C'. Scale bar = 10 μm.

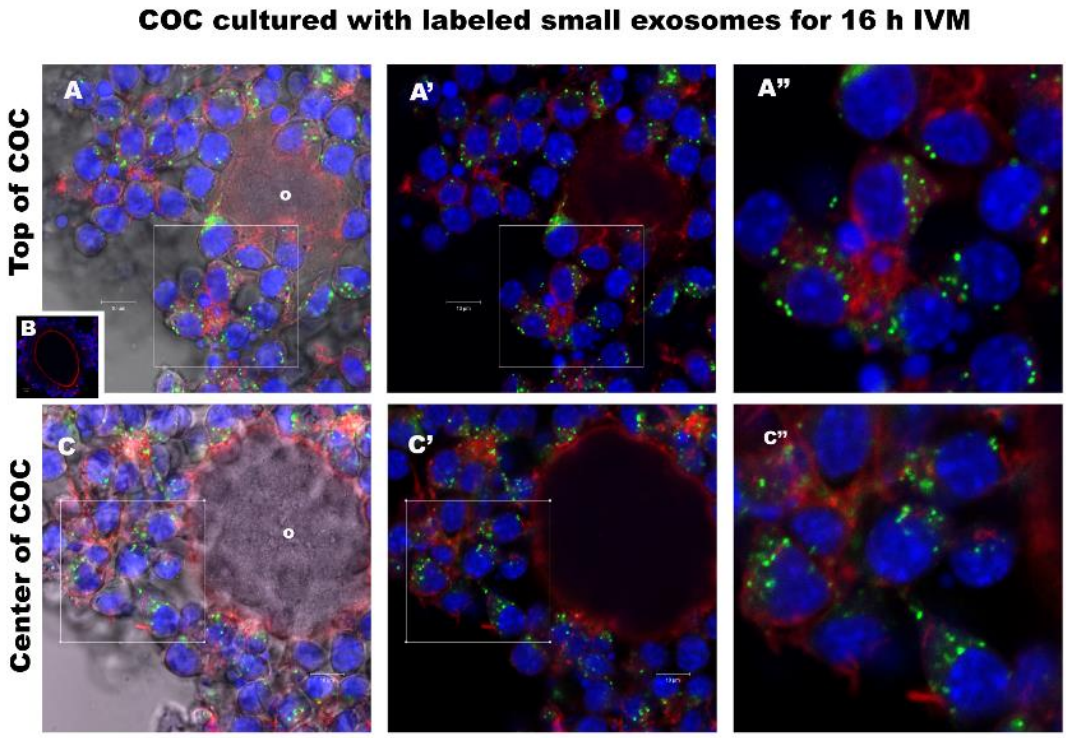
COC cultured with labeled small exosomes for 16 h IVM
Top of COC
Center of COC
A
A'
A"
B
C
C'
C"
o
o

Follicular EVs induce cumulus expansion

To determine if follicular EVs have a physical effect on the expansion of the COC, we *in vitro* matured mouse COC with or without the addition of bovine follicular EVs (Fig III-3). Differential interference contrast (Nomarski) imaging was used to determine the diameter of COC at the beginning (0 hr) and at the completion of the 16 hr mouse IVM protocol. The COC cultured without serum (PVA only control) did not expand during culture (negative control; Fig III-3A). Addition of 10% FBS (positive control) caused an increase in the diameter of the COC (cumulus expansion; Fig III-3B). Similar, to the positive control, follicular EVs from both small (3-5 mm) and large (>9 mm) bovine antral follicles induced cumulus expansion (Fig III-3C, 3D). Analysis of changes in COC diameter (percentage) confirmed that follicular EVs from both small and large antral follicles could induce cumulus expansion significantly greater than occurred in medium alone (i.e., negative control; Fig III-3E). Paradoxically, EVs isolated from small antral follicles exhibited a greater effect on cumulus expansion than those isolated from larger preovulatory follicles when cultured without FBS. To determine if the observed effects of follicular EVs was due to contaminants of EV from blood serum, we next tested COC expansion in media which contained 10% FBS plus follicular EVs. The follicular EVs from both small and large follicles increased cumulus expansion over that

observed for COC cultured with FBS (EV containing) alone, indicating that follicular EVs had an additive effect over any possible effects of FBS EVs (Fig III-3F). Since whole serum such as FBS contains endogenous EVs we also cultured COC with either whole FBS or FBS that was processed by ultra-centrifugation and filtration to remove endogenous EVs (EV-free FBS; EF-FBS). In these experiments there was no difference between FBS with or without the native serum EVs (Fig III-3G). These results indicate that cumulus expansion in response to EV from antral follicles is specific to follicular EVs and not a general of effect EVs from serum.

Next, we evaluated whether the effects of bovine follicular EVs on mouse COC could be duplicated using bovine follicular EVs on bovine COC. Consistent with the mixed species experiments using bovine EVs with mouse COC, bovine follicular EVs from both small (Fig III-4B) and large (Fig III-4C) antral follicles induced expansion of bovine COC.

Figure III- 3 Bovine follicular EVs induce mouse cumulus cell expansion.

Mouse COC were matured with follicular EVs from either small or large antral bovine follicles. COC were imaged by DIC at the beginning of culture (0 hr) and end (16 hr). Negative control COC cultured with no FBS and with no follicular EVs did not expand (A). COC cultured with either FBS (B; positive controls), or with follicular EVs from small antral (C) or large antral (D) follicles induced cumulus expansion. Cumulus expansion was quantified and the percent change in diameter of the COCs after 16 hr of in vitro maturation is shown. **Panel E** - COCs cultured with no serum or EV exhibited very little expansion. In the absence of serum, cumulus expansion induced by follicular EVs from the large antral follicles was significantly less than that induced by small antral follicle EVs (A). **Panel F** - COC matured with follicular EVs added to media containing FBS. COC cultured in FBS exhibited some expansion and follicular EVs increased cumulus expansion over that of whole FBS (i.e., FBS containing endogenous EVs). **Panel G** – COC matured in whole FBS, extracellular vesicle-free FBS (EV-FBS), with and without follicular EVs from small or large follicles. Removing serum endogenous EVs from the FBS had no effect on cumulus expansion, while addition of follicular EVs still significantly increased COC expansion (C). [a, b, c]Means ±SEM with different superscripts are significantly different ($P<0.05$).

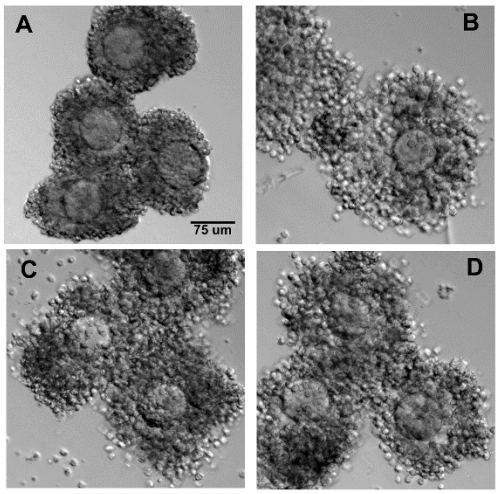
A
B
75 um
C
D

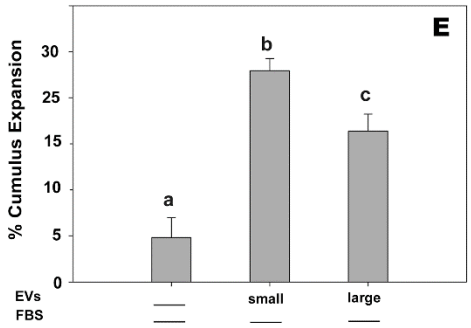
E
% Cumulus Expansion
30
25
15
10
5
0
a
b
c
EVs
FBS
small
large

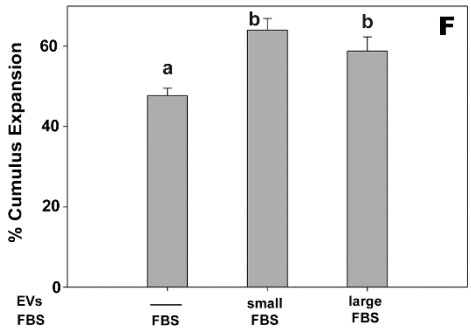
F
% Cumulus Expansion
60
40
20
0
a
b
b
EVs
FBS
FBS
small
FBS
large
FBS

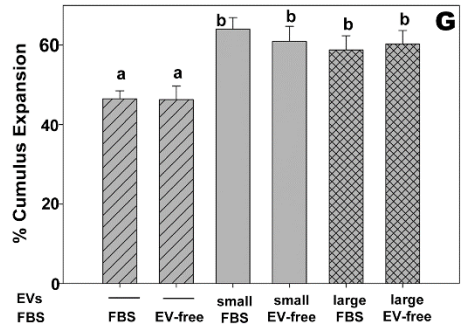
G
% Cumulus Expansion
60
40
20
0
a
a
b
b
b
b
EVs
FBS
FBS
EV-free
small
FBS
small
EV-free
large
FBS
large
EV-free

Figure III- 4 Bovine follicular EVs induce cumulus expansion of bovine COC.

Bovine COC were matured with follicular EVs from either small or large antral bovine follicles. COC were imaged by DIC at the beginning of culture (0 hr) and following in vitro maturation (24 hr). Negative control COC cultured with no FBS and with no follicular EVs did not expand (A). COC cultured with either small follicle EVs (B), or with large follicle EVs (C) exhibited increased cumulus expansion. Scale bar = 50 μm.

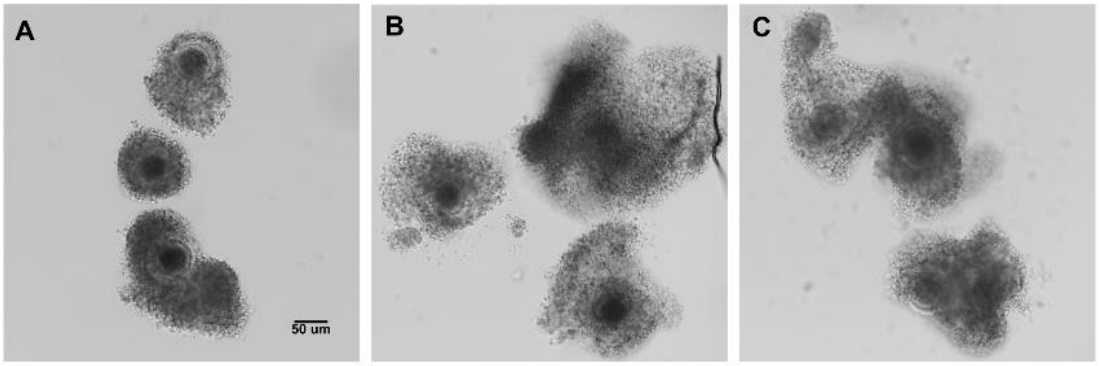
A
50 um
B
C

Analysis of COC expansion marker genes

To determine if follicular EVs affect the expression of genes associated with cumulus expansion, we examined the expression of three genes with known functions in COC expansion: *Ptgs2*, *Ptx3* and *Tnfaisp6*. Treatment of mouse COC with bovine follicular EVs from small antral follicles significantly increased expression of *Ptgs2* and *Ptx3* with the fold change of 2.7 and 20.3, respectively (Fig III-5A). There was also a trend for increased expression of *Tnfaisp6* (average fold change of 3.5) although this change did not reach significance ($P<0.08$). Bovine COC matured with bovine follicular EVs from small antral follicles also significantly up regulated expression of *Ptgs2* (7.1 fold), *Ptx3* (5.1 fold) and *Tnfaip6* (7.5 fold; Fig III-5B). Follicular EVs from large antral follicles did not induce the expression of *Ptx3* or *Tnfaip6,* however, there was a decrease in the expression of *Ptgs2* in mouse COC.

Figure III- 5 Follicular fluid EVs induce genes involved in cumulus expansion. COC from mice (A) and cows (B) were matured for 16 hr and 24 hr, respectively, followed by quantitative RT-PCR analysis of *Ptgs2*, *Ptx3* and *Tnfaip6* levels. Small follicle EVs increased cumulus gene expression in both mouse (A) and bovine COC (B), while large follicle EVs did not. Mouse COC *Tnfaip6* expression trended ($p= 0.08$) to increase. [a, b]Means ±SEM with different superscripts are significantly different ($P<0.05$).

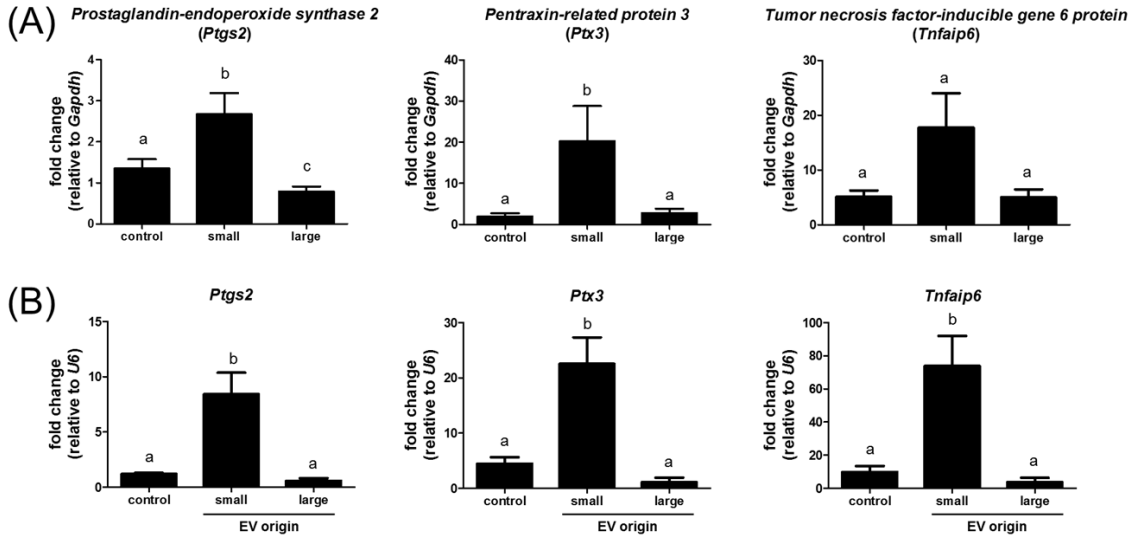
(A)
Prostaglandin-endoperoxide synthase 2 (Ptgs2)
Pentraxin-related protein 3 (Ptx3)
Tumor necrosis factor-inducible gene 6 protein (Tnfaip6)
fold change (relative to Gapdh)
control
small
large
(B)
Ptgs2
Ptx3
Tnfaip6
fold change (relative to U6)
EV origin

DISCUSSION

Ovarian follicular fluid is enriched with proteins, RNA, and extracellular vesicles. Our studies have demonstrated for the first time that follicular EVs can impact ovarian function. Follicular EVs were able to modify cumulus gene expression and to support cumulus expansion. Interestingly, follicular EVs isolated from small antral follicles exhibited more activity than those from large follicles (Fig. III-3), even though *in vivo*, COC from small follicles do not undergo expansion. However, when bovine COC from small antral follicles are released into culture they are functionally capable to undergo expansion (Fig III-4). And, similar to the murine COC, the bovine COC exhibited significant increased gene expression when exposed to EV from small but not large antral follicles (Fig. III-5A and 5B). This is an interesting phenomenon, which is discussed below and poses many questions for examination in future studies.

Mammalian COC secrete a hyaluronan-enriched extracellular matrix that separates the cumulus cells and the oocyte leading to what is termed cumulus expansion in response to the LH surge. LH receptors are found primarily in the theca and mural granulosa of antral follicles but not in the early cumulus cells. It is theorized that cumulus expansion is triggered *in vivo* in response to signals that are generated first by the mural granulosa cells and transmitted through the follicular fluid to affect the cumulus

cells. Indeed, many studies support a model by which EGF ligands; such as amphiregulin, epiregulin and epigen are released from mural granulosa cells to subsequently effect the cumulus cell gene expression and expansion (Carletti and Christenson 2009, Conti 2010). Whether these growth factors are simply released into the follicular fluid and work in a juxtacrine manner down a concentration gradient, or whether they are also partially released as a constituent of EVs is currently unknown. Interestingly, EGF-ligands and active receptors (ErbB1) have been detected in EVs released from cancer cells (Sanderson, Keller et al. 2008). While we did not detect any EGF-ligands in the follicular fluid EVs, the negative results may be partially due to problems with antibody specificity to the bovine molecules (data not shown). RNAseq, proteomic and lipidomic studies that can unbiasedly identify follicular EV RNAs, proteins and phospholipids are underway in our laboratory to address this question. The fact that small follicle EVs exhibited the greatest increase in cumulus expansion however argues against an EGF-ligand as being the active component within or on the surface of the follicular EVs as these ligands are not typically expressed by mural granulosa cells until after the LH (Park, Su et al. 2004, Sekiguchi, Mizutani et al. 2004).

Our recent studies on the content of follicular EVs have identified changes in the EV cargo from bovine follicles of different sizes (Navakanitworakul, Hung et al. 2016).

EVs from small antral follicles contained higher copy numbers of miRNA than did those EVs from large follicles and the miRNA present were also different. In spite of this general trend for decreasing quantities of miRNA, the levels of five specific miRNA significantly increased: miR-92b, miR-150, miR-328a-3p, miR-450a-5p, and miR-2419-5p. Two additional miRNA declined as follicle size increased: miR19a-3p and miR-335 (Navakanitworakul, Hung et al. 2016). The function of these changes is unknown. These differences between small (younger) and large (advanced) antral follicles might imply either an active and selective mechanism exists for the loading of cargo into follicular EVs, or that simply the content of the EVs changes as a reflection of cellular changes in miRNA expression. Studies are ongoing in our laboratories to identify the mechanisms of loading of miRNA into follicular EVs and to determine if this process is passive or controlled as our earlier study indicates.

Follicular EVs have been characterized by multiple groups (Revelli, Delle Piane et al. 2009, da Silveira, Veeramachaneni et al. 2012, Sang, Yao et al. 2013, Sohel, Hoelker et al. 2013), yet we still do not yet know which cells produce the EVs found in follicular fluid. We theorize that EVs are likely released by the neighboring granulosa cells (mural and cumulus) with lesser contributions from the oocyte and the theca cells because it is the granulosa cells that contact the follicular fluid directly. However, until

properly tested this remains unknown. It is generally considered that EVs would be too large to have entered from the theca vasculature, based on observations that large serum proteins >100 kDa are rate limited do enter the follicular fluid freely (reviewed in (Rodgers and Irving-Rodgers 2010)). A protein of 100 kDa is generally considered to be less than 10 nm in diameter whereas our nanoparticle tracking analysis and electron microscopy (Fig. 2) found that follicular EVs range from the 30 nm to 350 nm in diameter. Thus, EVs would be considered to be much larger than the largest serum proteins and as a result may be limited in their ability to pass through the basement membrane separating the theca and granulosa. Of note however, the lipid bilayer of EVs could also dramatically impact their transport. The passage of EVs through a cellular barrier by cell uptake, intracellular transport and subsequent export cannot be ruled out and ongoing studies are underway to determine the original source and transport mechanisms of follicular EVs (da Silveira, Veeramachaneni et al. 2012). In addition to our lack of knowledge regarding the cells that release follicular EVs, our current work as well as previous published studies that describe follicular exosomes and microvesicles (Revelli, Delle Piane et al. 2009, da Silveira, Veeramachaneni et al. 2012, Sang, Yao et al. 2013, Sohel, Hoelker et al. 2013), do not directly address the mechanism of follicular EV biogenesis or release. Without this knowledge, it is impossible to differentiate between

large exosomes and small microvesicles. Therefore, we have chosen to call the bi-lipid vesicles we observe in follicular fluid as extracellular vesicles (EVs), indicating that the material is probably a mixture of exosomes and/or microvesicles, and not a population of one type or the other. In addition to an overlap in size, it is now known that many of the so called "exosome specific" markers can also be associated with some microvesicles. This may not be a trivial concern, as major differences in the cargo and membrane components derived from these two different pathways may exist.

EVs isolated from follicles of different sizes differ in their ability to affect gene expression in the cumulus cells. We found increased expression of genes with known functions in cumulus expansion were activated by EVs from small but not large follicles (Fig. III-5). This result is counter intuitive since it might be assumed that the COC within the large follicles that normally reacts to the LH surge to induce cumulus expansion. One possible explanation is that small follicles contain EVs that support cumulus expansion and that these EVs are bound / taken up by COC during follicular development and the remaining (or newly produced) EVs in large follicles lack the ability to promote cumulus expansion. Another possibility is that follicular fluid from large follicles contains inhibitory factors that are not active in small antral follicles. Hosoda and Terada (2007) (Hosoda and Terada 2007) used filtration fractionation of follicle fluid

from large bovine follicles and determined that a >100 kDa fraction was associated with an inhibitory factor that blocked the cumulus expanding activity of EGF (Hosoda and Terada 2007). Since our isolation techniques used centrifugation primarily rather than filtration, the type of vesicles from our studies and the isolates from the Hosoda and Terada (Hosoda and Terada 2007) might overlap in size. It is therefore possible that an inhibitory factor associated with our EVs isolated from large follicles might limit their biologic activity. Future studies will be aimed at determining the differences in follicular EV cargos as follicles mature.

In conclusion, our studies have found a physiological effect of follicular EVs. These EVs were able to stimulate cumulus expansion and to up-regulate cumulus gene expression *in vitro*. Our current and futures studies are directed towards further defining the miRNA and protein cargos associated with follicular EVs and mechanisms of uptake, release, and transport within and between cells of the ovarian antral follicle.

X. Chapter IV: Follicular Extracellular Vesicles Differentially Regulate Bovine Granulosa Cell Proliferation in a Stage-Specific and Src/JNK-Dependent Manner

Introduction

The most important role of the female gonad, the ovary, is to produce fertilizable and healthy eggs. In the ovary, the oocyte is enclosed within the ovarian follicle, which is one of the most dynamic tissues in the body, with tremendous proliferation, differentiation, and apoptosis happening within days. At the later stages of folliculogenesis (the process of follicle growth), the antral follicle is defined by means of the formation of an antrum in a follicle, which is filled with a serum-like fluid called follicular fluid (FF) (Hennet and Combelles 2012). Follicular fluid is a rich, complex fluid containing nucleic acids, proteins, steroids, and hormones, and is thought to isolate the oocyte and its associated cumulus cells from the endocrine mural granulosa cells. This isolation however, has given rise to complicated and intricate cellular networks that facilitate the exchange of cellular messages between the cumulus-enclosed oocyte and the segregated mural granulosa cells (Rodgers and Irving-Rodgers 2010). Recently, extracellular vesicles (EVs) have also been found in the FF, and they have been hypothesized to act as yet another cellular mechanism to facilitate cross talk across the follicular antrum (da Silveira, Veeramachaneni et al. 2012, Sang, Yao et al. 2013, Sohel, Hoelker et al. 2013, Diez-Fraile, Lammens et al. 2014, Santonocito, Vento et al. 2014).

Release of EVs appears to be a phenomenon exhibited by all cells with two major

known mechanisms of EV biogenesis (Cocucci and Meldolesi 2015). This includes exosome biogenesis, where inward budding of the multivesicular body (MVB) membrane generates intraluminal vesicles (i.e., exosomes of 30-200 nm diameter) that are released into the extracellular space upon fusion of MVB with the plasma membrane (Kowal, Tkach et al. 2014). Microvesicles are produced by plasma membrane blebbing and results in a broad range (30-1000 nm) of vesicles sizes (Alenquer and Amorim 2015). Due to the overlap of markers and sizes of exosomes and microvesicles, "extracellular vesicle" (EV) has been adopted as an inclusive term that encompasses both kinds of vesicles outside the plasma membrane (Cheung, Keerthikumar et al. 2016). Exosomes and microvesicles both have been implicated in transmission of signaling molecules including nucleic acids, lipids and proteins to influence cellular behaviors (Tkach and Thery 2016). The first observation of functional EVs outside of cells was made in 1967 by Dr. H. Clarke Anderson in his pioneering studies of bone calcification (Anderson 1967). Recently, EVs have been implicated in a variety of physiologic and pathologic processes within various tissues. In the cardiovascular system, EVs has been shown to have a cardioprotective role in which they are enriched in cardioprotective miRNA (Barile, Moccetti et al. 2016). Extracellular vesicles also have known to be able to serve as the communication mediators between myelinating glia and neurons, which is

important for neuronal survival and synapse plasticity (Budnik, Ruiz-Canada et al. 2016). In pathological conditions, EVs have been described participating in the pathogenesis of neurodegenerative diseases and have been applied as potential biomarkers (Thompson, Gray et al. 2016). Moreover, tumor cells are known to secrete substantial amounts of EVs, and the tumor secreted EVs appear to be critical for tumor survival, proliferation, and metastasis (Tkach and Thery 2016).

Extracellular vesicles isolated from follicular fluid are known to differentially carry miRNA dependent upon the origin of the samples be it from different stages of the follicular maturation, different ages of the donor females, and under different disease conditions such as polycystic ovarian syndrome (da Silveira, Veeramachaneni et al. 2012, Sang, Yao et al. 2013, Sohel, Hoelker et al. 2013, Diez-Fraile, Lammens et al. 2014, Roth, McCallie et al. 2014, Santonocito, Vento et al. 2014, da Silveira, Winger et al. 2015, Moreno, Nunez et al. 2015). In addition, ovarian granulosa cells have been shown to take up fluorescently labeled vesicles (da Silveira, Veeramachaneni et al. 2012, Sang, Yao et al. 2013, Sohel, Hoelker et al. 2013, Diez-Fraile, Lammens et al. 2014, Roth, McCallie et al. 2014, Santonocito, Vento et al. 2014, da Silveira, Winger et al. 2015, Moreno, Nunez et al. 2015). Recently, follicular fluid EV treatment of cumulus-oocyte-complexes was shown to induce cumulus expansion and initiate the corresponding

cumulus gene expression changes associated with expansion (Hung, Christenson et al. 2015). Additionally, treatment of granulosa cells with follicular EVs from both mid-estrus and pre-ovulatory follicles which had abundant levels of miR-27b, miR-372, and miR-382 was shown to decrease expression of inhibitor of DNA binding/differentiation 2 (ID2), a target of these abundant miRNA (da Silveira, Carnevale et al. 2014). Both of these studies while indicating a functional effect of EVs are compromised by the purity of EV preparations, as EV isolation even under "gold-standard" ultracentrifugation protocols are still far from 100% pure. This has raised concerns of whether material that co-precipitates may also be contributing to the functional effects attributed to EVs. In our original study, we observed different functional effects of the follicular EVs based on the size of the follicle from which the fluid was isolated (Hung, Christenson et al. 2015). In this current study, we investigate whether stage-specific follicular EVs have differential effects on granulosa cell proliferation, a cellular function critical for rapidly growing follicles as they develop into ovulatory follicles. In this study we applied a combination of EV isolation methodologies to yield highly purified EVs and then examined their effects on cell signaling pathways involved in cellular proliferation and EV uptake by cultured granulosa cells.

Results

EV characterization and uptake of EVs by granulosa cells

Follicular fluid EVs were characterized using a battery of different molecular and visual methods. Western blot analysis for the exosomal marker, CD81, indicated that the amount of CD81 decreased as follicle size increased [equivalent protein loaded (10 μg)/lane; Figure IV-1A]. Nanoparticle tracking analysis indicated a single peak of 100-150 nm diameter particles across the different sized follicles (Figure IV-1B), and follicular fluid from 3-5mm follicles (hereafter called small follicles) was more concentrated in particles than those from 6-9mm and >9mm follicles (hereafter called medium and large follicles, respectively). Electron microscopy of EVs negatively stained on grids indicated the presence of a typical cup shape morphology in all the samples indicating the existence of EVs, smaller material (10-20 nm) was prominently observed in the background (Figure IV-1C).

In order to confirm that the granulosa cell can take up EVs, granulosa cells were exposed to PKH67-fluorescently labeled EVs. Green puncta were observed in the cytosol of granulosa cells indicating that EVs were taken up by granulosa cells (Figure IV-2B). Furthermore, flow-cytometry of granulosa cells exposed to the fluorescently labeled EVs also indicated uptake (Figure IV-2B). The potential effect of residual dye

was excluded using a negative control (Figure IV-2A).

Figure IV- 1 **Characterization of follicular fluid EVs.**

Extracellular vesicles from small (3-5mm), medium (6-9mm), and large (>9mm) antral follicles were subjected to A) Western blot analysis for the EV marker, CD81, using equal volumes of protein as demonstrated by a total protein staining, B) nanoparticle tracking analysis (NTA) shows the mean size distribution and numbers of particles for 3 independent samples at the three follicle sizes and C) transmission electron microscopy of negative stained EVs. Sizes of select individual EVs are show in nanometers.

(A)

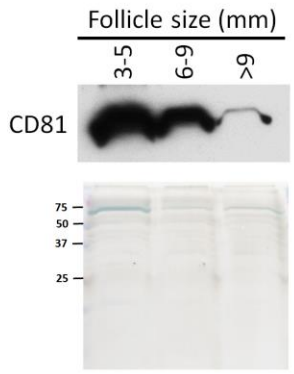
Follicle size (mm)
3-5
6-9
>9
CD81
75
50
37
25

(B)

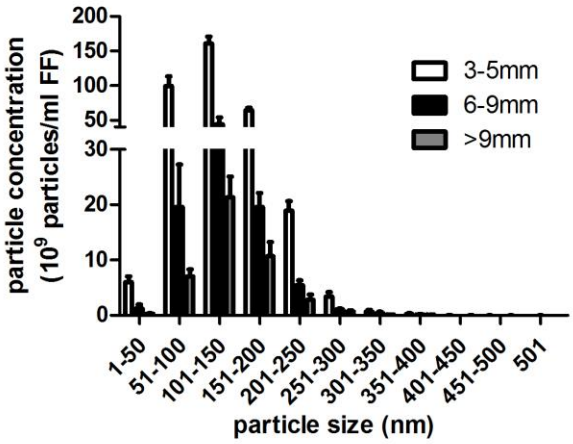
particle concentration
(10^9 particles/ml FF)
200
150
100
50
30
20
10
0
3-5mm
6-9mm
>9mm
1-50
51-100
101-150
151-200
201-250
251-300
301-350
351-400
401-450
451-500
501
particle size (nm)

(C)

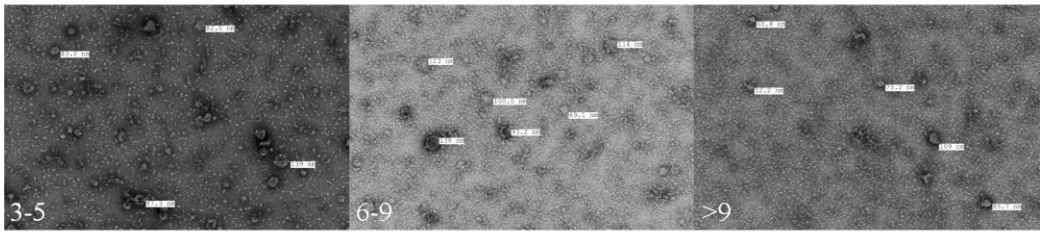
3-5
6-9
>9

Figure IV- 2 **Uptake of fluorescently labeled EVs by bovine granulosa cells.**

Bovine granulosa cells from 3-5 mm follicles were exposed to PKH67-labeled EVs isolated from small bovine antral follicles and then subjected to confocal imaging (upper) and flow cytometry (lower). A) Granulosa cells exposed to negative control showed no staining and complete lack of fluorescence by flow cytometry. B) Treatment of granulosa cells with labeled EVs showed punctate staining after 24 h of incubation and FITC intensity detected by flow cytometry was confirmed by confocal microscopy.

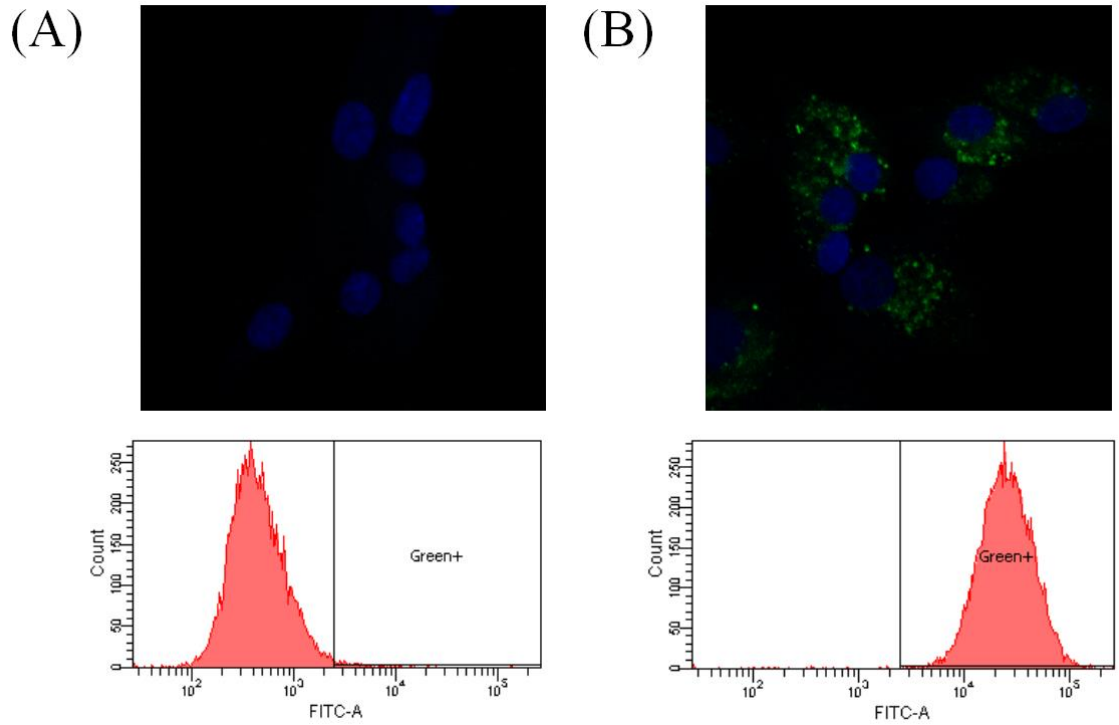
(A)
(B)
Count
Green+
FITC-A
Count
Green+
FITC-A

Follicular-stage specific EVs modulate granulosa cell proliferation

Treatment of granulosa cells for 24 h with EVs (100 μg protein/ml) from small antral follicles induced a 3.4-fold increase in BrdU incorporation compared to the non-treated controls while EVs from medium and large follicles only increased BrdU incorporation 2.3- and 1.6-fold, respectively (Figure IV-3A). The effect of small follicle EVs on BrdU incorporation were further strengthen by showing that the effect of EVs was concentration-dependent (5, 20, 100 μg/ml; Figure IV-3B). Treatment with EVs from small follicles increased granulosa cell number by 2.03 and 2.11 fold as determined by hematocytmetry counting in two independent experiments (n=2). In order to eliminate other confounding aspects that might influence the cell proliferation assay, we examined cell attachment and cell apoptosis following exposure to EVs. After 30 min of simultaneously seeding of granulosa cells and EVs, the number of granulosa cells, which attached on the plate were not different across treatment groups but were higher than control (Figure IV-3C). Additionally, we observed no differences in granulosa cell apoptosis after treatment with EVs for 24 h as determined by propidium iodide staining followed by flow cytometry (Figure IV-3D).

Because the cell proliferative activity was greatest in small follicles and these collections contain a mix of atretic and non-atretic follicular fluid, we further refined the

experiment by collecting follicular fluid from large numbers (~100 follicles/each replicate) of individual small antral follicles. These follicles were then individually determined to be either non-atretic or atretic based on granulosa cell expression of tissue inhibitor of metallopeptidase 1 (TIMP1) for each follicle. Three independent collections were done to generate three pools of follicular fluid from atretric and 3 pools from non-atretic FF and the EVs isolated from these pools were characterized for CD81 and ability to influence cell proliferation. Follicular EVs from non-atretic and atretic follicles carried similar levels of exosome marker CD81 and showed equivalent activities on GC proliferation (Figure IV-4).

To further eliminate the possibility that residual molecules co-precipitating with EVs might be influencing cell proliferation, which can be seen in Figure 1C, EVs were further purified through size exclusion columns. This purification step removed most of the residual molecules in the background yielding a highly purified preparation of follicular EVs (Figure IV-5A). This additional column purification step retained the activity on inducing granulosa cell proliferation (Figure IV-5B), and further indicates that the EVs are having a major influence on granulosa cell proliferation.

Figure IV- 3 **Effects of follicular fluid EVs on granulosa cell proliferation, attachment, and apoptosis.**

Granulosa cells were exposed to follicular fluid EVs from small (3-5mm), medium (6-9mm), and large (>9mm) follicles and evaluated for effects on: A, B) cell proliferation, C) cell attachment, and D) apoptosis. A) Depicts changes following 24 h exposure to EVs (100 μg/ml) from the different sized follicles, B) Depicts a concentration-dependent effect of EVs from small antral follicles on cell proliferation. C) Depicts effect of EVs from different sized follicles on cell attachment, while D) depicts effect of EVs from different sized follicles on apoptosis. ^{a,b,c,d}Means ± SEM (n=3) with different superscripts were statistically different ($p<0.05$).

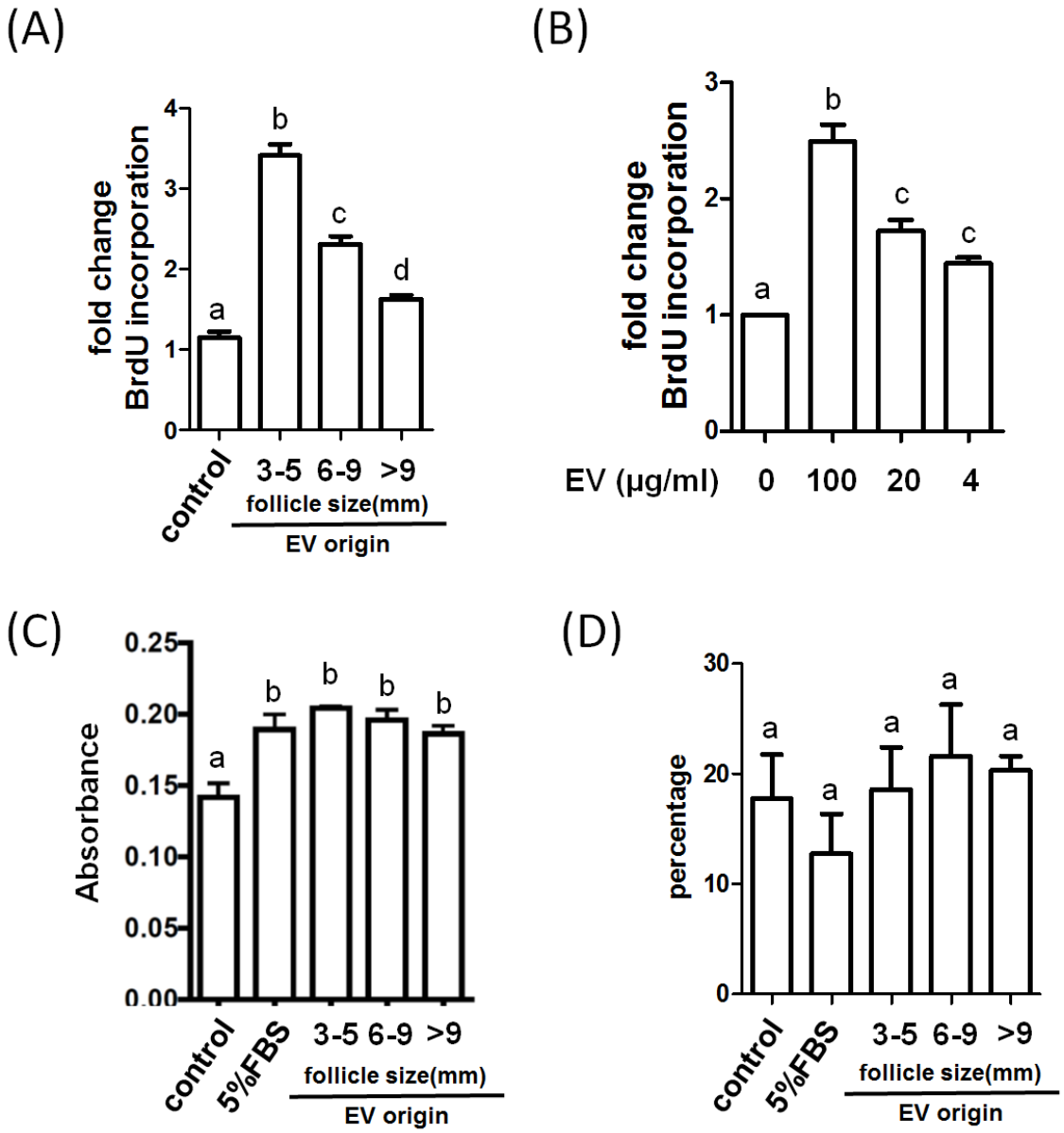
(A)
fold change BrdU incorporation
0
1
2
3
4
a
b
c
d
control
3-5
6-9
>9
follicle size(mm)
EV origin
(B)
fold change BrdU incorporation
0
1
2
3
a
b
c
c
EV (μg/ml)
0
100
20
4
(C)
Absorbance
0.00
0.05
0.10
0.15
0.20
0.25
a
b
b
b
b
control
5%FBS
3-5
6-9
>9
follicle size(mm)
EV origin
(D)
percentage
0
10
20
30
a
a
a
a
a
control
5%FBS
3-5
6-9
>9
follicle size(mm)
EV origin

Figure IV- 4 **Comparison of EVs from non-atretic and atretic follicles.**

A) Follicles were categorized by expression of TIMP1 (delta Ct method) as non-atretic or atretic. For each replication (n), a three Ct difference was used to define the groups, FF from all follicles that exhibited an intermediate delta Ct were discarded. B) The fold change in BrdU incorporation for the pooled follicular EVs from non-atretic (n=3) or atretic (n=3) follicles are shown. ^{a,b}Means ± SEM with different superscripts were statistically different ($p<0.05$)

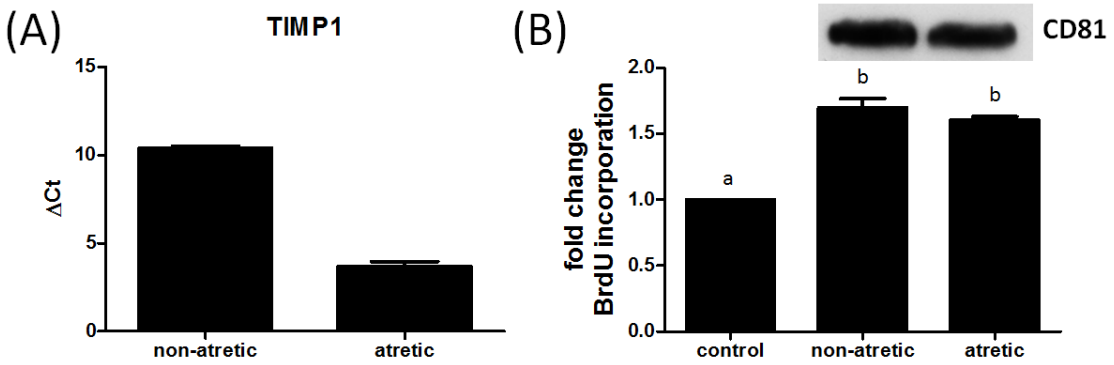
(A)
TIMP1
ΔCt
15
10
5
0
non-atretic
atretic
(B)
CD81
fold change BrdU incorporation
2.0
1.5
1.0
0.5
0.0
a
b
b
control
non-atretic
atretic

Figure IV- 5 **Comparison of the purity and activity of EV preparations following isolation by ultracentrifugation or ultracentrifugation plus size exclusion chromatography.**

Extracellular vesicles isolated by both protocols were A) imaged under TEM, and B) activities on cell proliferation were tested. ^{a,b} Means ± SEM (n=3) with different superscripts were statistically different ($p<0.05$).

(A)

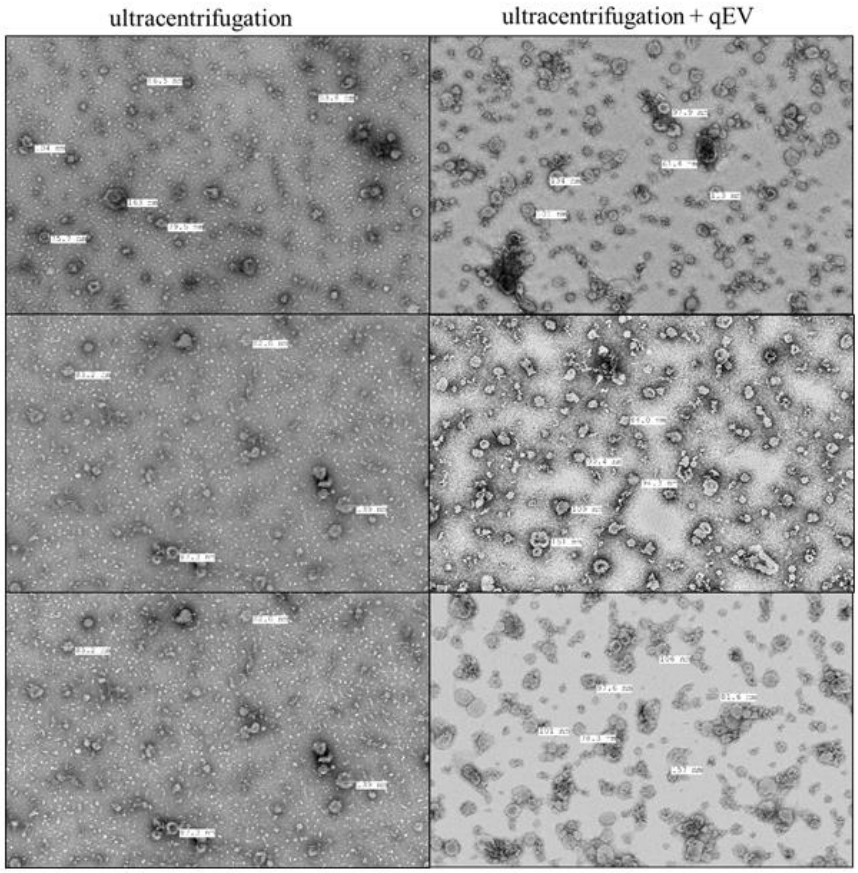
ultracentrifugation
ultracentrifugation + qEV

(B)

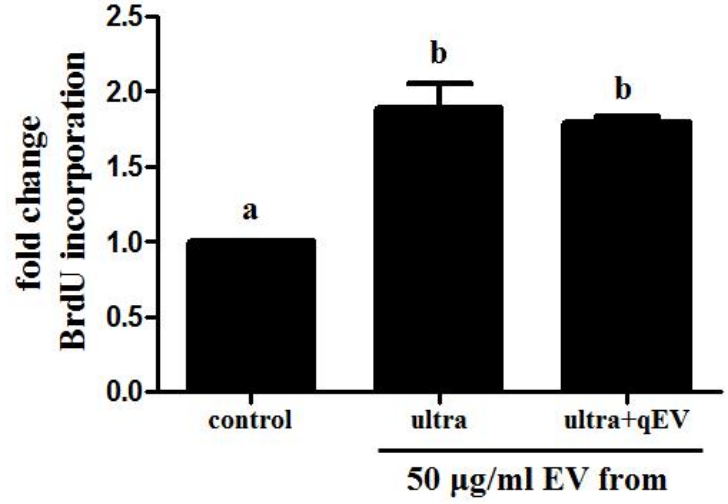
fold change
BrdU incorporation
2.5
2.0
1.5
1.0
0.5
0.0
a
b
b
control
ultra
ultra+qEV
50 µg/ml EV from

Small follicle EVs affect granulosa cell protein kinase cell signaling factors

To examine the cell signaling pathways that mediate EV action within the granulosa cells, we used a Kinexus antibody-based array that examines 877 cell signaling proteins. Bovine granulosa cells from small follicles were treated with or without EVs (100 μg protein/ml) for 24 hour as above and then cell lysates were collected and subjected to the antibody array. A total of 106 cell signaling proteins changed more than 25% after EV treatment in granulosa cells, with 66 increasing and 40 decreasing in total protein levels. Post-translational modifications of proteins (i.e., phosphorylation) also changed in granulosa cells exposed to EV, again looking at only those that changed 25% or more after EV treatment, we observed that 67 exhibited increased and 19 that had decreased phosphorylation (Table 1). Two of the top upregulated genes, Akt and Mcl-1 were verified by western blot (Figure IV-6).

Table IV- 1 Proteins showed 25% increase or decrease upon EVs treatment in the kinase array

Name	fold change	Name	fold change	Name	fold change	Name	fold change
Src*	39.72	PP4C (X/C)*	1.46	p38g MAPK*	1.31	ASK1	0.71
Mcl1*	3.53	B-Raf	1.45	Histone H2A.X	1.30	Cdc25C	0.70
p53*	3.02	PKR1*	1.44	PKCe*	1.30	Rb	0.70
RSK1*	2.67	MEK2*	1.43	SMG1*	1.30	DUSP6	0.69
Akt1 (PKBa)*	2.59	Hsp90b	1.43	ERK5	1.30	Kit	0.69
GSK3a*	2.22	Csk*	1.43	ZIPK*	1.30	Cyclin D1	0.68
PKA R2a (PKR2)*	2.16	COX2*	1.43	Hsp70*	1.29	PDK1	0.68
MEK2*	2.10	Ezrin*	1.42	Bcr*	1.29	CD63	0.68
ERK3*	2.06	ALK*	1.42	Kit*	1.29	Krs-1	0.68
PKCh*	2.01	ERK1	1.42	Hpk1*	1.29	Myc	0.68
Ephrin-B2*	1.88	p21 CDKI1*	1.42	BRD2*	1.29	CDK6	0.68
Hsp27*	1.86	CDK2*	1.41	mTOR*	1.29	CDK4	0.67
Tau*	1.86	KDEL Receptor (KR10)*	1.41	I1PP2A (PHAPI)*	1.29	ErbB2	0.66
PI3-Kinase*	1.84	B23 (NPM)*	1.41	PAK1*	1.28	CDK9	0.66
NIK*	1.82	Cdc2 p34	1.41	hHR23B*	1.28	AMPKa2	0.66
BCL*	1.80	p53*	1.41	CaMK2a*	1.28	Synapsin 1	0.65
MEK3b	1.80	Rac1/cdc42*	1.40	MAPKAPK2*	1.28	Paxillin	0.65
Trail*	1.79	FAK*	1.40	MEK5	1.27	FAS	0.64
MEK1*	1.75	MEK1*	1.40	MEK2*	1.27	PAKa	0.64
eIF2a*	1.75	VIM*	1.39	PYKSD8	1.27	IRS1	0.64
CaMK1d*	1.74	VEGF-C*	1.38	MyoD*	1.27	WNK1	0.64
Chk1*	1.74	RIP2/RICK*	1.38	PTP1D/SHP2*	1.27	Fos	0.63
MEK3/6	1.70	ERK5*	1.38	MST3*	1.26	MEK1 + B23(NPM)	0.63
GNB2L1	1.69	Rac1	1.37	ErbB4*	1.26	STAT3	0.62
Nek2*	1.69	Akt1 (PKBa)*	1.37	PLCg1*	1.26	Bcl-xS/L	0.61
EGFR*	1.67	eIF4E*	1.37	Tau*	1.26	PTEN	0.60
c-Cbl*	1.66	B23 (NPM)*	1.37	PKCg*	1.26	STAT4	0.60
Caveolin 1*	1.64	PYK*	1.37	LIMK1/2*	1.26	NMDAR2B	0.59
Nek2*	1.62	Catenin a*	1.36	PKCd*	1.25	Src	0.57
PKCg*	1.61	ILK1*	1.36	ERK1	1.25	PKG1b-NT	0.56
ZAP70*	1.60	HDAC4/5/9*	1.36	JAK2*	1.25	PKCt	0.53
Fes*	1.59	MEK3*	1.35	Smad2*	1.25	JAK1	0.53
Hsp47*	1.58	PKCl*	1.35	Elk1*	1.25	HDAC4	0.51
FAK*	1.58	MLC*	1.35	MEKK2	0.75	Abl	0.50
MST3*	1.58	NFKB p65*	1.35	CD45	0.75	CDK2	0.50
Csk*	1.56	MST1*	1.34	STAT2	0.75	IRAK1	0.45
Hsp27*	1.54	Jun*	1.34	Chk1	0.75	Integrin a4	0.43
PKCt*	1.53	LAR*	1.34	PKA Ca/b	0.74	Hsc70	0.42
PKCm (PKD)*	1.52	Lck*	1.34	CDK5	0.74	VEGFR2	0.39
Crystallin aB	1.52	ERK1*	1.33	RONa	0.74	STAT1	0.35
NME7*	1.52	CAMK2d*	1.32	Progesterone Receptor	0.74	STAT6	0.21
NFkappaB p65*	1.52	DNAPK	1.32	Rb	0.73	PKCl	0.05
CDK1*	1.51	SIK3*	1.32	Lck	0.73		
CPG16/CaMKinase VI*	1.51	Met*	1.32	JAK1	0.73		
FRK*	1.49	Cofilin*	1.31	GRK2	0.73		
TYK2	1.48	p70 S6K*	1.31	MEK3	0.73		
ANKRD3*	1.48	PKD (PKCm)*	1.31	IkBa	0.73		
CDK1/CDC2*	1.48	PP2A/Aa/b*	1.31	DUSP1 (MKP1)	0.72		
Caspase 3*	1.47	Cortactin*	1.31	MEK4	0.72		
HDAC5*	1.46	SOCS2*	1.31	Akt2 (PKBb)	0.71		

Covered box: phosphorylated antibodies

*target of abundant miRNA in large antral follicle

Figure IV- 6 **Western blot validation of kinase array results.**

Western blot analysis for Mcl1 and Akt confirmed that these top Kinase array proteins were increased. Equal protein loading was observed as indicated by similar actin levels.

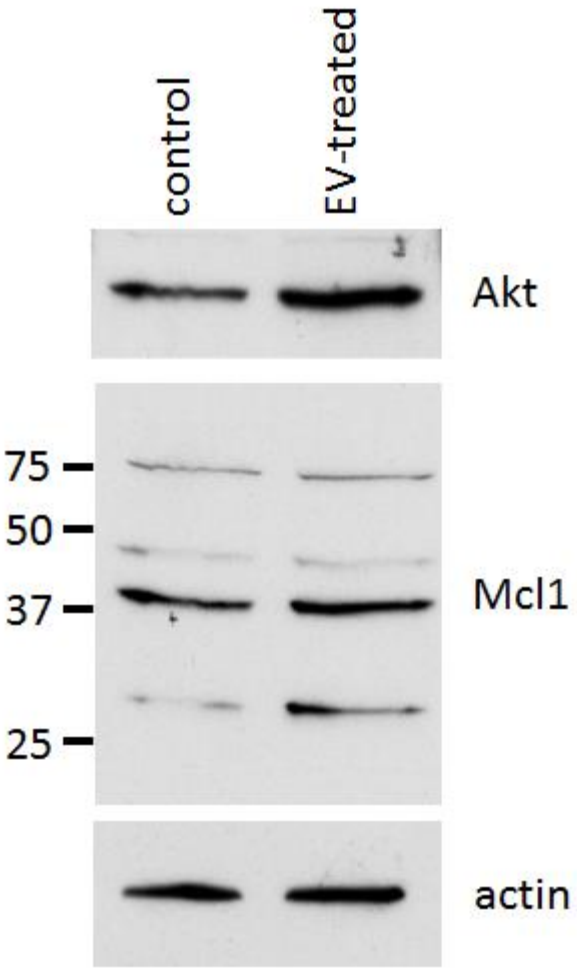
control
EV-treated
Akt
75
50
37
25
Mcl1
actin

Analysis of cellular signalling pathways

In order to elucidate possible cell signalling pathways, we used a combined approach using kinase array data and miRNA expression data. Breifly, we examined those proteins/translational modifcations which were up-regulated in response to EV treatment (from small follicles) and might be essential for EV-induced cell proliferation in small antral follicles. These genes would be predicted to decline as small follicles become large follicles as cellular proliferation decreases during this transititon. Since, microRNA (miRNA) function primarily to suppress expression of their target transcripts, we evaluated whether abundant miRNA present in EVs from large follicles (compared to small follicles) from our previous study (GEO-GSE74879) (Navakanitworakul, Hung et al. 2016), could modulate the kinase array identified proteins. We did this by comparing those predicted miRNA target genes to the list of kinase array identified genes which increased in cells treated with EVs. This resulted in an overlap of 101 genes that were subsequently analysed by IPA. These 101 genes were highly related to post-translational modification, cell growth, proliferation, and survival and to the signalling pathways of HGF, Erbb, GnRH, and Src (Figure IV-7).

Src and JNK signaling implicated in EV-mediated cell proliferation

In order to test the IPA analysis predictions and dissect out specific signaling pathways contributing to the EV-mediated cellular events, specific kinase inhibitors were applied into the cell culture system with/without the presence of EVs. Treatment with the Src inhibitor (PP2; 0-50 μM) and with the JNK inhibitor (SP600125; 0-50 μM) completely blocked induction of cell proliferation (i.e., BrdU incorporation) by EV treatment while not affecting the proliferation of GC receiving no treatment (Figure IV-8). Granulosa cells treated with the PI3K inhibitor LY294002; 0-50 μM) or with the MEK1/2 inhibitor (U0126; 0-50 μM) had decreased levels of EV-mediated proliferation with a dose-dependent trend but also affected the proliferation in the no-EV control groups (Figure IV-8). Treatment of GC with the p38 inhibitor (SB203580; 0-50 μM) did not influence the ability of EV to stimulate proliferation (Figure IV-8). To exclude the off-target effects, granulosa cells were exposed to PP3 (a non-functional PP2 analogue) in combination with EV treatment. PP3 did not influence EV-mediated cell proliferation at any concentration tested (Figure IV-8).

Src influenced EV-mediated cell proliferation was independent of regulation of uptake

Src is known to regulate endocytosis which is one way for EVs to enter the cell (Donaldson, Porat-Shliom et al. 2009). To test if inhibition of Src kinase activity

affected the uptake of EVs by granulosa cells, flow-cytometry was used to define the level of uptake of PKH67-fluorescently labeled EVs following treatment with the Src kinase inhibitor, PP2. Treatment of PP2 did not influence uptake of EVs in granulosa cells as the numbers of green-positive cells were similar despite increasing the concentration of the Src inhibitor (Figure IV-9).

Figure IV- 7 **Predicted downstream pathways involved in EV mediated cellular proliferation.**

Targets of miRNA which are abundant in the large follicles (GEO-GSE74879) were predicted by IPA in advance and then compared to the genes which were regulated with the treatment of EVs from small follicles. The overlapping 101 genes were then subjected to IPA in order to predict the following regulator molecules and canonical signaling pathways in response to EV treatment.

Top Canonical Pathways		
Name	p-value	Overlap
Molecular Mechanisms of Cancer	2.35E-36	9.6 % 35/365
HGF Signaling	2.91E-36	23.8 % 25/105
GNRH Signaling	8.56E-34	19.4 % 25/129
ErbB Signaling	1.06E-32	25.6 % 22/86
LPS-stimulated MAPK Signaling	1.87E-32	28.8 % 21/73

Top Upstream Regulators		
Upstream Regulator	p-value of overlap	Predicted Activation
nocodazole	6.45E-36	
TP53	1.58E-26	
ESR1	1.53E-21	
curcumin	1.36E-18	
SRC	2.28E-18	

Figure IV- 8 **Identification of downstream signaling pathways affected by EV treatment.**

Specific inhibitors were used to elucidate downstream cell signaling pathways in granulosa cells following EV treatment. Pathways evaluated included Src (PP2), JNK (SP600125), PI3K (LY294002), MEK1/2 (U0126), and p38 (SB203580). A non-functional analog of PP2, PP3, was used to rule out potential off-target effects for the Src inhibition study. *Means ± SEM (n=3) with different superscripts were statistically different ($p<0.05$).

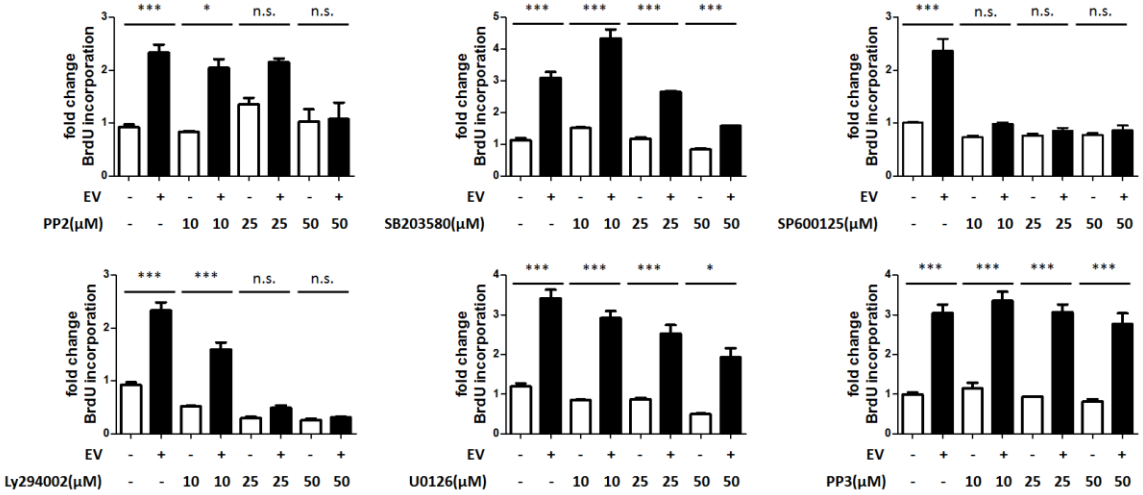
fold change BrdU incorporation
EV
PP2(μM)
SB203580(μM)
SP600125(μM)
Ly294002(μM)
U0126(μM)
PP3(μM)
***
*
n.s.
- + - + - + - +
- - 10 10 25 25 50 50

Figure IV- 9 **Effect of Src inhibition by PP2 on EV uptake.**

Influence of PP2 on EV uptake was tested by flow cytometry. A) Representative image of effect of PP2 on EV uptake under flow cytometry (PP2: 50 μM), and B) effect of PP2 on EV uptake in a dose-dependent design. ^{a,b}Means ± SEM with different superscripts were statistically different ($p<0.05$).

(A)

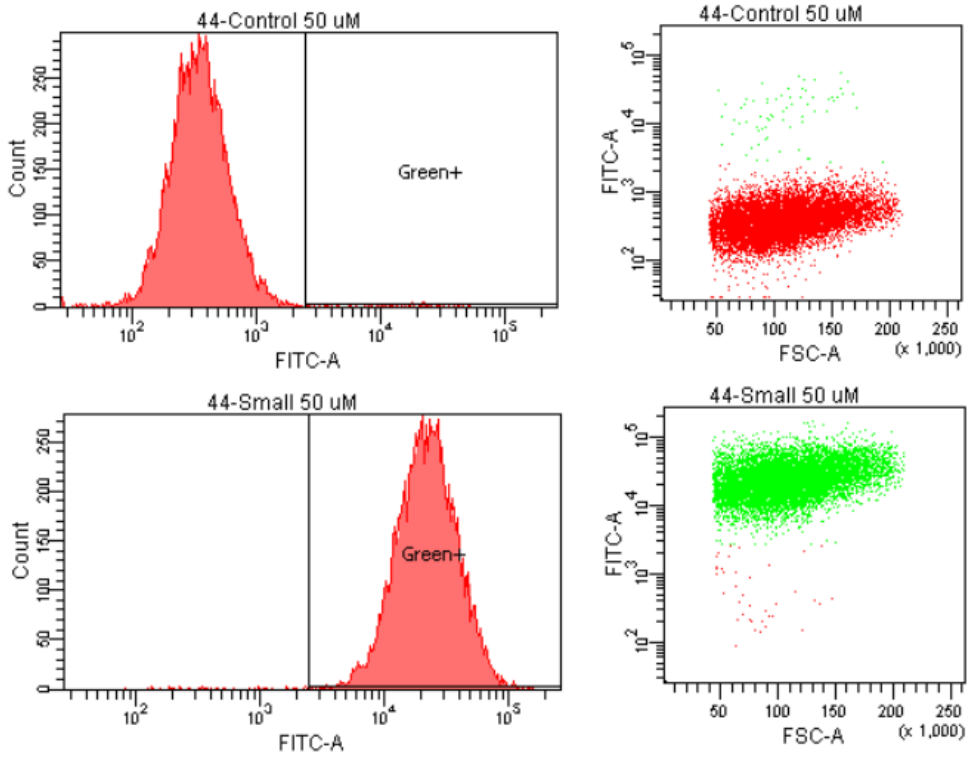
44-Control 50 uM
Count
Green+
FITC-A
44-Control 50 uM
FITC-A
FSC-A
(x 1,000)
44-Small 50 uM
Count
Green+
FITC-A
44-Small 50 uM
FITC-A
FSC-A
(x 1,000)

(B)

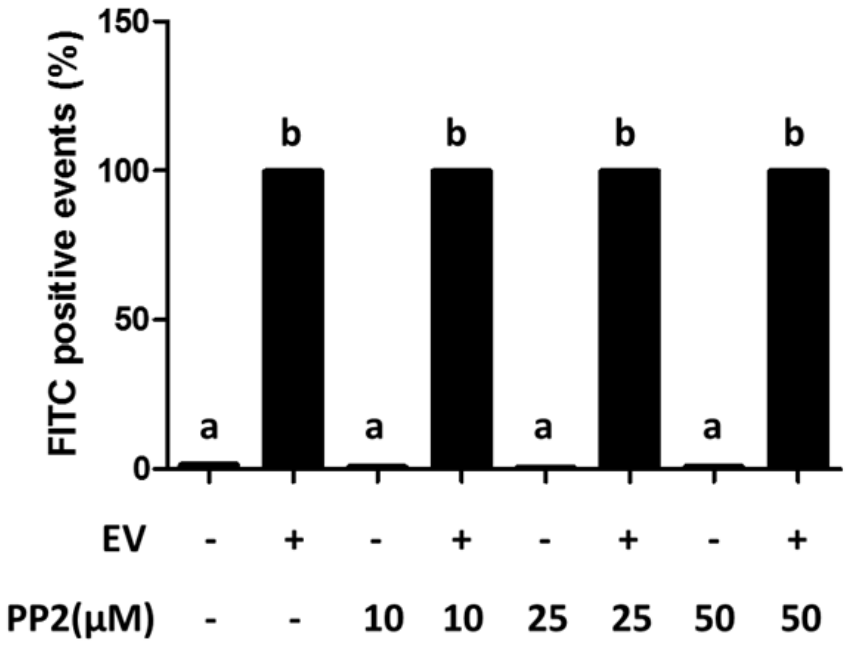
FITC positive events (%)
150
100
50
0
a
b
a
b
a
b
a
b
EV - + - + - + - +
PP2(μM) - - 10 10 25 25 50 50

EVs from different size follicles were taken up by granulosa cells at different levels

One explanation for the differential ability of EVs from small, medium and large follicles to promote cell proliferation is that they may be taken up by the cell differently. To test this hypothesis, EVs from different size follicles were labeled with PKH67 before treatment of granulosa cells. Extracellular vesicles from small antral follicles exhibited a preferential uptake by granulosa cells. The intensity of green positive cells following treatment with EVs from small follicles was twice that observed following treatment of EVs from medium and large antral follicles at both 2 h and 24 h (Figure IV-10A). To further evaluate cellular uptake, another preparation of EVs from small follicles, which had half the numbers of EVs as determined by protein concentration were tested (particle concentration of FF-EV is proportional to its protein concentration, Figure IV-11). Even with half the number of small follicle EVs, granulosa cell uptake was still greater for the small versus medium and large follicles (Figure IV-10B). Meanwhile, this phenomenon was consistent regardless of the source of granulosa cells [i.e., small, medium (Figure IV-12A) and large (Figure IV-12B) antral follicles. To demonstrate that EVs were in the cells and not just associated with the cells, we used the ImageStream imaging flow cytometer. The amount of EVs loaded was based on protein concentration. Additionally, in order to prove that a similar number of EVs were used, particle

concentrations of EVs from small and large follicles were quantified by nanoparticle tracking analysis and Imagestream flow cytometry. Both of these methods confirmed that similar concentrations of EVs from small and large follicles were used in these experiments (Figure IV-10E-G). Granulosa cells took up EVs isolated from small follicles at twice the level as EVs isolated from large follicles (Figure IV-10C), which was consistent with standard flow cytometry results in Figure 8A. The internalized EVs were observed in the cells as green puncta in the cytosol (Figure IV-10D).

Figure IV- 10 **Extracellular vesicles from different sized antral follicles are differentially taken up by granulosa cells.**

Bovine granulosa cells from small antral follicles were cultured with labeled EVs from small, medium, or large antral follicles for 2 h or 24 h, and the level of uptake was measured by flow cytometry. A) Level of EV uptake by FITC intensity under flow cytometry, and B) overlap image showed the levels of uptake of EV from different sized follicles, including a set where EVs from small follicles were given at one half the dose (Small 0.5). Uptake was also examined by Imagestream (imaging flow cytometry) with labeled EVs from small and large follicles. C) Level of EV uptake were presented by FITC intensity under imageflow cytometry, and D) corresponding images of granulosa cells treated with EVs from small and large follicles showed the internalized labeled EVs (green). The equal number loading was determined by E) imaging flow cytometry and F) nanoparticle tracking analysis and G) the images of labeled EVs (green spots) acquired by imaging flow cytometry are also shown.

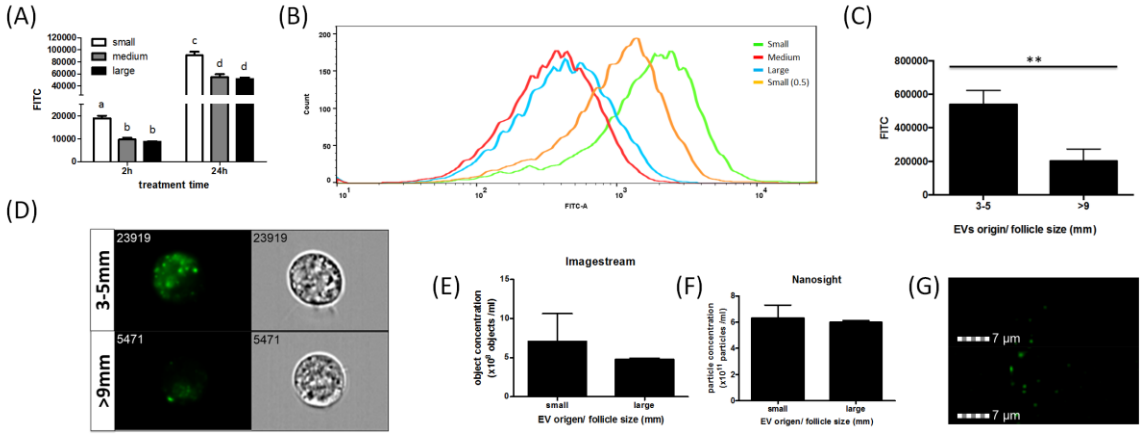
(A)
small
medium
large
FITC
treatment time
2h
24h
(B)
Small
Medium
Large
Small (0.5)
Count
FITC-A
(C)
FITC
EVs origin/ follicle size (mm)
3-5
>9
(D)
3-5mm
>9mm
23919
5471
(E)
Imagestream
object concentration
EV origen/ follicle size (mm)
small
large
(F)
Nanosight
particle concentration
EV origen/ follicle size (mm)
(G)
7 µm

Figure IV- 11 **Particle concentration of FF-EV is proportional to its protein concentration.**

Three independent collection of EVs were collected from FF. Their particle and protein concentrations were then determined and plotted into a histogram.

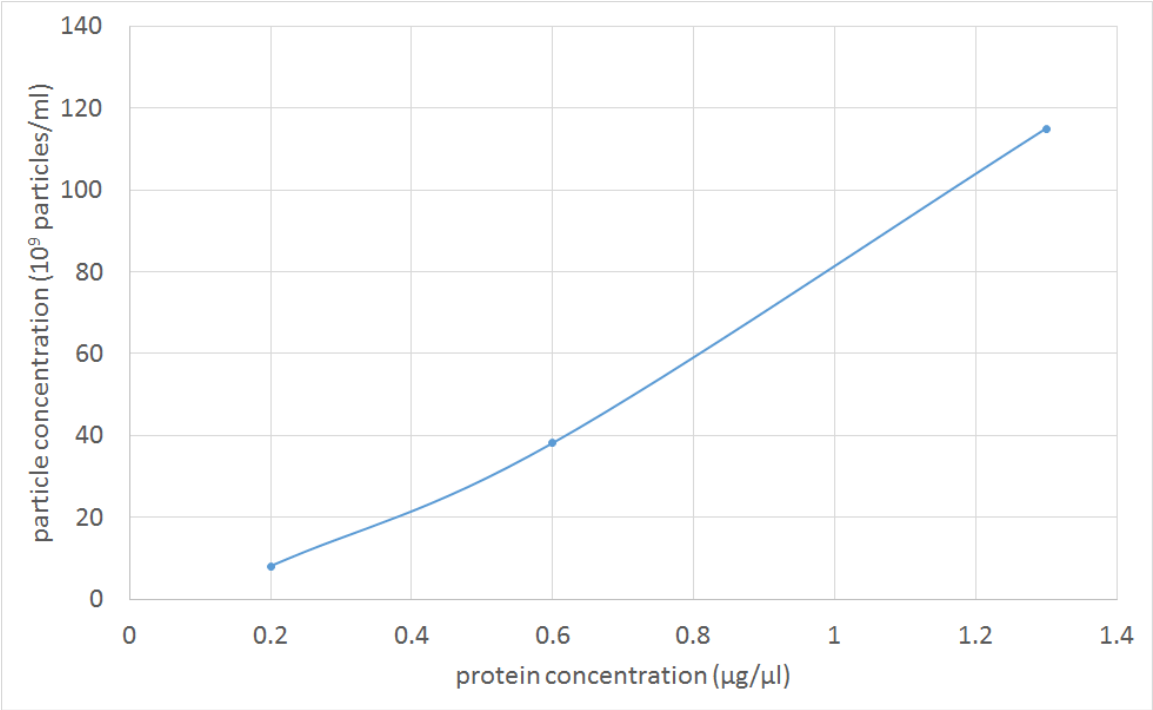
140
120
100
80
60
40
20
0
particle concentration (10^9 particles/ml)
0
0.2
0.4
0.6
0.8
1
1.2
1.4
protein concentration (µg/µl)

Figure IV-12 **Extracellular vesicles from different sized antral follicles are differentially taken up by granulosa cells of medium and large follicles.**

Bovine granulosa cells from A) medium and B) large antral follicles were cultured with labeled EVs from small, medium, or large antral follicles for 2h, and the level of uptake was measured under flow cytometry.

(A)

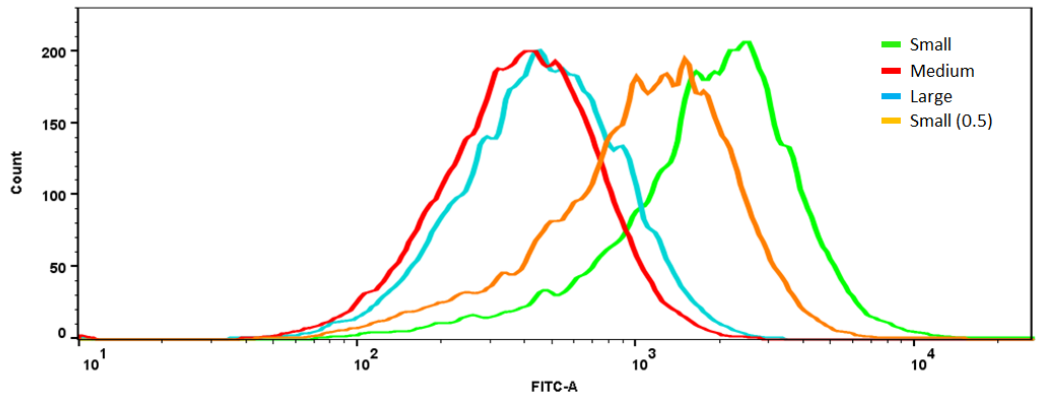
Small
Medium
Large
Small (0.5)
Count
200
150
100
50
0
10^1
10^2
10^3
10^4
FITC-A

(B)

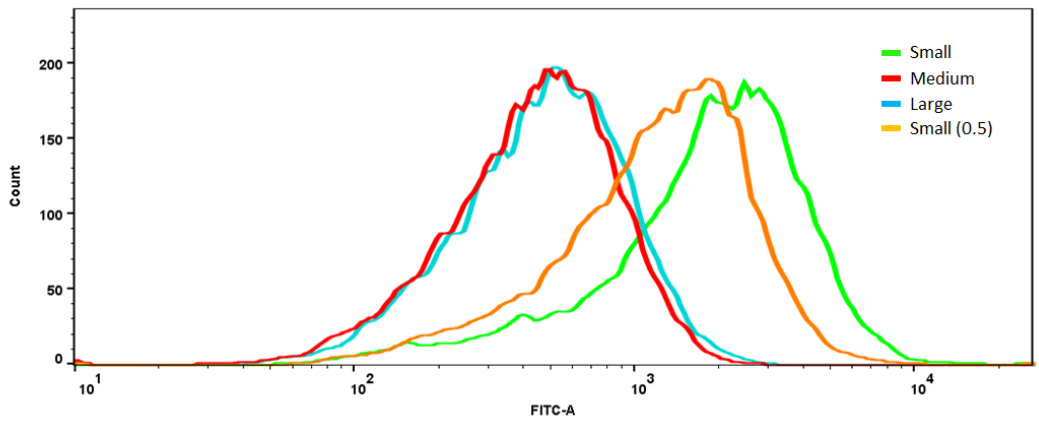
Small
Medium
Large
Small (0.5)
Count
200
150
100
50
0
10^1
10^2
10^3
10^4
FITC-A

Discussion

This study provides the first evidence that EVs isolated from ovarian FF can impact granulosa cell proliferation. Additionally, we were able to show that the Src and JNK pathways were involved in this stage-specific cell proliferation response as EVs isolated from small follicles exhibited the greatest activity on proliferation. We also proved that this differential activity of EVs was a result of the differential capacity of EVs themselves being taken up, which provides a potential model for studying the membrane proteins crucial for EV uptake. Additionally, in this study we developed a combination approach using the "gold" standard ultracentrifugation method combined with a column size exclusion method to significantly reduce/eliminate residual precipitants within the EV preparation.

Folliculogenesis is a well-orchestrated process regulated by endocrine, paracrine, and autocrine signaling (Roy 1994). Gonadotropins, which include follicle stimulating hormone (FSH) and luteinizing hormone (LH), are certainly the most critical and well-defined players serving as endocrine signaling hormones from the pituitary (Kumar 2005). However, there are also paracrine and autocrine factors such as insulin-like growth factor (IGF), epidermal growth factor superfamily (Erb family, EGF ligands), transforming growth factor beta (TGFβ) superfamily, fibroblast growth factor (FGF),

within the ovary, which have proven to be essential in stage specific manners (Monget and Bondy 2000, Knight and Glister 2006, Chaves, de Matos et al. 2012). Extracellular vesicles isolated from FF of different conditions have been reported to carry different miRNA, indicating a role as stage-specific signaling mediators (da Silveira, Veeramachaneni et al. 2012, Sang, Yao et al. 2013, Sohel, Hoelker et al. 2013, Diez-Fraile, Lammens et al. 2014, Roth, McCallie et al. 2014, Santonocito, Vento et al. 2014, da Silveira, Winger et al. 2015, Moreno, Nunez et al. 2015). In this study, we showed follicular EVs from different size antral follicles exhibiting differential activity on granulosa cell proliferation in which EVs from small follicles were most active, and this differential activity was correlated to physiological condition where proliferation is highly activated in small antral follicles.

Granulosa cell proliferation is controlled by a complex signaling network (Field, Dasgupta et al. 2014). Application of antibody-based array provided a comprehensive evaluation of EVs effects on signaling within recipient granulosa cells. Combined with our previous small RNA-seq on follicular EVs from different size follicles (GEO-GSE74879), we were able to identify several pathways (Src, HGF, GnRH, and ErbB pathways) that follicular EVs from small follicles may use to regulate granulosa cell proliferation. Further inhibitor studies enabled us to dissect these predicted pathways,

and to elucidate the JNK pathway as another critical pathway for EV-induced cell proliferation. Src kinase has been shown as downstream of several signaling pathways in the granulosa cells, which include FSH, LH, growth differentiation factor 9 (GDF9)/ bone morphogenetic protein 15 (BMP15), protein kinase C (PKC), and progesterone (Rice, Chaudhery et al. 2001, Du, Huang et al. 2012, Mottershead, Ritter et al. 2012, Yamashita, Okamoto et al. 2014). Similarly, the JNK pathway has been reported to affect granulosa cell proliferation by regulating the cell cycle, and also is associated with pathways such as FSH and GDF9/BMP15 (Sriraman, Modi et al. 2008, Miyoshi, Otsuka et al. 2010, Oktem, Buyuk et al. 2011, Mottershead, Ritter et al. 2012). While the experiments used a fairly late time point (24 h) in relationship to FF exposure to examine cell signaling molecules via the Kinome array, we were able to identify several pathways. Most importantly blockade of these pathways with inhibitors simultaneous with exposure to FF-EV was able to confirm these pathways involvement. Here, we showed that follicular EVs can affect granulosa cells through these cell signaling pathways.

Isolation of follicular EVs began with a standard multi-step ultracentrifugation protocol (Thery, Amigorena et al. 2006). Differential ultracentrifugation is regarded as the best protocol to collect EVs from various body fluids because of its ability to pull down materials simply based on their density (Szatanek, Baran et al. 2015). With a

further step of sucrose gradient, we proved that the majority of vesicles collected by ultracentrifugation from FF were exosomes in our previous study (Navakanitworakul, Hung et al. 2016). However, the purity of post-ultracentrifugation EVs is still debated, and concern arises mainly because of the residual background materials observed under EM. To further eliminate and produce a highly purified EV preparation, we combined ultracentrifugation with a size exclusion column and successfully removed most of the small residual materials. The subsequent BrdU assays showed that the additional step of removing contaminating non-vesicle material did not influence the result of BrdU assay, and thus strengthens the observation that EVs contributed most of the activity on inducing granulosa cell proliferation. Our study provides an improved protocol for purifying EVs and provide strong evidence that EVs are the functional components. The effects of EVs on cellular functions can be regulated through several manners including EV secretion, EV cargo selection, as well as EV uptake. Most studies on EV uptake focus on the ability of recipient cells to take up EVs (Mulcahy, Pink et al. 2014). Conventional and imaging flow cytometry were used to quantify the level of EV uptake after treatment of granulosa cells with fluorescently labeled EVs, and both of them yielded very similar results. Three different approaches were used to ensure that the cells were given similar amount of labeled EVs including determining protein

concentration of EVs by the bicinchoninic acid (BCA) assay, determining particle concentration by nanoparticle tracking analysis and imaging flow cytometry. Extracellular vesicles were equally applied across treatment groups (small and large follicles) in the individual experiments based on these methods. Interestingly, nanoparticle tracking analysis and imaging flow cytometry however yielded different absolute levels of EVs, this can be attributed to methodological differences. Imaging flow cytometry relies on fluorescent labeling of EVs and subsequent detection, conversely, nanoparticle tracking analysis does not rely on fluorescence and individual particles are more likely to be counted. Based on our knowledge, this is the first demonstration showing that a single tissue (follicle) is able to produce stage-specific EVs, which have differential capacities of being taken up by specific target cells. This finding also enables follicular EVs as a potential model to identify surface proteins, which could be critical for EV uptake.

The bovine model for the study reproduction is useful not only because of because of its importance to agriculture but also because it has many similarities to human reproduction; both species generate multiple follicular waves resulting in a single ovulation and the bovine reproductive cycle is nearly as long as the menstrual cycle of women. The availability of tissue and size of the bovine ovary makes it an effective

model for studying the physiological role of follicular EVs and even the basic biology of EVs. When collecting EVs from the FF, one concern is the existence of atretic follicles. In our previous study, we proved that the majority of FF originating from 3-5 mm and >9 mm follicles was from non-atretic follicles (Navakanitworakul, Hung et al. 2016). In this study, we compared follicular EVs from non-atretic and atretic small follicles, which were separated based on expression of TIMP1, a marker previously shown to be increased in atretic follicles (Hatzirodos, Hummitzsch et al. 2014). Surprisingly, follicular EVs from non-atretic and atretic small follicles exerted similar effects on the proliferation of granulosa cells. This suggests that EVs isolated from small follicles inherently stimulate cell proliferation, regardless of the physiologic state the follicle is in. This might suggest that the EVs isolated are highly similar and that the differences between these two types of follicles resides in the cell's ability to respond to the EVs. Further studies will be necessary to establish what differences/similarities exist in the atretic and non-atretic follicle EVs and/or whether cell responsiveness to EVs in these two types of follicles differ.

In conclusion, this study provides evidence that follicular EVs from different sized follicles exhibit different functional outcomes on granulosa cells. Extracellular vesicles

from highly proliferative small follicles were shown to induce granulosa cell proliferation while those from large antral follicles were only able to moderately stimulate proliferation. We also proved the activity is mainly from EVs and not residual materials that simultaneously co-precipitate with the EVs, therefore these studies support the use of the ultracentrifugation EV collection methodology. The ability of EVs to induce cell proliferation was clearly prevented by inhibitors of the Src and JNK signaling pathways, while less compelling evidence for PI3K and ERK pathways were obtained. We also observed a differentially capacity of EVs being taken up by granulosa cells, which might explain the differential effects of EVs on cell proliferation. Interestingly, this difference in EV uptake was dependent upon the source of follicular EVs (i.e., small or large follicles), and was not dependent upon the size of the follicle from which the cells were isolated. These studies support a role for EVs in cellular function within the developing antral follicle.

Material and Method

Follicular fluid collection

Bovine ovaries were collected from a local abattoir and because the animals were not used specifically for research purposes our Institutional Animal Care and Use Committee

ruled that the collection of ovaries from the abattoir does not constitute animal research and is exempt from further review. Ovaries (~150 ovaries / collection) were placed immediately into PBS and then transported 2.5 h to the University of Kansas Medical Center at 20-24 C temperature in preparation for ovarian FF aspiration. Follicular diameters were determined by individually measuring follicle diameters; follicles were designated into three different groups based on diameter (3-5 mm - small, 6-9 mm – medium and > 9 mm – large). Follicular fluid was aspirated using a tuberculin syringe (28 gauge needle) for small follicles and a 5 ml syringe with a 20-gauge needle for medium and large follicles. Follicular fluid from individual follicles was then stored independently or pooled into 15ml aliquots based on experimental designs.

Isolation of extracellular vesicles

Extracellular vesicles were isolated using a differential ultracentrifugation method developed for serum isolation of exosomes(Thery, Amigorena et al. 2006) and recently validated for follicular fluid (Navakanitworakul, Hung et al. 2016). Follicular fluid was diluted 1:1 with PBS and then spun at 800g for 5 min to pellet all cells including oocytes (the cell pellets were snap frozen at -80C or placed in Trizol). Follicular fluid was then centrifuged at 2000g for 20 min followed by 12000g for 45 min to remove cellular debris and other large particles (large microvesicles and apoptotic blebs). Samples were then

filtered through a 0.22 μm pore filter (Millipore) to further remove vesicles greater than 220 nm. Ultracentrifugation of the 1:1 mix follicular fluid:PBS was performed at 110000g for 3 hours. Above centrifuge steps were perform in an Optima^{TM} L-100XP ultracentrifuge, using a swinging bucket SW32Ti rotor for large scale collection (15ml FF). The resulting EV pellets were then resuspended in 4 ml PBS and spun again for 1.5 hours at 110000 g in a TLA 100.4 fixed angle rotor. A final wash with 1 ml of PBS was then performed and spun at 110000 g for 1.5 hours using a TLA 55 fixed angle rotor. All centrifugations were performed at 4°C. The obtained pellets were re-suspended in PBS for further analysis. When FF volumes were below 2ml the TLA110.4 rotor was used in place of SW32Ti until the last ultracentrifugation with TLA55 rotor.

Nanoparticle tracking analysis

To determine particle size and concentration, nanoparticle-tracking analysis (NTA) was performed with a Nanosight LM10 instrument (Nanosight, Salisbury, UK) outfitted with a LM14C laser. Each EV preparation was sampled three times to generate 3 independent dilutions. These dilutions range from ~1:1000 to 1:10,000 for each sample (the dilution is determined empirically for each sample) and then each of the three dilutions is analyzed 3 times. The overall average of these three dilutions was used as the experimental result for each sample. From validation studies using dilution series, we

determined that NTA is most accurate between particle concentrations in the range of 2×10^8 /ml to 2×10^9 /ml. Thus samples were diluted to this level and absolute concentrations were then back calculated according to the dilution factor.

Transmission electron microscopy

EVs (10 mg/ml) were fixed overnight (2% glutaraldehyde and 0.1 M cacodylate buffer) and washed with 0.1 M sodium cacodylate buffer. A glow discharge treated carbon film 300 mesh grid was inverted and floated upside down on the drop containing fixed EVs (20 min). Each grid was rinsed 7x with filtered distilled water then stained with 1% uranyl acetate. All samples are examined in a JEOL-JEM-1400 transmission electron microscope at an 80-100 kV with 15,000x magnification.

Western blot Analysis

EV samples (10 μg protein) were lysed in SDS sample buffer with 50 mM DTT, heated for 5 min at 95 °C and subjected to electrophoresis using 12% SDS-PAGE in running buffer at constant 120 V for 1.5 hours. Proteins were then electrotransferred onto polyvinylidenedifluoride membranes, and the membranes were blocked with 5 % (w/v) skim milk powder in Tris-buffered saline with 0.05 % (v/v) Tween-20 (TTBS) for 1 hour at RT. Membranes were then probed with primary anti-CD81 (sc-166029), anti-Mcl1 (sc-819), anti-Akt (sc-8312) and anti-Actin (sc-1616) antibodies for overnight at 4 °C in

TTBS (50 mM Tris, 150 mM NaCl, 0.05 % Tween20) followed by incubation with the secondary anti-mouse IgG or anti-sheep goat antibodies for 1 h. All primary antibodies were purchased from Santa Cruz Biotechnology Inc. Membranes were washed three times in TTBS for 10 min after each incubation step and detected by enhanced chemiluminescence (ECL) (GE Healthcare Bio-science, PA) per manufacturer's instructions. To ensure that similar levels of total proteins were loaded on to westerns, we stained the membranes with Swift Membrane Stain (G Biosciences, St Louis MO) per manual instructions.

Granulosa cell culture

Primary granulosa cells isolated from small, medium and large follicles were cultured in DMEM/F12 supplemented with 1000 IU/ml penicillin, 1000 µg/ml streptomycin, 2 µg/ml recombinant human insulin, 1.1 µg/ml human transferrin, 1 ng/ml sodium selenite, and 10% fetal bovine serum. Fetal bovine serum was diluted with equal volume of DMEM/F12 and spun for 3 hours at 110000g to remove vesicles in advance. Cells were cultured at 38.5℃ supplemented with 6% CO_2. Plating densities and specifics to assay are described.

EVs labeling and imaging

EVs were stained using the PKH67 Green Fluorescent Cell Linker Kit (Sigma Chemical

Corp, St Louis, MO) per manual protocol and pelleted by ultracentrifugation following several washes in PBS before final resuspension in PBS. To test if there is any residual or precipitant dye with this protocol, a negative control was performed in parallel under same protocol but without EVs. For the negative control the same volume of PBS was added to the centrifuged tube. Granulosa cells from small follicles were cultured as previously described and treated with an equal volume of labeled EVs or negative control solution in a chamber slide. Extracellular vesicle uptake was then observed under a Zeiss Pascal 510 confocal microscope.

Flow cytometry

Bovine granulosa cells from small follicles were plated in 24-well dish at 10^5 cells/well with/without the treatment of labeled EVs and PP2, Src kinase inhibitor. After treatment, granulosa cells were washed with PBS once before detaching by trypsinization. Trypsin was neutralized by adding complete medium and cells were collected by centrifugation. For apoptosis assay, granulosa cells were treated with 100 µg/ml EV from small follicle and then stained with propidium iodide staining in advance to analysis. The fluorescence level of cells was used to determine the level of EVs uptake under a BD LSR II (BD Biosciences), and data were analyzed with BD FACSDiva software (BD Biosciences). For imaging flow cytometry, samples were run

on a Amnis ImageStream®^{X} Mark II Imaging Flow Cytometer and analyzed with IDEAS® Software (EMD Millipore, Darmstadt, Germany). In each of the cell and EV samples, 10000 and 100000 objects were collected, respectively.

BrdU incorporation assay and cell attachment assay

Bovine granulosa cells from small follicles were cultured in 96 well culture dishes at 5 x 10^3 cells/well with or without EVs (see individual figure for concentration) collected from specific size follicles as indicated. Cell proliferation was measured 24 hours later as BrdU incorporation according to the manufacturer's protocol (Roche). For inhibitor study, granulosa cells were cultured as described with addition of indicated kinase inhibitors, including PP2 (Millipore) for Src kinase, Ly294002 (Sigma-Aldrich) for PI3K kinase, SB203580 (LC laboratories) for p38 kinase, U0126 (Promega) for MEK1/2, and SP600125 (Sigma-Aldrich) for JNK kinase. PP3 (Millipore) a PP2 analog was also used in specific experiments. The concentration of each was described in individual figure legends.

For analyzing effect of EV on cell attachment, bovine granulosa cells from small follicles were cultured with EVs from small, medium, or large follicles with controls with/without FBS. Cells were seeded at the density of 4 x 10^5 cells/ml simultaneously with indicated supplements into 96 well plates. Cells were then rinsed with PBS for three times and

fixed with 4% paraformaldehyde for 15mins. After washing with PBS, the fixed cells were stained with crystal violet (5 mg/ml in 2% ethanol) for 10 mins. Following with washing with water to remove the residual dye, the plate was air dried and then 2% SDS was used to dissolve crystal violet. The plate was read at absorbance 550 nm on a FlexStation 3 Multi-Mode Microplate Reader (Molecular Devices).

.

KAM-880 antibody microarray

Twenty-four hours after treatment, GC with EV treatment (100 μg/ml EVs from small follicle) and non-treatment control were washed twice with cold PBS before adding 200μl of lysis buffer (20 mM MOPS pH7.0, 2 mM EGTA, 5 mM EDTA, 30 mM sodium fluoride, 60 mM β-glycerophosphate, 20 mM sodium pyrophosphate, 1 mM sodium orthovanadate, 1% Triton X-100, 1 mM phenylmethylsulfonylfluoride, 3 mM benzamidine, 5 μM pepstatin A, 10 μM leupeptin, 1 mM dithiothreitol). Lysates were sonicated (Model Q800R, Active Motif, CA) with the following protocol: amplification 75%, pulse on 15 s, pulse off 45 s, temperature 3°C. Samples were then spun twice at 16000 g for 30 mins each at 4°C before submitting on dry ice to Kinexus Bioinformatics Corp. (Vancouver BC, Canada). The KAM-880 antibody microarray includes 518 pan-specific and 359 phospho-site specific antibodies. The background of this specific array

was described by McGinnis *et al*. (McGinnis, Pelech et al. 2014).

Ingenuity pathway analysis (IPA)

MicroRNA which are abundant in the large follicles (i.e., might be predicted to be inhibitory to cell proliferation) were identified from our small RNA-seq (GEO-GSE74879) study. Their respective target genes were predicted through the use of Ingenuity® Pathway Analysis (IPA®, QIAGEN Redwood City, www.qiagen.com/ingenuity) and these predicted target genes were then compared to the differentially expressed proteins/translation modifications (kinase array results) following EV treatment. The overlapping miRNA target genes and the kinase array identified proteins were then subjected to IPA analysis in order to identify possible cell signaling pathways.

RNA preparation

Total RNA was isolated from granulosa cells (GC) of individual follicle with Trizol (Invitrogen) according to the manufacturer's protocol. Briefly, GC were disrupted in 1 ml of Trizol reagent and incubated for 15 min at room temperature following addition of 200 µl of chloroform. Subsequently, the aqueous solution was mixed with 500 µl of isopropanol. In facilitate precipitation and visualization of RNA pellet, 1 µl glycogen (20 µg/µl) was added together with the RNA-isopropanol mixture solution and incubated

at RT for 10 min and spun at 12000 g for 15 min at 4 °C. The pellet was washed with 500 µl of 75 % ethanol followed by centrifugation at 12000 g for 5 min at 4 °C. The RNA pellet was dried at room temperature and dissolved in 15 µl of RNase free water. The RNA solution was then stored at -80 °C. The concentration of RNA was determined using Nanodrop spectrophotometer ND-1000 (Thermo Scientific, Wilmington, DE).

Quantitative RT-PCR

Total RNA was reverse-transcribed using SuperScriptTM II Reverse Transcriptase (Life Technologies) with random primer per manufacturer's instruction. Quantitative PCR was then performed with 1:5 dilution of cDNA on an Applied Biosystems HT7900 sequence detector. Primer sets for bovine *Timp1* (forward: CAG AAC CGC AGT GAG GAG TTT, reverse: GAT GTG CAG GTG CCC ATT C), and U6 (forward: CTC GCT TCG GCA GCA CA, reverse: AAC GCT TCA CGA ATT TGC GT) were designed using Primer Express 3.0 software (Applied Biosystems). Samples were run in triplicate, and the ΔCt method was used to calculate the relative expression between the samples after normalization with U6. The presence of a single dissociation curve confirmed the amplification of a single transcript and lack of primer dimers.

Statistical Analysis

All of the quantitative experiments were repeated at least with three biological replicates

and were analyzed by one-way ANOVA with Newman-Kuels multiple comparison test was performed using GraphPad Prism version 5.00 for Windows, GraphPad Software, San Diego California USA, www.graphpad.com. $P<0.05$ was considered statistically significant.

XI. Chapter VI: Conclusion

Since the first study showing the presence of EVs in ovarian follicular fluid in 2012, several additional studies were completed that focused on understanding the microRNA carried in the follicular EVs. The potential functions of these specific EVs were predicted, but there is still a lack of knowledge on the role of EVs in ovarian follicle physiology. In the studies presented in my dissertation, I have provided evidence that follicular EVs can induce cumulus expansion and granulosa cell proliferation, and these functions are dependent on the size of follicles where EVs are collected. These studies were conducted during the later stages of folliculogenesis in which there is an antrum filled with follicular fluid. We first characterized follicular EVs from antral follicles of different sizes (representing different stages of follicle growth) with regard to their physical features as well as their contained cargos (protein and small RNA). The functions of EVs were tested in vitro using cultured granulosa cells and an ex vivo cumulus-oocyte-complex expansion assay.

In my initial experiments, I observed that follicular EVs have a typical lipid bi-layer structure or a cup-shape morphology under electronic microscopy (EM) depending on the preparation methodology, and a standard size distribution between 50 to 200 nm observed by EM or nanosight. When the comparison was made across different sizes of follicles, follicular EVs carry different microRNA contents and are functionally relevant

to the physiological state of the follicles isolated from based on bioinformatics prediction. For example, miR-204 has been addressed as a cell proliferation inhibitor in several cell types (Shi, Huang et al. 2015, Wu, Pan et al. 2015, Wu, Zeng et al. 2015, Wu, Wang et al. 2015, Xia, Liu et al. 2015, Yin, Liang et al. 2015), and it presented at a higher level in larger follicles. Interestingly, the level of one EV marker, CD81, decreased with the growth of follicles while the level of the other marker, β-actin, remained relatively unchanged, which brings out the possibility of the existence of different groups of EVs in the follicular fluid. Whether different populations of EVs carry out different functions or whether the ovarian cells (granulosa cell, cumulus cell, and oocyte) are able to use them differentially according to the physiological condition still needs further investigation.

We first tested the function of EVs on cumulus-oocyte-complex. EVs showed the ability to support cumulus expansion through induction of *Ptgs2*, *Ptx3*, and *Tnfaip6*, expression, all of which are known to be critical for the expansion process. Interestingly, while both EVs from small and large antral follicles were able to induce the expansion, only EVs from small follicles caused the normal increase in expression of these genes. This is an interesting yet perplexing problem. One possibility is that the increasing diameter of cumulus-oocyte-complex that occurs after EV exposure is not a

typical cumulus expansion but an effect of cell proliferation or migration. Another possibility is that EVs provide some but not all of the required components for normal expansion. Because cumulus expansion is an event that happens right before ovulation we logically, expected EVs from large follicles to have the major effect on cumulus expansion, compared to those from small follicles. Our results showed the opposite response. Therefore, it again raises the idea that there are populations of EVs in the follicular fluid and they may be taken up by the cells differentially throughout follicular growth. A possible explanation could be that EVs in favor of cumulus expansion are taken up by cumulus cells before the follicles reach a large size and then either a suppressive mechanism prevents the expansion in the early stage or another signal (maturation) is required to initiate the process.

During follicular growth, the size of the follicle increases dramatically due to pronounced cell proliferation and antrum formation. The level of cell proliferation remains high during the growth of the follicle and slows down approaching ovulation. We have shown that EVs are able to increase granulosa cell proliferation and the activity of the EVs is follicle size dependent, with EVs from small follicles inducing high levels of proliferation while EVs from large follicles do not. In order to understand the cellular pathways that EVs stimulate cellular proliferation through, an antibody-based

array was applied to the cell lysate after treating the granulosa cells with EVs from small antral follicles. Proteins that showed a differential expression were subjects for bioinformatics analysis, and the results pointed to several signaling pathways including ErbB and src signalings. Treatment of granulosa cells with inhibitors against the kinase activities of src and JNK, a downstream molecule of ErbB, abolished the effect of EVs on inducing cell proliferation. Whether EVs induced cell proliferation directly or indirectly through these pathways, and what molecules associated with EVs are responsible for the effect still need more work. One of the experiments that can be done next will be applying siRNA against these kinases and observing whether this influences the EV-induced granulosa cell proliferation.

The functional effects of EVs are likely to be determined by the cargos associated with them or by their interaction with recipient cells. We observed that EVs from different sizes of follicles exhibited different activities on inducing granulosa cells. Therefore, we tested if these EVs are different in terms of the interaction with the granulosa cells. Interestingly, we found that EVs from small antral follicles, which highly induced granulosa cell proliferation, were also more accessible for being taken up by the granulosa cells. Regulated uptake of extracellular materials usually requires the involvement of cell surface proteins and it would be very intriguing if the follicular EVs

can serve as a model for the study of EV uptake. A follow up experiment to compare the protein composition of EVs from small and large follicles will help to identify candidate proteins important for EV uptake.

In summary, my studies provide the first comprehensive analysis of follicular EVs through folliculogenesis. I collected follicular EVs from different sized antral follicles and characterized their containing miRNA. I also characterized their functional effects on inducing cumulus expansion and granulosa cell proliferation. My results indicate that follicular EVs have effects on both cumulus-oocyte-complex expansion and granulosa cell proliferation indicating another possible layer of cell-to-cell communication system that has not been previously considered within the ovarian follicle. Our studies also provide an improved protocol for collecting EVs, based on the "gold standard" ultracentrifugation method combined with a size exclusion method. Moreover, the observation that follicular EVs from different sized follicles have differential potential for being taken up by granulosa cells provides a unique model for studying molecules important for EV uptake. In conclusion, this dissertation describes several physiologic roles for follicular EVs within the ovarian follicle and also demonstrates that the ovarian follicle has great potential for furthering our understanding of extracellular vesicle biology in general and specifically in the reproductive system.

XII. References

Abrami, L., L. Brandi, M. Moayeri, M. J. Brown, B. A. Krantz, S. H. Leppla and F. G. van der Goot (2013). "Hijacking multivesicular bodies enables long-term and exosome-mediated long-distance action of anthrax toxin." Cell Rep **5**(4): 986-996.
Accili, D. and K. C. Arden (2004). "FoxOs at the crossroads of cellular metabolism, differentiation, and transformation." Cell **117**(4): 421-426.
Adashi, E. Y., C. E. Resnick, A. J. D'Ercole, M. E. Svoboda and J. J. Van Wyk (1985). "Insulin-like growth factors as intraovarian regulators of granulosa cell growth and function." Endocr Rev **6**(3): 400-420.
Adashi, E. Y., C. E. Resnick, D. W. Payne, R. G. Rosenfeld, T. Matsumoto, M. K. Hunter, S. E. Gargosky, J. Zhou and C. A. Bondy (1997). "The mouse intraovarian insulin-like growth factor I system: departures from the rat paradigm." Endocrinology **138**(9): 3881-3890.
Akison, L. K., E. R. Alvino, K. R. Dunning, R. L. Robker and D. L. Russell (2012). "Transient invasive migration in mouse cumulus oocyte complexes induced at ovulation by luteinizing hormone." Biol Reprod **86**(4): 125.
Alenquer, M. and M. J. Amorim (2015). "Exosome Biogenesis, Regulation, and Function in Viral Infection." Viruses **7**(9): 5066-5083.
Alvarez-Erviti, L., Y. Seow, H. Yin, C. Betts, S. Lakhal and M. J. Wood (2011). "Delivery of siRNA to the mouse brain by systemic injection of targeted exosomes." Nat Biotechnol **29**(4): 341-345.
Ambekar, A. S., R. S. Nirujogi, S. M. Srikanth, S. Chavan, D. S. Kelkar, I. Hinduja, K. Zaveri, T. S. Prasad, H. C. Harsha, A. Pandey and S. Mukherjee (2013). "Proteomic analysis of human follicular fluid: a new perspective towards understanding folliculogenesis." J Proteomics **87**: 68-77.
Anasti, J. N., S. N. Kalantaridou, L. M. Kimzey, M. George and L. M. Nelson (1998). "Human follicle fluid vascular endothelial growth factor concentrations are correlated with luteinization in spontaneously developing follicles." Hum Reprod **13**(5): 1144-1147.
Andersen, C. Y., K. T. Schmidt, S. G. Kristensen, M. Rosendahl, A. G. Byskov and E. Ernst (2010). "Concentrations of AMH and inhibin-B in relation to follicular diameter in normal human small antral follicles." Hum Reprod **25**(5): 1282-1287.
Anderson, H. C. (1967). "Electron microscopic studies of induced cartilage development and calcification." J Cell Biol **35**(1): 81-101.
Angelucci, S., D. Ciavardelli, F. Di Giuseppe, E. Eleuterio, M. Sulpizio, G. M. Tiboni, F. Giampietro, P. Palumbo and C. Di Ilio (2006). "Proteome analysis of human follicular fluid." Biochim Biophys Acta **1764**(11): 1775-1785.

Armstrong, D. G., C. G. Gutierrez, G. Baxter, A. L. Glazyrin, G. E. Mann, K. J. Woad, C. O. Hogg and R. Webb (2000). "Expression of mRNA encoding IGF-I, IGF-II and type 1 IGF receptor in bovine ovarian follicles." J Endocrinol **165**(1): 101-113.
Baerwald, A. R., G. P. Adams and R. A. Pierson (2012). "Ovarian antral folliculogenesis during the human menstrual cycle: a review." Hum Reprod Update **18**(1): 73-91.
Bahrini, I., J. H. Song, D. Diez and R. Hanayama (2015). "Neuronal exosomes facilitate synaptic pruning by up-regulating complement factors in microglia." Sci Rep **5**: 7989.
Baietti, M. F., Z. Zhang, E. Mortier, A. Melchior, G. Degeest, A. Geeraerts, Y. Ivarsson, F. Depoortere, C. Coomans, E. Vermeiren, P. Zimmermann and G. David (2012). "Syndecan-syntenin-ALIX regulates the biogenesis of exosomes." Nat Cell Biol **14**(7): 677-685.
Baker, J., M. P. Hardy, J. Zhou, C. Bondy, F. Lupu, A. R. Bellve and A. Efstratiadis (1996). "Effects of an Igf1 gene null mutation on mouse reproduction." Mol Endocrinol **10**(7): 903-918.
Barile, L., T. Moccetti, E. Marban and G. Vassalli (2016). "Roles of exosomes in cardioprotection." Eur Heart J.
Barres, C., L. Blanc, P. Bette-Bobillo, S. Andre, R. Mamoun, H. J. Gabius and M. Vidal (2010). "Galectin-5 is bound onto the surface of rat reticulocyte exosomes and modulates vesicle uptake by macrophages." Blood **115**(3): 696-705.
Batiz, L. F., M. A. Castro, P. V. Burgos, Z. D. Velasquez, R. I. Munoz, C. A. Lafourcade, P. Troncoso-Escudero and U. Wyneken (2015). "Exosomes as Novel Regulators of Adult Neurogenic Niches." Front Cell Neurosci **9**: 501.
Bedaiwy, M., A. Y. Shahin, A. M. AbulHassan, J. M. Goldberg, R. K. Sharma, A. Agarwal and T. Falcone (2007). "Differential expression of follicular fluid cytokines: relationship to subsequent pregnancy in IVF cycles." Reprod Biomed Online **15**(3): 321-325.
Beg, M. A. and O. J. Ginther (2006). "Follicle selection in cattle and horses: role of intrafollicular factors." Reproduction **132**(3): 365-377.
Bender, K., S. Walsh, A. C. Evans, T. Fair and L. Brennan (2010). "Metabolite concentrations in follicular fluid may explain differences in fertility between heifers and lactating cows." Reproduction **139**(6): 1047-1055.
Benjamini, Y., D. Drai, G. Elmer, N. Kafkafi and I. Golani (2001). "Controlling the false discovery rate in behavior genetics research." Behav Brain Res **125**(1-2): 279-284.
Berisha, B., M. W. Pfaffl and D. Schams (2002). "Expression of estrogen and progesterone receptors in the bovine ovary during estrous cycle and pregnancy."

Endocrine **17**(3): 207-214.
Bianco, F., C. Perrotta, L. Novellino, M. Francolini, L. Riganti, E. Menna, L. Saglietti, E. H. Schuchman, R. Furlan, E. Clementi, M. Matteoli and C. Verderio (2009). "Acid sphingomyelinase activity triggers microparticle release from glial cells." EMBO J **28**(8): 1043-1054.
Biggers, J. D. and L. K. McGinnis (2001). "Evidence that glucose is not always an inhibitor of mouse preimplantation development in vitro." Hum Reprod **16**(1): 153-163.
Bissig, C. and J. Gruenberg (2014). "ALIX and the multivesicular endosome: ALIX in Wonderland." Trends Cell Biol **24**(1): 19-25.
Bobrie, A., S. Krumeich, F. Reyal, C. Recchi, L. F. Moita, M. C. Seabra, M. Ostrowski and C. Thery (2012). "Rab27a supports exosome-dependent and -independent mechanisms that modify the tumor microenvironment and can promote tumor progression." Cancer Res **72**(19): 4920-4930.
Britt, K. L., A. E. Drummond, V. A. Cox, M. Dyson, N. G. Wreford, M. E. Jones, E. R. Simpson and J. K. Findlay (2000). "An age-related ovarian phenotype in mice with targeted disruption of the Cyp 19 (aromatase) gene." Endocrinology **141**(7): 2614-2623.
Brunet, A., A. Bonni, M. J. Zigmond, M. Z. Lin, P. Juo, L. S. Hu, M. J. Anderson, K. C. Arden, J. Blenis and M. E. Greenberg (1999). "Akt promotes cell survival by phosphorylating and inhibiting a Forkhead transcription factor." Cell **96**(6): 857-868.
Budnik, V., C. Ruiz-Canada and F. Wendler (2016). "Extracellular vesicles round off communication in the nervous system." Nat Rev Neurosci **17**(3): 160-172.
Camussi, G., M. C. Deregibus and C. Tetta (2010). "Paracrine/endocrine mechanism of stem cells on kidney repair: role of microvesicle-mediated transfer of genetic information." Curr Opin Nephrol Hypertens **19**(1): 7-12.
Caplan, M. J., E. J. Kamsteeg and A. Duffield (2007). "Tetraspan proteins: regulators of renal structure and function." Curr Opin Nephrol Hypertens **16**(4): 353-358.
Carletti, M. Z. and L. K. Christenson (2009). "Rapid effects of LH on gene expression in the mural granulosa cells of mouse periovulatory follicles." Reproduction **137**(5): 843-855.
Carletti, M. Z., S. D. Fiedler and L. K. Christenson (2010). "MicroRNA 21 blocks apoptosis in mouse periovulatory granulosa cells." Biol Reprod **83**(2): 286-295.
Cavender, J. L. and W. J. Murdoch (1988). "Morphological studies of the microcirculatory system of periovulatory ovine follicles." Biol Reprod **39**(4): 989-997.
Chaves, R. N., M. H. de Matos, J. Buratini, Jr. and J. R. de Figueiredo (2012). "The fibroblast growth factor family: involvement in the regulation of folliculogenesis."

Reprod Fertil Dev **24**(7): 905-915.
Cheung, K. H., S. Keerthikumar, P. Roncaglia, S. L. Subramanian, M. E. Roth, M. Samuel, S. Anand, L. Gangoda, S. Gould, R. Alexander, D. Galas, M. B. Gerstein, A. F. Hill, R. R. Kitchen, J. Lotvall, T. Patel, D. C. Procaccini, P. Quesenberry, J. Rozowsky, R. L. Raffai, A. Shypitsyna, A. I. Su, C. Thery, K. Vickers, M. H. Wauben, S. Mathivanan, A. Milosavljevic and L. C. Laurent (2016). "Extending gene ontology in the context of extracellular RNA and vesicle communication." J Biomed Semantics **7**: 19.
Chevillet, J. R., Q. Kang, I. K. Ruf, H. A. Briggs, L. N. Vojtech, S. M. Hughes, H. H. Cheng, J. D. Arroyo, E. K. Meredith, E. N. Gallichotte, E. L. Pogosova-Agadjanyan, C. Morrissey, D. L. Stirewalt, F. Hladik, E. Y. Yu, C. S. Higano and M. Tewari (2014). "Quantitative and stoichiometric analysis of the microRNA content of exosomes." Proc Natl Acad Sci U S A **111**(41): 14888-14893.
Choi, W. J., J. Banerjee, T. Falcone, J. Bena, A. Agarwal and R. K. Sharma (2007). "Oxidative stress and tumor necrosis factor-alpha-induced alterations in metaphase II mouse oocyte spindle structure." Fertil Steril **88**(4 Suppl): 1220-1231.
Christenson, L. K., S. Gunewardena, X. Hong, M. Spitschak, A. Baufeld and J. Vanselow (2013). "Research resource: preovulatory LH surge effects on follicular theca and granulosa transcriptomes." Mol Endocrinol **27**(7): 1153-1171.
Christianson, H. C., K. J. Svensson, T. H. van Kuppevelt, J. P. Li and M. Belting (2013). "Cancer cell exosomes depend on cell-surface heparan sulfate proteoglycans for their internalization and functional activity." Proc Natl Acad Sci U S A **110**(43): 17380-17385.
Ciardiello, C., L. Cavallini, C. Spinelli, J. Yang, M. Reis-Sobreiro, P. de Candia, V. R. Minciacchi and D. Di Vizio (2016). "Focus on Extracellular Vesicles: New Frontiers of Cell-to-Cell Communication in Cancer." Int J Mol Sci **17**(2).
Clancy, J. W., A. Sedgwick, C. Rosse, V. Muralidharan-Chari, G. Raposo, M. Method, P. Chavrier and C. D'Souza-Schorey (2015). "Regulated delivery of molecular cargo to invasive tumour-derived microvesicles." Nat Commun **6**: 6919.
Clarke, H. G., S. A. Hope, S. Byers and R. J. Rodgers (2006). "Formation of ovarian follicular fluid may be due to the osmotic potential of large glycosaminoglycans and proteoglycans." Reproduction **132**(1): 119-131.
Cocucci, E. and J. Meldolesi (2015). "Ectosomes and exosomes: shedding the confusion between extracellular vesicles." Trends Cell Biol.
Cocucci, E. and J. Meldolesi (2015). "Ectosomes and exosomes: shedding the confusion between extracellular vesicles." Trends Cell Biol **25**(6): 364-372.
Cocucci, E., G. Racchetti and J. Meldolesi (2009). "Shedding microvesicles: artefacts no

more." Trends Cell Biol **19**(2): 43-51.
Colombo, M., C. Moita, G. van Niel, J. Kowal, J. Vigneron, P. Benaroch, N. Manel, L. F. Moita, C. Thery and G. Raposo (2013). "Analysis of ESCRT functions in exosome biogenesis, composition and secretion highlights the heterogeneity of extracellular vesicles." J Cell Sci **126**(Pt 24): 5553-5565.
Conti, M. (2010). "Signaling networks in somatic cells and oocytes activated during ovulation." Ann Endocrinol (Paris) **71**(3): 189-190.
Conti, M., M. Hsieh, J. Y. Park and Y. Q. Su (2006). "Role of the epidermal growth factor network in ovarian follicles." Mol Endocrinol **20**(4): 715-723.
Conti, M., M. Hsieh, A. M. Zamah and J. S. Oh (2012). "Novel signaling mechanisms in the ovary during oocyte maturation and ovulation." Mol Cell Endocrinol **356**(1-2): 65-73.
Costa-Silva, B., N. M. Aiello, A. J. Ocean, S. Singh, H. Zhang, B. K. Thakur, A. Becker, A. Hoshino, M. T. Mark, H. Molina, J. Xiang, T. Zhang, T. M. Theilen, G. Garcia-Santos, C. Williams, Y. Ararso, Y. Huang, G. Rodrigues, T. L. Shen, K. J. Labori, I. M. Lothe, E. H. Kure, J. Hernandez, A. Doussot, S. H. Ebbesen, P. M. Grandgenett, M. A. Hollingsworth, M. Jain, K. Mallya, S. K. Batra, W. R. Jarnagin, R. E. Schwartz, I. Matei, H. Peinado, B. Z. Stanger, J. Bromberg and D. Lyden (2015). "Pancreatic cancer exosomes initiate pre-metastatic niche formation in the liver." Nat Cell Biol **17**(6): 816-826.
Crawford, N. (1971). "The presence of contractile proteins in platelet microparticles isolated from human and animal platelet-free plasma." Br J Haematol **21**(1): 53-69.
Cui, L. L., G. Yang, J. Pan and C. Zhang (2011). "Tumor necrosis factor alpha knockout increases fertility of mice." Theriogenology **75**(5): 867-876.
da Silveira, J. C., E. M. Carnevale, Q. A. Winger and G. J. Bouma (2014). "Regulation of ACVR1 and ID2 by cell-secreted exosomes during follicle maturation in the mare." Reprod Biol Endocrinol **12**: 44.
da Silveira, J. C., D. N. Veeramachaneni, Q. A. Winger, E. M. Carnevale and G. J. Bouma (2012). "Cell-secreted vesicles in equine ovarian follicular fluid contain miRNAs and proteins: a possible new form of cell communication within the ovarian follicle." Biol Reprod **86**(3): 71.
da Silveira, J. C., Q. A. Winger, G. J. Bouma and E. M. Carnevale (2015). "Effects of age on follicular fluid exosomal microRNAs and granulosa cell transforming growth factor-? signalling during follicle development in the mare." Reprod Fertil Dev.
Diez-Fraile, A., T. Lammens, K. Tilleman, W. Witkowski, B. Verhasselt, P. De Sutter, Y. Benoit, M. Espeel and K. D'Herde (2014). "Age-associated differential microRNA levels

in human follicular fluid reveal pathways potentially determining fertility and success of in vitro fertilization." Hum Fertil (Camb) **17**(2): 90-98.
Dijkers, P. F., K. U. Birkenkamp, E. W. Lam, N. S. Thomas, J. W. Lammers, L. Koenderman and P. J. Coffer (2002). "FKHR-L1 can act as a critical effector of cell death induced by cytokine withdrawal: protein kinase B-enhanced cell survival through maintenance of mitochondrial integrity." J Cell Biol **156**(3): 531-542.
Donaldson, J. G., N. Porat-Shliom and L. A. Cohen (2009). "Clathrin-independent endocytosis: a unique platform for cell signaling and PM remodeling." Cell Signal **21**(1): 1-6.
Du, X. Y., J. Huang, L. Q. Xu, D. F. Tang, L. Wu, L. X. Zhang, X. L. Pan, W. Y. Chen, L. P. Zheng and Y. H. Zheng (2012). "The proto-oncogene c-src is involved in primordial follicle activation through the PI3K, PKC and MAPK signaling pathways." Reprod Biol Endocrinol **10**: 58.
Dupont, S., A. Krust, A. Gansmuller, A. Dierich, P. Chambon and M. Mark (2000). "Effect of single and compound knockouts of estrogen receptors alpha (ERalpha) and beta (ERbeta) on mouse reproductive phenotypes." Development **127**(19): 4277-4291.
Eppig, J. J. (2001). "Oocyte control of ovarian follicular development and function in mammals." Reproduction **122**(6): 829-838.
Escola, J. M., M. J. Kleijmeer, W. Stoorvogel, J. M. Griffith, O. Yoshie and H. J. Geuze (1998). "Selective enrichment of tetraspan proteins on the internal vesicles of multivesicular endosomes and on exosomes secreted by human B-lymphocytes." J Biol Chem **273**(32): 20121-20127.
Escrevente, C., S. Keller, P. Altevogt and J. Costa (2011). "Interaction and uptake of exosomes by ovarian cancer cells." BMC Cancer **11**: 108.
Espey, L. L. (1980). "Ovulation as an inflammatory reaction--a hypothesis." Biol Reprod **22**(1): 73-106.
Espey, L. L. and J. S. Richards (2002). "Temporal and spatial patterns of ovarian gene transcription following an ovulatory dose of gonadotropin in the rat." Biol Reprod **67**(6): 1662-1670.
Fatehi, A. N., R. van den Hurk, B. Colenbrander, A. J. Daemen, H. T. van Tol, R. M. Monteiro, B. A. Roelen and M. M. Bevers (2005). "Expression of bone morphogenetic protein2 (BMP2), BMP4 and BMP receptors in the bovine ovary but absence of effects of BMP2 and BMP4 during IVM on bovine oocyte nuclear maturation and subsequent embryo development." Theriogenology **63**(3): 872-889.
Feng, D., W. L. Zhao, Y. Y. Ye, X. C. Bai, R. Q. Liu, L. F. Chang, Q. Zhou and S. F. Sui

(2010). "Cellular internalization of exosomes occurs through phagocytosis." Traffic **11**(5): 675-687.
Field, S. L., T. Dasgupta, M. Cummings and N. M. Orsi (2014). "Cytokines in ovarian folliculogenesis, oocyte maturation and luteinisation." Mol Reprod Dev **81**(4): 284-314.
Fitzgerald, J. B., J. George and L. K. Christenson (2016). "Non-coding RNA in Ovarian Development and Disease." Adv Exp Med Biol **886**: 79-93.
Fitzner, D., M. Schnaars, D. van Rossum, G. Krishnamoorthy, P. Dibaj, M. Bakhti, T. Regen, U. K. Hanisch and M. Simons (2011). "Selective transfer of exosomes from oligodendrocytes to microglia by macropinocytosis." J Cell Sci **124**(Pt 3): 447-458.
Fortune, J. E. (1994). "Ovarian follicular growth and development in mammals." Biol Reprod **50**(2): 225-232.
Frick, M., N. A. Bright, K. Riento, A. Bray, C. Merrified and B. J. Nichols (2007). "Coassembly of flotillins induces formation of membrane microdomains, membrane curvature, and vesicle budding." Curr Biol **17**(13): 1151-1156.
Frohlich, D., W. P. Kuo, C. Fruhbeis, J. J. Sun, C. M. Zehendner, H. J. Luhmann, S. Pinto, J. Toedling, J. Trotter and E. M. Kramer-Albers (2014). "Multifaceted effects of oligodendroglial exosomes on neurons: impact on neuronal firing rate, signal transduction and gene regulation." Philos Trans R Soc Lond B Biol Sci **369**(1652).
Fruhbeis, C., D. Frohlich, W. P. Kuo, J. Amphornrat, S. Thilemann, A. S. Saab, F. Kirchhoff, W. Mobius, S. Goebbels, K. A. Nave, A. Schneider, M. Simons, M. Klugmann, J. Trotter and E. M. Kramer-Albers (2013). "Neurotransmitter-triggered transfer of exosomes mediates oligodendrocyte-neuron communication." PLoS Biol **11**(7): e1001604.
Fruhbeis, C., D. Frohlich, W. P. Kuo and E. M. Kramer-Albers (2013). "Extracellular vesicles as mediators of neuron-glia communication." Front Cell Neurosci **7**: 182.
Galloway, S. M., S. M. Gregan, T. Wilson, K. P. McNatty, J. L. Juengel, O. Ritvos and G. H. Davis (2002). "Bmp15 mutations and ovarian function." Mol Cell Endocrinol **191**(1): 15-18.
Ghossoub, R., F. Lembo, A. Rubio, C. B. Gaillard, J. Bouchet, N. Vitale, J. Slavik, M. Machala and P. Zimmermann (2014). "Syntenin-ALIX exosome biogenesis and budding into multivesicular bodies are controlled by ARF6 and PLD2." Nat Commun **5**: 3477.
Glebov, O. O., N. A. Bright and B. J. Nichols (2006). "Flotillin-1 defines a clathrin-independent endocytic pathway in mammalian cells." Nat Cell Biol **8**(1): 46-54.
Glister, C., D. S. Tannetta, N. P. Groome and P. G. Knight (2001). "Interactions between follicle-stimulating hormone and growth factors in modulating secretion of steroids and

inhibin-related peptides by nonluteinized bovine granulosa cells." Biol Reprod **65**(4): 1020-1028.
Goren, Y., M. Kushnir, B. Zafrir, S. Tabak, B. S. Lewis and O. Amir (2012). "Serum levels of microRNAs in patients with heart failure." Eur J Heart Fail **14**(2): 147-154.
Gosden, R. G., R. H. Hunter, E. Telfer, C. Torrance and N. Brown (1988). "Physiological factors underlying the formation of ovarian follicular fluid." J Reprod Fertil **82**(2): 813-825.
Griffiths-Jones, S., H. K. Saini, S. van Dongen and A. J. Enright (2008). "miRBase: tools for microRNA genomics." Nucleic Acids Res **36**(Database issue): D154-158.
Grondahl, M. L., M. E. Nielsen, M. B. Dal Canto, R. Fadini, I. A. Rasmussen, L. G. Westergaard, S. G. Kristensen and C. Yding Andersen (2011). "Anti-Mullerian hormone remains highly expressed in human cumulus cells during the final stages of folliculogenesis." Reprod Biomed Online **22**(4): 389-398.
Gyorgy, B., T. G. Szabo, M. Pasztoi, Z. Pal, P. Misjak, B. Aradi, V. Laszlo, E. Pallinger, E. Pap, A. Kittel, G. Nagy, A. Falus and E. I. Buzas (2011). "Membrane vesicles, current state-of-the-art: emerging role of extracellular vesicles." Cell Mol Life Sci **68**(16): 2667-2688.
Haggarty, P., M. Wood, E. Ferguson, G. Hoad, A. Srikantharajah, E. Milne, M. Hamilton and S. Bhattacharya (2006). "Fatty acid metabolism in human preimplantation embryos." Hum Reprod **21**(3): 766-773.
Hanrieder, J., A. Nyakas, T. Naessen and J. Bergquist (2008). "Proteomic analysis of human follicular fluid using an alternative bottom-up approach." J Proteome Res **7**(1): 443-449.
Hanson, P. I. and A. Cashikar (2012). "Multivesicular body morphogenesis." Annu Rev Cell Dev Biol **28**: 337-362.
Hao, S., O. Bai, F. Li, J. Yuan, S. Laferte and J. Xiang (2007). "Mature dendritic cells pulsed with exosomes stimulate efficient cytotoxic T-lymphocyte responses and antitumour immunity." Immunology **120**(1): 90-102.
Hastie, P. M. and W. Haresign (2006). "A role for LH in the regulation of expression of mRNAs encoding components of the insulin-like growth factor (IGF) system in the ovine corpus luteum." Anim Reprod Sci **96**(1-2): 196-209.
Hattori, M., K. Sakamoto, N. Fujihara and I. Kojima (1996). "Nitric oxide: a modulator for the epidermal growth factor receptor expression in developing ovarian granulosa cells." Am J Physiol **270**(3 Pt 1): C812-818.
Hatzirodos, N., K. Hummitzsch, H. F. Irving-Rodgers, M. L. Harland, S. E. Morris and R.

J. Rodgers (2014). "Transcriptome profiling of granulosa cells from bovine ovarian follicles during atresia." BMC Genomics **15**: 40.
Hennet, M. L. and C. M. Combelles (2012). "The antral follicle: a microenvironment for oocyte differentiation." Int J Dev Biol **56**(10-12): 819-831.
Hong, X., L. J. Luense, L. K. McGinnis, W. B. Nothnick and L. K. Christenson (2008). "Dicer1 is essential for female fertility and normal development of the female reproductive system." Endocrinology **149**(12): 6207-6212.
Hoshino, A., B. Costa-Silva, T. L. Shen, G. Rodrigues, A. Hashimoto, M. Tesic Mark, H. Molina, S. Kohsaka, A. Di Giannatale, S. Ceder, S. Singh, C. Williams, N. Soplop, K. Uryu, L. Pharmer, T. King, L. Bojmar, A. E. Davies, Y. Ararso, T. Zhang, H. Zhang, J. Hernandez, J. M. Weiss, V. D. Dumont-Cole, K. Kramer, L. H. Wexler, A. Narendran, G. K. Schwartz, J. H. Healey, P. Sandstrom, K. J. Labori, E. H. Kure, P. M. Grandgenett, M. A. Hollingsworth, M. de Sousa, S. Kaur, M. Jain, K. Mallya, S. K. Batra, W. R. Jarnagin, M. S. Brady, O. Fodstad, V. Muller, K. Pantel, A. J. Minn, M. J. Bissell, B. A. Garcia, Y. Kang, V. K. Rajasekhar, C. M. Ghajar, I. Matei, H. Peinado, J. Bromberg and D. Lyden (2015). "Tumour exosome integrins determine organotropic metastasis." Nature **527**(7578): 329-335.
Hosoda, K. and T. Terada (2007). "Bovine follicular fluid contains antagonist activity for cumulus expansion promoting effect by epidermal growth factor." Reprod Domest Anim **42**(3): 225-229.
Hsu, C., Y. Morohashi, S. Yoshimura, N. Manrique-Hoyos, S. Jung, M. A. Lauterbach, M. Bakhti, M. Gronborg, W. Mobius, J. Rhee, F. A. Barr and M. Simons (2010). "Regulation of exosome secretion by Rab35 and its GTPase-activating proteins TBC1D10A-C." J Cell Biol **189**(2): 223-232.
Hsu, C. J. and J. M. Hammond (1987). "Gonadotropins and estradiol stimulate immunoreactive insulin-like growth factor-I production by porcine granulosa cells in vitro." Endocrinology **120**(1): 198-207.
Hung, W., L. Christenson and L. McGinnis (2015). "Extracellular vesicles from bovine follicular fluid support cumulus expansion." Biol Reprod.
Hurley, J. H. (2015). "ESCRTs are everywhere." EMBO J **34**(19): 2398-2407.
Hwang, I., X. Shen and J. Sprent (2003). "Direct stimulation of naive T cells by membrane vesicles from antigen-presenting cells: distinct roles for CD54 and B7 molecules." Proc Natl Acad Sci U S A **100**(11): 6670-6675.
Jahn, R. and T. C. Sudhof (1999). "Membrane fusion and exocytosis." Annu Rev Biochem **68**: 863-911.

Ji, R., Y. Cheng, J. Yue, J. Yang, X. Liu, H. Chen, D. B. Dean and C. Zhang (2007). "MicroRNA expression signature and antisense-mediated depletion reveal an essential role of MicroRNA in vascular neointimal lesion formation." Circ Res **100**(11): 1579-1588.
Jiang, P., H. Wu, W. Wang, W. Ma, X. Sun and Z. Lu (2007). "MiPred: classification of real and pseudo microRNA precursors using random forest prediction model with combined features." Nucleic Acids Res **35**(Web Server issue): W339-344.
Johnstone, R. M., M. Adam, J. R. Hammond, L. Orr and C. Turbide (1987). "Vesicle formation during reticulocyte maturation. Association of plasma membrane activities with released vesicles (exosomes)." J Biol Chem **262**(19): 9412-9420.
Juengel, J. L., D. A. Heath, L. D. Quirke and K. P. McNatty (2006). "Oestrogen receptor alpha and beta, androgen receptor and progesterone receptor mRNA and protein localisation within the developing ovary and in small growing follicles of sheep." Reproduction **131**(1): 81-92.
Kawashima, I., Z. Liu, L. K. Mullany, T. Mihara, J. S. Richards and M. Shimada (2012). "EGF-like factors induce expansion of the cumulus cell-oocyte complexes by activating calpain-mediated cell movement." Endocrinology **153**(8): 3949-3959.
Kerr, M. C. and R. D. Teasdale (2009). "Defining macropinocytosis." Traffic **10**(4): 364-371.
Khalid, M., W. Haresign and M. R. Luck (2000). "Secretion of IGF-1 by ovine granulosa cells: effects of growth hormone and follicle stimulating hormone." Anim Reprod Sci **58**(3-4): 261-272.
Kim, C. W., H. M. Lee, T. H. Lee, C. Kang, H. K. Kleinman and Y. S. Gho (2002). "Extracellular membrane vesicles from tumor cells promote angiogenesis via sphingomyelin." Cancer Res **62**(21): 6312-6317.
Kimura, N., Y. Hoshino, K. Totsukawa and E. Sato (2007). "Cellular and molecular events during oocyte maturation in mammals: molecules of cumulus-oocyte complex matrix and signalling pathways regulating meiotic progression." Soc Reprod Fertil Suppl **63**: 327-342.
Kirchhausen, T. (2000). "Clathrin." Annu Rev Biochem **69**: 699-727.
Knight, P. G. and C. Glister (2006). "TGF-beta superfamily members and ovarian follicle development." Reproduction **132**(2): 191-206.
Korkut, C., Y. Li, K. Koles, C. Brewer, J. Ashley, M. Yoshihara and V. Budnik (2013). "Regulation of postsynaptic retrograde signaling by presynaptic exosome release." Neuron **77**(6): 1039-1046.

Koumangoye, R. B., A. M. Sakwe, J. S. Goodwin, T. Patel and J. Ochieng (2011). "Detachment of breast tumor cells induces rapid secretion of exosomes which subsequently mediate cellular adhesion and spreading." PLoS One **6**(9): e24234.
Kowal, J., M. Tkach and C. Thery (2014). "Biogenesis and secretion of exosomes." Curr Opin Cell Biol **29**: 116-125.
Kramer-Albers, E. M., N. Bretz, S. Tenzer, C. Winterstein, W. Mobius, H. Berger, K. A. Nave, H. Schild and J. Trotter (2007). "Oligodendrocytes secrete exosomes containing major myelin and stress-protective proteins: Trophic support for axons?" Proteomics Clin Appl **1**(11): 1446-1461.
Kumar, D., D. Gupta, S. Shankar and R. K. Srivastava (2014). "Biomolecular characterization of exosomes released from cancer stem cells: Possible implications for biomarker and treatment of cancer." Oncotarget **6**(5): 3280-3291.
Kumar, T. R. (2005). "What have we learned about gonadotropin function from gonadotropin subunit and receptor knockout mice?" Reproduction **130**(3): 293-302.
Lakkaraju, A. and E. Rodriguez-Boulan (2008). "Itinerant exosomes: emerging roles in cell and tissue polarity." Trends Cell Biol **18**(5): 199-209.
Laulagnier, K., D. Grand, A. Dujardin, S. Hamdi, H. Vincent-Schneider, D. Lankar, J. P. Salles, C. Bonnerot, B. Perret and M. Record (2004). "PLD2 is enriched on exosomes and its activity is correlated to the release of exosomes." FEBS Lett **572**(1-3): 11-14.
LaVoie, H. A., D. C. DeSimone, C. Gillio-Meina and Y. Y. Hui (2002). "Cloning and characterization of porcine ovarian estrogen receptor beta isoforms." Biol Reprod **66**(3): 616-623.
Ledee, N., V. Gridelet, S. Ravet, C. Jouan, O. Gaspard, F. Wenders, F. Thonon, N. Hincourt, M. Dubois, J. M. Foidart, C. Munaut and S. Perrier d'Hauterive (2013). "Impact of follicular G-CSF quantification on subsequent embryo transfer decisions: a proof of concept study." Hum Reprod **28**(2): 406-413.
Ledee, N., C. Munaut, V. Serazin, S. Perrier d'Hauterive, L. Lombardelli, F. Logiodice, R. Wainer, V. Gridelet, G. Chaouat, F. Frankenne, J. M. Foidart and M. P. Piccinni (2010). "Performance evaluation of microbead and ELISA assays for follicular G-CSF: a non-invasive biomarker of oocyte developmental competence for embryo implantation." J Reprod Immunol **86**(2): 126-132.
Ledee, N., M. Petitbarat, M. Rahmati, S. Dubanchet, G. Chaouat, O. Sandra, S. Perrier-d'Hauterive, C. Munaut and J. M. Foidart (2011). "New pre-conception immune biomarkers for clinical practice: interleukin-18, interleukin-15 and TWEAK on the endometrial side, G-CSF on the follicular side." J Reprod Immunol **88**(2): 118-123.

Li, H. and R. Durbin (2009). "Fast and accurate short read alignment with Burrows-Wheeler transform." Bioinformatics **25**(14): 1754-1760.
Li, R., D. M. Phillips and J. P. Mather (1995). "Activin promotes ovarian follicle development in vitro." Endocrinology **136**(3): 849-856.
Liu, G., W. Zhou, L. I. Wang, S. Park, D. P. Miller, L. L. Xu, J. C. Wain, T. J. Lynch, L. Su and D. C. Christiani (2004). "MPO and SOD2 polymorphisms, gender, and the risk of non-small cell lung carcinoma." Cancer Lett **214**(1): 69-79.
Liu, J., A. T. Koenigsfeld, T. C. Cantley, C. K. Boyd, Y. Kobayashi and M. C. Lucy (2000). "Growth and the initiation of steroidogenesis in porcine follicles are associated with unique patterns of gene expression for individual componentsof the ovarian insulin-like growth factor system." Biol Reprod **63**(3): 942-952.
Londin, E., P. Loher, A. G. Telonis, K. Quann, P. Clark, Y. Jing, E. Hatzimichael, Y. Kirino, S. Honda, M. Lally, B. Ramratnam, C. E. Comstock, K. E. Knudsen, L. Gomella, G. L. Spaeth, L. Hark, L. J. Katz, A. Witkiewicz, A. Rostami, S. A. Jimenez, M. A. Hollingsworth, J. J. Yeh, C. A. Shaw, S. E. McKenzie, P. Bray, P. T. Nelson, S. Zupo, K. Van Roosbroeck, M. J. Keating, G. A. Calin, C. Yeo, M. Jimbo, J. Cozzitorto, J. R. Brody, K. Delgrosso, J. S. Mattick, P. Fortina and I. Rigoutsos (2015). "Analysis of 13 cell types reveals evidence for the expression of numerous novel primate- and tissue-specific microRNAs." Proc Natl Acad Sci U S A **112**(10): E1106-1115.
Maalouf, S. W., W. S. Liu, I. Albert and J. L. Pate (2014). "Regulating life or death: potential role of microRNA in rescue of the corpus luteum." Mol Cell Endocrinol **398**(1-2): 78-88.
Marei, W. F., D. C. Wathes and A. A. Fouladi-Nashta (2010). "Impact of linoleic acid on bovine oocyte maturation and embryo development." Reproduction **139**(6): 979-988.
Maruo, T., M. Hayashi, H. Matsuo, Y. Ueda, H. Morikawa and M. Mochizuki (1988). "Comparison of the facilitative roles of insulin and insulin-like growth factor I in the functional differentiation of granulosa cells: in vitro studies with the porcine model." Acta Endocrinol (Copenh) **117**(2): 230-240.
Mathivanan, S., H. Ji and R. J. Simpson (2010). "Exosomes: extracellular organelles important in intercellular communication." J Proteomics **73**(10): 1907-1920.
Matsuda, F., N. Inoue, A. Maeda, Y. Cheng, T. Sai, H. Gonda, Y. Goto, K. Sakamaki and N. Manabe (2011). "Expression and function of apoptosis initiator FOXO3 in granulosa cells during follicular atresia in pig ovaries." J Reprod Dev **57**(1): 151-158.
Matzuk, M. M., K. H. Burns, M. M. Viveiros and J. J. Eppig (2002). "Intercellular communication in the mammalian ovary: oocytes carry the conversation." Science

296(5576): 2178-2180.
Mazerbourg, S. and A. J. Hsueh (2003). "Growth differentiation factor-9 signaling in the ovary." Mol Cell Endocrinol **202**(1-2): 31-36.
McConnell, N. A., R. S. Yunus, S. A. Gross, K. L. Bost, M. G. Clemens and F. M. Hughes, Jr. (2002). "Water permeability of an ovarian antral follicle is predominantly transcellular and mediated by aquaporins." Endocrinology **143**(8): 2905-2912.
McConnell, R. E., J. N. Higginbotham, D. A. Shifrin, Jr., D. L. Tabb, R. J. Coffey and M. J. Tyska (2009). "The enterocyte microvillus is a vesicle-generating organelle." J Cell Biol **185**(7): 1285-1298.
McConnell, R. E. and M. J. Tyska (2007). "Myosin-1a powers the sliding of apical membrane along microvillar actin bundles." J Cell Biol **177**(4): 671-681.
McGinnis, L. K., S. Pelech and W. H. Kinsey (2014). "Post-ovulatory aging of oocytes disrupts kinase signaling pathways and lysosome biogenesis." Mol Reprod Dev **81**(10): 928-945.
Menck, K., F. Klemm, J. C. Gross, T. Pukrop, D. Wenzel and C. Binder (2013). "Induction and transport of Wnt 5a during macrophage-induced malignant invasion is mediated by two types of extracellular vesicles." Oncotarget **4**(11): 2057-2066.
Mendoza, C., E. Ruiz-Requena, E. Ortega, N. Cremades, F. Martinez, R. Bernabeu, E. Greco and J. Tesarik (2002). "Follicular fluid markers of oocyte developmental potential." Hum Reprod **17**(4): 1017-1022.
Miro, F. and S. G. Hillier (1996). "Modulation of granulosa cell deoxyribonucleic acid synthesis and differentiation by activin." Endocrinology **137**(2): 464-468.
Miyanishi, M., K. Tada, M. Koike, Y. Uchiyama, T. Kitamura and S. Nagata (2007). "Identification of Tim4 as a phosphatidylserine receptor." Nature **450**(7168): 435-439.
Miyoshi, T., F. Otsuka, M. Yamashita, K. Inagaki, E. Nakamura, N. Tsukamoto, M. Takeda, J. Suzuki and H. Makino (2010). "Functional relationship between fibroblast growth factor-8 and bone morphogenetic proteins in regulating steroidogenesis by rat granulosa cells." Mol Cell Endocrinol **325**(1-2): 84-92.
Monget, P. and C. Bondy (2000). "Importance of the IGF system in early folliculogenesis." Mol Cell Endocrinol **163**(1-2): 89-93.
Monniaux, D. and C. Pisselet (1992). "Control of proliferation and differentiation of ovine granulosa cells by insulin-like growth factor-I and follicle-stimulating hormone in vitro." Biol Reprod **46**(1): 109-119.
Montecalvo, A., A. T. Larregina, W. J. Shufesky, D. B. Stolz, M. L. Sullivan, J. M. Karlsson, C. J. Baty, G. A. Gibson, G. Erdos, Z. Wang, J. Milosevic, O. A. Tkacheva, S.

J. Divito, R. Jordan, J. Lyons-Weiler, S. C. Watkins and A. E. Morelli (2012). "Mechanism of transfer of functional microRNAs between mouse dendritic cells via exosomes." Blood **119**(3): 756-766.
Morelli, A. E., A. T. Larregina, W. J. Shufesky, M. L. Sullivan, D. B. Stolz, G. D. Papworth, A. F. Zahorchak, A. J. Logar, Z. Wang, S. C. Watkins, L. D. Falo, Jr. and A. W. Thomson (2004). "Endocytosis, intracellular sorting, and processing of exosomes by dendritic cells." Blood **104**(10): 3257-3266.
Moreno, J. M., M. J. Nunez, A. Quinonero, S. Martinez, M. de la Orden, C. Simon, A. Pellicer, C. Diaz-Garcia and F. Dominguez (2015). "Follicular fluid and mural granulosa cells microRNA profiles vary in in vitro fertilization patients depending on their age and oocyte maturation stage." Fertil Steril **104**(4): 1037-1046 e1031.
Mottershead, D. G., L. J. Ritter and R. B. Gilchrist (2012). "Signalling pathways mediating specific synergistic interactions between GDF9 and BMP15." Mol Hum Reprod **18**(3): 121-128.
Mu, W., S. Rana and M. Zoller (2013). "Host matrix modulation by tumor exosomes promotes motility and invasiveness." Neoplasia **15**(8): 875-887.
Mulcahy, L. A., R. C. Pink and D. R. Carter (2014). "Routes and mechanisms of extracellular vesicle uptake." J Extracell Vesicles **3**.
Muralidharan-Chari, V., J. W. Clancy, A. Sedgwick and C. D'Souza-Schorey (2010). "Microvesicles: mediators of extracellular communication during cancer progression." J Cell Sci **123**(Pt 10): 1603-1611.
Nabhan, J. F., R. Hu, R. S. Oh, S. N. Cohen and Q. Lu (2012). "Formation and release of arrestin domain-containing protein 1-mediated microvesicles (ARMMs) at plasma membrane by recruitment of TSG101 protein." Proc Natl Acad Sci U S A **109**(11): 4146-4151.
Nabi, I. R. and P. U. Le (2003). "Caveolae/raft-dependent endocytosis." J Cell Biol **161**(4): 673-677.
Nanbo, A., E. Kawanishi, R. Yoshida and H. Yoshiyama (2013). "Exosomes derived from Epstein-Barr virus-infected cells are internalized via caveola-dependent endocytosis and promote phenotypic modulation in target cells." J Virol **87**(18): 10334-10347.
Naslund, T. I., D. Paquin-Proulx, P. T. Paredes, H. Vallhov, J. K. Sandberg and S. Gabrielsson (2014). "Exosomes from breast milk inhibit HIV-1 infection of dendritic cells and subsequent viral transfer to CD4+ T cells." AIDS **28**(2): 171-180.
Navakanitworakul, R., W. T. Hung, S. Gunewardena, J. S. Davis, W. Chotigeat and L. K. Christenson (2016). "Characterization and Small RNA Content of Extracellular Vesicles

in Follicular Fluid of Developing Bovine Antral Follicles." Sci Rep **6**: 25486.
Nazarenko, I., S. Rana, A. Baumann, J. McAlear, A. Hellwig, M. Trendelenburg, G. Lochnit, K. T. Preissner and M. Zoller (2010). "Cell surface tetraspanin Tspan8 contributes to molecular pathways of exosome-induced endothelial cell activation." Cancer Res **70**(4): 1668-1678.
Nolte-'t Hoen, E. N., S. I. Buschow, S. M. Anderton, W. Stoorvogel and M. H. Wauben (2009). "Activated T cells recruit exosomes secreted by dendritic cells via LFA-1." Blood **113**(9): 1977-1981.
Ohnami, N., A. Nakamura, M. Miyado, M. Sato, N. Kawano, K. Yoshida, Y. Harada, Y. Takezawa, S. Kanai, C. Ono, Y. Takahashi, K. Kimura, T. Shida, K. Miyado and A. Umezawa (2012). "CD81 and CD9 work independently as extracellular components upon fusion of sperm and oocyte." Biol Open **1**(7): 640-647.
Oktem, O., E. Buyuk and K. Oktay (2011). "Preantral follicle growth is regulated by c-Jun-N-terminal kinase (JNK) pathway." Reprod Sci **18**(3): 269-276.
Ostrowski, M., N. B. Carmo, S. Krumeich, I. Fanget, G. Raposo, A. Savina, C. F. Moita, K. Schauer, A. N. Hume, R. P. Freitas, B. Goud, P. Benaroch, N. Hacohen, M. Fukuda, C. Desnos, M. C. Seabra, F. Darchen, S. Amigorena, L. F. Moita and C. Thery (2010). "Rab27a and Rab27b control different steps of the exosome secretion pathway." Nat Cell Biol **12**(1): 19-30; sup pp 11-13.
Otsuka, M., Q. Jing, P. Georgel, L. New, J. Chen, J. Mols, Y. J. Kang, Z. Jiang, X. Du, R. Cook, S. C. Das, A. K. Pattnaik, B. Beutler and J. Han (2007). "Hypersusceptibility to vesicular stomatitis virus infection in Dicer1-deficient mice is due to impaired miR24 and miR93 expression." Immunity **27**(1): 123-134.
Otsuka, M., M. Zheng, M. Hayashi, J. D. Lee, O. Yoshino, S. Lin and J. Han (2008). "Impaired microRNA processing causes corpus luteum insufficiency and infertility in mice." J Clin Invest **118**(5): 1944-1954.
Otto, G. P. and B. J. Nichols (2011). "The roles of flotillin microdomains--endocytosis and beyond." J Cell Sci **124**(Pt 23): 3933-3940.
Palecek, S. P., C. E. Schmidt, D. A. Lauffenburger and A. F. Horwitz (1996). "Integrin dynamics on the tail region of migrating fibroblasts." J Cell Sci **109 (Pt 5)**: 941-952.
Park, J. Y., Y. Q. Su, M. Ariga, E. Law, S. L. Jin and M. Conti (2004). "EGF-like growth factors as mediators of LH action in the ovulatory follicle." Science **303**(5658): 682-684.
Parolini, I., C. Federici, C. Raggi, L. Lugini, S. Palleschi, A. De Milito, C. Coscia, E. Iessi, M. Logozzi, A. Molinari, M. Colone, M. Tatti, M. Sargiacomo and S. Fais (2009). "Microenvironmental pH is a key factor for exosome traffic in tumor cells." J Biol Chem

284(49): 34211-34222.
Peinado, H., M. Aleckovic, S. Lavotshkin, I. Matei, B. Costa-Silva, G. Moreno-Bueno, M. Hergueta-Redondo, C. Williams, G. Garcia-Santos, C. Ghajar, A. Nitadori-Hoshino, C. Hoffman, K. Badal, B. A. Garcia, M. K. Callahan, J. Yuan, V. R. Martins, J. Skog, R. N. Kaplan, M. S. Brady, J. D. Wolchok, P. B. Chapman, Y. Kang, J. Bromberg and D. Lyden (2012). "Melanoma exosomes educate bone marrow progenitor cells toward a pro-metastatic phenotype through MET." Nat Med **18**(6): 883-891.
Png, K. J., M. Yoshida, X. H. Zhang, W. Shu, H. Lee, A. Rimner, T. A. Chan, E. Comen, V. P. Andrade, S. W. Kim, T. A. King, C. A. Hudis, L. Norton, J. Hicks, J. Massague and S. F. Tavazoie (2011). "MicroRNA-335 inhibits tumor reinitiation and is silenced through genetic and epigenetic mechanisms in human breast cancer." Genes Dev **25**(3): 226-231.
Raposo, G., H. W. Nijman, W. Stoorvogel, R. Liejendekker, C. V. Harding, C. J. Melief and H. J. Geuze (1996). "B lymphocytes secrete antigen-presenting vesicles." J Exp Med **183**(3): 1161-1172.
Revelli, A., L. Delle Piane, S. Casano, E. Molinari, M. Massobrio and P. Rinaudo (2009). "Follicular fluid content and oocyte quality: from single biochemical markers to metabolomics." Reprod Biol Endocrinol **7**: 40.
Rice, V. M., A. R. Chaudhery, O. Oluola, S. D. Limback, K. F. Roby and P. F. Terranova (2001). "Herbimycin, a tyrosine kinase inhibitor with Src selectivity, reduces progesterone and estradiol secretion by human granulosa cells." Endocrine **15**(3): 271-276.
Robinson, M. D. and G. K. Smyth (2008). "Small-sample estimation of negative binomial dispersion, with applications to SAGE data." Biostatistics **9**(2): 321-332.
Rodgers, R. J. and H. F. Irving-Rodgers (2010). "Formation of the ovarian follicular antrum and follicular fluid." Biol Reprod **82**(6): 1021-1029.
Romancino, D. P., G. Paterniti, Y. Campos, A. De Luca, V. Di Felice, A. d'Azzo and A. Bongiovanni (2013). "Identification and characterization of the nano-sized vesicles released by muscle cells." FEBS Lett **587**(9): 1379-1384.
Rosenfeld, C. S., J. S. Wagner, R. M. Roberts and D. B. Lubahn (2001). "Intraovarian actions of oestrogen." Reproduction **122**(2): 215-226.
Roth, L. W., B. McCallie, R. Alvero, W. B. Schoolcraft, D. Minjarez and M. G. Katz-Jaffe (2014). "Altered microRNA and gene expression in the follicular fluid of women with polycystic ovary syndrome." J Assist Reprod Genet **31**(3): 355-362.
Roy, S. K. (1994). "Regulation of ovarian follicular development: a review of microscopic studies." Microsc Res Tech **27**(2): 83-96.

Rubinstein, E., A. Ziyyat, M. Prenant, E. Wrobel, J. P. Wolf, S. Levy, F. Le Naour and C. Boucheix (2006). "Reduced fertility of female mice lacking CD81." Dev Biol **290**(2): 351-358.
Russell, D. L. and A. Salustri (2006). "Extracellular matrix of the cumulus-oocyte complex." Semin Reprod Med **24**(4): 217-227.
Sanderson, M. P., S. Keller, A. Alonso, S. Riedle, P. J. Dempsey and P. Altevogt (2008). "Generation of novel, secreted epidermal growth factor receptor (EGFR/ErbB1) isoforms via metalloprotease-dependent ectodomain shedding and exosome secretion." J Cell Biochem **103**(6): 1783-1797.
Sang, Q., Z. Yao, H. Wang, R. Feng, H. Wang, X. Zhao, Q. Xing, L. Jin, L. He, L. Wu and L. Wang (2013). "Identification of microRNAs in human follicular fluid: characterization of microRNAs that govern steroidogenesis in vitro and are associated with polycystic ovary syndrome in vivo." J Clin Endocrinol Metab **98**(7): 3068-3079.
Santonocito, M., M. Vento, M. R. Guglielmino, R. Battaglia, J. Wahlgren, M. Ragusa, D. Barbagallo, P. Borzi, S. Rizzari, M. Maugeri, P. Scollo, C. Tatone, H. Valadi, M. Purrello and C. Di Pietro (2014). "Molecular characterization of exosomes and their microRNA cargo in human follicular fluid: bioinformatic analysis reveals that exosomal microRNAs control pathways involved in follicular maturation." Fertil Steril **102**(6): 1751-1761 e1751.
Sarapik, A., A. Velthut, K. Haller-Kikkatalo, G. C. Faure, M. C. Bene, M. de Carvalho Bittencourt, F. Massin, R. Uibo and A. Salumets (2012). "Follicular proinflammatory cytokines and chemokines as markers of IVF success." Clin Dev Immunol **2012**: 606459.
Savchev, S. I., V. A. Moragianni, D. Senger, A. S. Penzias, K. Thornton and A. Usheva (2010). "Follicular fluid-specific distribution of vascular endothelial growth factor isoforms and sFlt-1 in patients undergoing IVF and their correlation with treatment outcomes." Reprod Sci **17**(11): 1036-1042.
Savina, A., C. M. Fader, M. T. Damiani and M. I. Colombo (2005). "Rab11 promotes docking and fusion of multivesicular bodies in a calcium-dependent manner." Traffic **6**(2): 131-143.
Schneider, C. A., W. S. Rasband and K. W. Eliceiri (2012). "NIH Image to ImageJ: 25 years of image analysis." Nat Methods **9**(7): 671-675.
Schweigert, F. J., B. Gericke, W. Wolfram, U. Kaisers and J. W. Dudenhausen (2006). "Peptide and protein profiles in serum and follicular fluid of women undergoing IVF." Hum Reprod **21**(11): 2960-2968.
Sekiguchi, T., T. Mizutani, K. Yamada, T. Kajitani, T. Yazawa, M. Yoshino and K.

Miyamoto (2004). "Expression of epiregulin and amphiregulin in the rat ovary." J Mol Endocrinol **33**(1): 281-291.
Shi, Y., J. Huang, J. Zhou, Y. Liu, X. Fu, Y. Li, G. Yin and J. Wen (2015). "MicroRNA-204 inhibits proliferation, migration, invasion and epithelial-mesenchymal transition in osteosarcoma cells via targeting Sirtuin 1." Oncol Rep **34**(1): 399-406.
Shu, M., X. Zheng, S. Wu, H. Lu, T. Leng, W. Zhu, Y. Zhou, Y. Ou, X. Lin, Y. Lin, D. Xu, Y. Zhou and G. Yan (2011). "Targeting oncogenic miR-335 inhibits growth and invasion of malignant astrocytoma cells." Mol Cancer **10**: 59.
Shukla, D., J. Liu, P. Blaiklock, N. W. Shworak, X. Bai, J. D. Esko, G. H. Cohen, R. J. Eisenberg, R. D. Rosenberg and P. G. Spear (1999). "A novel role for 3-O-sulfated heparan sulfate in herpes simplex virus 1 entry." Cell **99**(1): 13-22.
Simpson, R. J., J. W. Lim, R. L. Moritz and S. Mathivanan (2009). "Exosomes: proteomic insights and diagnostic potential." Expert Rev Proteomics **6**(3): 267-283.
Skowronski, M. T., T. H. Kwon and S. Nielsen (2009). "Immunolocalization of aquaporin 1, 5, and 9 in the female pig reproductive system." J Histochem Cytochem **57**(1): 61-67.
Sohel, M. M., M. Hoelker, S. S. Noferesti, D. Salilew-Wondim, E. Tholen, C. Looft, F. Rings, M. J. Uddin, T. E. Spencer, K. Schellander and D. Tesfaye (2013). "Exosomal and Non-Exosomal Transport of Extra-Cellular microRNAs in Follicular Fluid: Implications for Bovine Oocyte Developmental Competence." PLoS One **8**(11): e78505.
Son, D. S., K. Y. Arai, K. F. Roby and P. F. Terranova (2004). "Tumor necrosis factor alpha (TNF) increases granulosa cell proliferation: dependence on c-Jun and TNF receptor type 1." Endocrinology **145**(3): 1218-1226.
Son, D. S., K. F. Roby and P. F. Terranova (2004). "Tumor necrosis factor-alpha induces serum amyloid A3 in mouse granulosa cells." Endocrinology **145**(5): 2245-2252.
Sriraman, V., S. R. Modi, Y. Bodenburg, L. A. Denner and R. J. Urban (2008). "Identification of ERK and JNK as signaling mediators on protein kinase C activation in cultured granulosa cells." Mol Cell Endocrinol **294**(1-2): 52-60.
Stahl, M., P. F. Dijkers, G. J. Kops, S. M. Lens, P. J. Coffer, B. M. Burgering and R. H. Medema (2002). "The forkhead transcription factor FoxO regulates transcription of p27Kip1 and Bim in response to IL-2." J Immunol **168**(10): 5024-5031.
Stein, J. M. and J. P. Luzio (1991). "Ectocytosis caused by sublytic autologous complement attack on human neutrophils. The sorting of endogenous plasma-membrane proteins and lipids into shed vesicles." Biochem J **274 (Pt 2)**: 381-386.
Stenmark, H. (2009). "Rab GTPases as coordinators of vesicle traffic." Nat Rev Mol Cell Biol **10**(8): 513-525.

Stephens, L., C. Ellson and P. Hawkins (2002). "Roles of PI3Ks in leukocyte chemotaxis and phagocytosis." Curr Opin Cell Biol **14**(2): 203-213.
Strauss, K., C. Goebel, H. Runz, W. Mobius, S. Weiss, I. Feussner, M. Simons and A. Schneider (2010). "Exosome secretion ameliorates lysosomal storage of cholesterol in Niemann-Pick type C disease." J Biol Chem **285**(34): 26279-26288.
Su, Y. Q., K. Sugiura, Q. Li, K. Wigglesworth, M. M. Matzuk and J. J. Eppig (2010). "Mouse oocytes enable LH-induced maturation of the cumulus-oocyte complex via promoting EGF receptor-dependent signaling." Mol Endocrinol **24**(6): 1230-1239.
Sugiyama, R., A. Fuzitou, C. Takahashi, O. Akutagawa, H. Ito, K. Nakagawa, R. Sugiyama and K. Isaka (2010). "Bone morphogenetic protein 2 may be a good predictor of success in oocyte fertilization during assisted reproductive technology." Hum Cell **23**(3): 83-88.
Sung, B. H., T. Ketova, D. Hoshino, A. Zijlstra and A. M. Weaver (2015). "Directional cell movement through tissues is controlled by exosome secretion." Nat Commun **6**: 7164.
Svensson, K. J., H. C. Christianson, A. Wittrup, E. Bourseau-Guilmain, E. Lindqvist, L. M. Svensson, M. Morgelin and M. Belting (2013). "Exosome uptake depends on ERK1/2-heat shock protein 27 signaling and lipid Raft-mediated endocytosis negatively regulated by caveolin-1." J Biol Chem **288**(24): 17713-17724.
Szatanek, R., J. Baran, M. Siedlar and M. Baj-Krzyworzeka (2015). "Isolation of extracellular vesicles: Determining the correct approach (Review)." Int J Mol Med **36**(1): 11-17.
Takami, M., S. L. Preston, V. A. Toyloy and H. R. Behrman (1999). "Antioxidants reversibly inhibit the spontaneous resumption of meiosis." Am J Physiol **276**(4 Pt 1): E684-688.
Tamura, H., A. Takasaki, I. Miwa, K. Taniguchi, R. Maekawa, H. Asada, T. Taketani, A. Matsuoka, Y. Yamagata, K. Shimamura, H. Morioka, H. Ishikawa, R. J. Reiter and N. Sugino (2008). "Oxidative stress impairs oocyte quality and melatonin protects oocytes from free radical damage and improves fertilization rate." J Pineal Res **44**(3): 280-287.
Tanigawa, M., K. Miyamoto, S. Kobayashi, M. Sato, H. Akutsu, M. Okabe, E. Mekada, K. Sakakibara, M. Miyado, A. Umezawa and K. Miyado (2008). "Possible involvement of CD81 in acrosome reaction of sperm in mice." Mol Reprod Dev **75**(1): 150-155.
Tartaglia, L. A., R. F. Weber, I. S. Figari, C. Reynolds, M. A. Palladino, Jr. and D. V. Goeddel (1991). "The two different receptors for tumor necrosis factor mediate distinct cellular responses." Proc Natl Acad Sci U S A **88**(20): 9292-9296.

Taurino, C., W. H. Miller, M. W. McBride, J. D. McClure, R. Khanin, M. U. Moreno, J. A. Dymott, C. Delles and A. F. Dominiczak (2010). "Gene expression profiling in whole blood of patients with coronary artery disease." Clin Sci (Lond) **119**(8): 335-343.
Thery, C., S. Amigorena, G. Raposo and A. Clayton (2006). "Isolation and characterization of exosomes from cell culture supernatants and biological fluids." Curr Protoc Cell Biol **Chapter 3**: Unit 3 22.
Thery, C., L. Duban, E. Segura, P. Veron, O. Lantz and S. Amigorena (2002). "Indirect activation of naive CD4+ T cells by dendritic cell-derived exosomes." Nat Immunol **3**(12): 1156-1162.
Thery, C., A. Regnault, J. Garin, J. Wolfers, L. Zitvogel, P. Ricciardi-Castagnoli, G. Raposo and S. Amigorena (1999). "Molecular characterization of dendritic cell-derived exosomes. Selective accumulation of the heat shock protein hsc73." J Cell Biol **147**(3): 599-610.
Thompson, A. G., E. Gray, S. M. Heman-Ackah, I. Mager, K. Talbot, S. E. Andaloussi, M. J. Wood and M. R. Turner (2016). "Extracellular vesicles in neurodegenerative disease - pathogenesis to biomarkers." Nat Rev Neurol **12**(6): 346-357.
Tkach, M. and C. Thery (2016). "Communication by Extracellular Vesicles: Where We Are and Where We Need to Go." Cell **164**(6): 1226-1232.
Toda, K., K. Takeda, T. Okada, S. Akira, T. Saibara, T. Kaname, K. Yamamura, S. Onishi and Y. Shizuta (2001). "Targeted disruption of the aromatase P450 gene (Cyp19) in mice and their ovarian and uterine responses to 17beta-oestradiol." J Endocrinol **170**(1): 99-111.
Trajkovic, K., C. Hsu, S. Chiantia, L. Rajendran, D. Wenzel, F. Wieland, P. Schwille, B. Brugger and M. Simons (2008). "Ceramide triggers budding of exosome vesicles into multivesicular endosomes." Science **319**(5867): 1244-1247.
Valadi, H., K. Ekstrom, A. Bossios, M. Sjostrand, J. J. Lee and J. O. Lotvall (2007). "Exosome-mediated transfer of mRNAs and microRNAs is a novel mechanism of genetic exchange between cells." Nat Cell Biol **9**(6): 654-659.
Vassilieva, E. V. and A. Nusrat (2008). "Vesicular trafficking: molecular tools and targets." Methods Mol Biol **440**: 3-14.
Vlassov, A. V., S. Magdaleno, R. Setterquist and R. Conrad (2012). "Exosomes: current knowledge of their composition, biological functions, and diagnostic and therapeutic potentials." Biochim Biophys Acta **1820**(7): 940-948.
Wandji, S. A., T. L. Wood, J. Crawford, S. W. Levison and J. M. Hammond (1998). "Expression of mouse ovarian insulin growth factor system components during follicular

development and atresia." Endocrinology **139**(12): 5205-5214.
Wang, L. H., K. G. Rothberg and R. G. Anderson (1993). "Mis-assembly of clathrin lattices on endosomes reveals a regulatory switch for coated pit formation." J Cell Biol **123**(5): 1107-1117.
Webber, J., V. Yeung and A. Clayton (2015). "Extracellular vesicles as modulators of the cancer microenvironment." Semin Cell Dev Biol **40**: 27-34.
Weng, Z., D. Wang, W. Zhao, M. Song, F. You, L. Yang and L. Chen (2011). "microRNA-450a targets DNA methyltransferase 3a in hepatocellular carcinoma." Exp Ther Med **2**(5): 951-955.
Williams, R. L. and S. Urbe (2007). "The emerging shape of the ESCRT machinery." Nat Rev Mol Cell Biol **8**(5): 355-368.
Wu, D., H. Pan, Y. Zhou, Z. Zhang, P. Qu, J. Zhou and W. Wang (2015). "Upregulation of microRNA-204 inhibits cell proliferation, migration and invasion in human renal cell carcinoma cells by downregulating SOX4." Mol Med Rep **12**(5): 7059-7064.
Wu, L. M., M. H. Hu, X. H. Tong, H. Han, N. Shen, R. T. Jin, W. Wang, G. X. Zhou, G. P. He and Y. S. Liu (2012). "Chronic unpredictable stress decreases expression of brain-derived neurotrophic factor (BDNF) in mouse ovaries: relationship to oocytes developmental potential." PLoS One **7**(12): e52331.
Wu, X., Y. Zeng, S. Wu, J. Zhong, Y. Wang and J. Xu (2015). "MiR-204, down-regulated in retinoblastoma, regulates proliferation and invasion of human retinoblastoma cells by targeting CyclinD2 and MMP-9." FEBS Lett **589**(5): 645-650.
Wu, Z. Y., S. M. Wang, Z. H. Chen, S. X. Huv, K. Huang, B. J. Huang, J. L. Du, C. M. Huang, L. Peng, Z. X. Jian and G. Zhao (2015). "MiR-204 regulates HMGA2 expression and inhibits cell proliferation in human thyroid cancer." Cancer Biomark **15**(5): 535-542.
Xia, Z., F. Liu, J. Zhang and L. Liu (2015). "Decreased Expression of MiRNA-204-5p Contributes to Glioma Progression and Promotes Glioma Cell Growth, Migration and Invasion." PLoS One **10**(7): e0132399.
Yamashita, Y., M. Okamoto, M. Ikeda, A. Okamoto, M. Sakai, Y. Gunji, R. Nishimura, M. Hishinuma and M. Shimada (2014). "Protein kinase C (PKC) increases TACE/ADAM17 enzyme activity in porcine ovarian somatic cells, which is essential for granulosa cell luteinization and oocyte maturation." Endocrinology **155**(3): 1080-1090.
Yang, J., Z. Zhang, C. Chen, Y. Liu, Q. Si, T. H. Chuang, N. Li, A. Gomez-Cabrero, R. A. Reisfeld, R. Xiang and Y. Luo (2014). "MicroRNA-19a-3p inhibits breast cancer progression and metastasis by inducing macrophage polarization through downregulated expression of Fra-1 proto-oncogene." Oncogene **33**(23): 3014-3023.

Yao, G., M. Yin, J. Lian, H. Tian, L. Liu, X. Li and F. Sun (2010). "MicroRNA-224 is involved in transforming growth factor-beta-mediated mouse granulosa cell proliferation and granulosa cell function by targeting Smad4." Mol Endocrinol **24**(3): 540-551.
Yin, J. J., B. Liang and X. R. Zhan (2015). "MicroRNA-204 inhibits cell proliferation in T-cell acute lymphoblastic leukemia by down-regulating SOX4." Int J Clin Exp Pathol **8**(8): 9189-9195.
Yuan, W., M. C. Lucy and M. F. Smith (1996). "Messenger ribonucleic acid for insulin-like growth factors-I and -II, insulin-like growth factor-binding protein-2, gonadotropin receptors, and steroidogenic enzymes in porcine follicles." Biol Reprod **55**(5): 1045-1054.
Yue, S., W. Mu, U. Erb and M. Zoller (2015). "The tetraspanins CD151 and Tspan8 are essential exosome components for the crosstalk between cancer initiating cells and their surrounding." Oncotarget **6**(4): 2366-2384.
Yuyama, K., H. Sun, S. Mitsutake and Y. Igarashi (2012). "Sphingolipid-modulated exosome secretion promotes clearance of amyloid-beta by microglia." J Biol Chem **287**(14): 10977-10989.
Zhou, J., E. Chin and C. Bondy (1991). "Cellular pattern of insulin-like growth factor-I (IGF-I) and IGF-I receptor gene expression in the developing and mature ovarian follicle." Endocrinology **129**(6): 3281-3288.
Zhou, J., T. R. Kumar, M. M. Matzuk and C. Bondy (1997). "Insulin-like growth factor I regulates gonadotropin responsiveness in the murine ovary." Mol Endocrinol **11**(13): 1924-1933.
Zhou, W., M. Y. Fong, Y. Min, G. Somlo, L. Liu, M. R. Palomares, Y. Yu, A. Chow, S. T. O'Connor, A. R. Chin, Y. Yen, Y. Wang, E. G. Marcusson, P. Chu, J. Wu, X. Wu, A. X. Li, Z. Li, H. Gao, X. Ren, M. P. Boldin, P. C. Lin and S. E. Wang (2014). "Cancer-secreted miR-105 destroys vascular endothelial barriers to promote metastasis." Cancer Cell **25**(4): 501-515.
Zoller, M. (2009). "Tetraspanins: push and pull in suppressing and promoting metastasis." Nat Rev Cancer **9**(1): 40-55.